

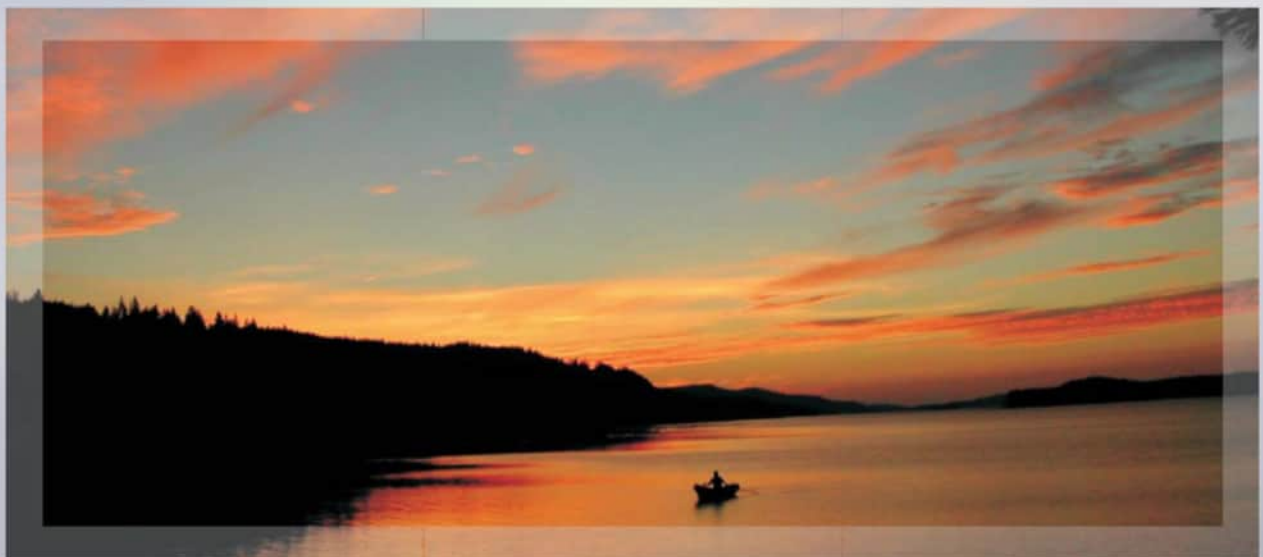
Proceedings



UNIVERSITY OF
EASTERN FINLAND

Ninth International Workshop **Nanocarbon Photonics and Optoelectronics**

4 - 9 August, 2024, Spa Hotel Rauhalampi,
Kuopio, Finland



Joensuu, 2024

University of Eastern Finland
Institute of Photonic Sciences

Proceedings

Ninth International Workshop Nanocarbon Photonics and Optoelectronics

Spa Hotel Rauhalampi, Kuopio, Finland

Editors:
Alexander Obraztsov
Zhipei Sun
Yuri Svirko

Joensuu, Finland

2024

NPO2024 Schedule-at-a Glance

| | | Sunday | Monday August 5 | Tuesday, August 6 | Wednesday August 7 | Thursday August 8 | Friday | | |
|-----------------------------------|-------|---------|--------------------|----------------------|-----------------------|----------------------|-------------------|----------------|--|
| 9 | 00-15 | | | Kaihui Liu | Hongbing Fu | Andrey Turchanin | Departure | | |
| | 15-30 | | | | | | | | |
| | 30-45 | | | | | | | | |
| | 45-00 | | | | | | | | |
| 10 | 00-15 | | | Natsuki Kanda | Ari Seitsonen | Andreas Liapis | | | |
| | 15-30 | | | Shuo Cao | Haruyuki Sakurai | Xu Cheng | | | |
| <i>Coffee Break 10:30 - 11:00</i> | | | | | | | | | |
| 11 | 00-15 | | | Opening | Misha Portnoi | Dmitry Golberg | | Andrea Ferrari | |
| | 15-30 | | | | | | | | |
| | 30-45 | | Vasili Perebeinos | Georgy Fedorov | Benedetta Bertoni | Leonas Valkunas | | | |
| | 45-00 | | | | | | | | |
| 12 | 00-15 | | Olivia Pulci | Georgy Fedorov | Maria Cojocari | Nianze Shang | | | |
| | 15-30 | | | | Patrizia Lamberti | | | | |
| <i>Lunch 12:30 - 14:30</i> | | | | | | | | | |
| 14 | 30-45 | | Maxim Shundalau | Alexander Obraztsov | Irmantas Kasalynas | Antonio Maffucci | | | |
| | 45-00 | | | | | | | | |
| 15 | 00-15 | | Radek Łapkiewicz | Sergey Malykhin | Ildiko Peter | Patrizia Lamberti | | | |
| | 15-30 | | | | | | | | |
| | 30-45 | | | Filip Steiner | Fedor Ogrin | | | | |
| | 45-00 | | | Michal Gulka | | | | | |
| <i>Coffee break 16:00 - 16:30</i> | | | | | | | | | |
| 16 | 30-45 | Arrival | Fiorenzo Vetrone | Fedor Jelezko | Junji Yumoto | Kuniaki Konishi | | | |
| | 45-00 | | | | | | | | |
| 17 | 00-15 | | | Marijonas Tutkus | Petr Cigler | Ladislau Matekovits | Peter Kazansky | | |
| | 15-30 | | | | | | | | |
| | 30-45 | | | | | Maria Cojocari | | | |
| | 45-00 | | | | | | | | |
| <i>Dinner 18:00 - 19:30</i> | | | | | | | | | |
| 19 | 30 | | | Kallavesi cruise | Smoke sauna | Poster Session | NPO2024 Reception | | |
| 21 | 30 | | | | | | | | |

Legend: FLORIN QUANTERA PREIN TERASSA CHARTIST

Workshop Co-Chairs

Alexander Obraztsov, University of Eastern Finland, Finland

Zhipai Sun, Aalto University University, Finland

Yuri Svirko, University of Eastern Finland, Finland

Program Committee

Polina Kuzhir, University of Eastern Finland, Finland

Alexander Obraztsov, University of Eastern Finland, Finland

Yuri Svirko, University of Eastern Finland, Finland

Organizing Committee

Polina Kuzhir, University of Eastern Finland, Finland

Yuri Svirko, University of Eastern Finland, Finland

NPO2024 Sponsor Organisations



Welcome to NPO2024

We are pleased to welcome you to the 9th International Workshop on Nanocarbon Photonics and Optoelectronics (NPO2024) that continues a series of meetings organized by the University of Eastern Finland. Since 2008, NPO Workshops have been bringing together research leaders from both academia and industry to discuss the latest achievements in this rapidly developing area of modern physics and nanotechnology with focus on carbon nanomaterials. We hope that you will enjoy both the scientific and the social program of NPO2024.

We invite all participants to contribute to a special issue of Nanotechnology (IOP Publishing) dedicated to the NPO2024. IOP Publishing also introduced cash prizes for the best poster presentations. Guest Editors of the special issue are Alexander Obraztsov and Yuri Svirko.

Despite ongoing turbulence NPO2024 has attracted seventy researchers and students from around the globe. We are very grateful to all participants for taking part in the Workshop. We also thank our sponsors for their financial backing, which has allowed us to support our lecturers.

We hope that the NPO2024 will expand on the success of previous Workshops, while the magnificent scenery will allow all participants to enjoy the beauty of the Finnish Lakeland.

Alexander Obraztsov
Zhipei Sun
Yuri Svirko
NPO2024 Co-Chairs

Contents

| | |
|---|-----------|
| Monday, August 5 | 1 |
| 11:15-12:00 Many-body effects on linear and nonlinear optical properties of low dimensional materials Vasili Perebeinos, <i>Electrical Engineering Department, University at Buffalo, Buffalo, New York, USA</i> | 3 |
| 12:00-12:30 Moiré-induced Dirac cones replicas and minigaps opening in graphene/hBN superlattices Simone Brozzesi ¹ , Alberto Zobelli ¹ , Maurizia Palumbo ^{1,2} , Olivia Pulci ¹ , <i>Department of Physics, University of Rome Tor Vergata, Rome, Italy</i> , <i>Université Paris-Saclay, CNRS, Laboratoire de Physique des Solides, Orsay, France</i> | 4 |
| 14:30-15:15 THz, Raman, and fluorescence characterization of a weak-bound complex of hBN and trans-stilbene Ivan Halimski ¹ , Daniil Pashnev ^{1,2} , Martynas Talaikis ¹ , Andrej Dementjev ¹ , Renata Karpicz ¹ , Irmantas Kašalynas ¹ , Andžej Urbanovič ^{1,2} , Patrizia Lamberti ³ , Maksim Shundalau ³ , <i>Center for Physical Sciences and Technology, Saulėtekio Av. 3, Vilnius, LT-10257, Lithuania</i> , <i>Teravil Ltd., Saulėtekio Av. 3, Vilnius, LT-10257, Lithuania</i> , <i>University of Salerno, via Giovanni Paolo II 132, Fisciano (SA), Italy</i> | 5 |
| 15:15-16:00 Three-dimensional fluctuation-based super-resolution bioimaging Alexander Krupinski-Ptaszek ¹ , Paweł Szczypkowski ¹ , Adrian Makowski ^{1,2} , Aleksandra Mielnicka ³ , Monika Pawłowska ¹ , Ron Tenne ⁴ , Radek Lapkiewicz ¹ , <i>Institute of Experimental Physics, Faculty of Physics, University of Warsaw, Pasteura 5, Warsaw 02-093, Poland</i> , <i>Laboratoire Kastler Brossel, ENS-PSL Universite, CNRS, Sorbonne Universite, College de France, 24 rue Lhomond, Paris 75005, France</i> , <i>The Nencki Institute of Experimental Biology, PAS, 02-093 Warsaw, Poland</i> , <i>Department of Physics, University of Konstanz, Universitätsstraße 10, D-78457 Konstanz, Germany</i> | 6 |
| 16:30-17:15 Luminescent rare Earth doped nanoparticles – light based theranostics Fiorenzo Vetrone, <i>Institut National de la Recherche Scientifique (INRS), Centre Énergie, Matériaux et Télécommunications, Université du Québec, Varennes (Montréal), QC, Canada</i> | 7 |
| 17:15-17:45 Super-resolution microscopy system for single-molecule tracking, including hardware and software, designed for bench-top use Marijonas Tutkus ^{1,2} , Mohammad Nour Alsamsam ^{1,2} , Aurimas Kopustas ^{1,2} , Meda Jureviciute ¹ , Juste Paksaite ¹ , <i>Vilnius University, Life Sciences Center, Institute of Biotechnology, Vilnius, Lithuania</i> , <i>Center For Physical Sciences And Technology, Vilnius, Lithuania</i> | 8 |
| 17:45-18:00 Stability of Graphene/Carbon/Boron nitride quantum dots and doxorubicin aggregates evaluated by optical methods Katsiaryna Chernyakova, Martynas Zaleckas, Yaraslau Padrez, Lena Golubewa, Giedrė Grincienė, Renata Karpicz, <i>Center for Physical Sciences and Technology, Saulėtekio Ave. 3, LT-10257 Vilnius, Lithuania</i> | 9 |
| Tuesday, August 6 | 11 |

| | | |
|----------------------------|---|-----------|
| 9:00-9:45 | Optical crystals of 2D materials Kaihui Liu, <i>School of Physics, Peking University, Beijing 100871, China</i> | 13 |
| 9:45-10:15 | Ultrafast spectroscopy of a Dirac semimetal Cd₃As₂ driven by intense multi-terahertz pulses Natsuki Kanda ^{1,2} , Yuta Murotani ² , Ryusuke Matsunaga ² , ¹ <i>Ultrafast Coherent Soft X-ray Photonics Research Team, RIKEN Center for Advanced Photonics, RIKEN, 2-1 Hirosawa, Wako, Saitama 351-0198, Japan</i> , ² <i>The Institute for Solid State Physics, The University of Tokyo, 5-1-5 Kashiwanoha, Kashiwa, Chiba 277-8581, Japan</i> | 14 |
| 10:15-10:30 | he dispersion energy strength of van der Waals interaction of the two-dimensional stacked structures Shuo Cao, Wen Liu, Changcheng Xu, Shaofeng Wang, Qing Wang, Jianjun Sun, Yong Ding, <i>School of Physics, Liaoning University, Shenyang, P.R. China</i> | 15 |
| 11:00-11:45 | Optical properties and terahertz applications of one-dimensional nanocarbons R. R. Hartmann ¹ , M. E. Portnoi ² , ¹ <i>Physics Department, De La Salle University, 2401 Taft Avenue, 0922 Manila, Philippines</i> , ² <i>Physics and Astronomy, University of Exeter, Stocker Road, Exeter EX4 4QL, United Kingdom</i> | 16 |
| 11:45-12:30 | Terahertz emission form optically pumped carbon nanotube films G. Fedorov ¹ , A. Saushin ¹ , D. Pashnev ² , I. Kašalynas ² , P. Kuzhir ¹ , M. Portnoi ³ , ¹ <i>Department of Physics and Mathematics, Center of Photonic Sciences, University of Eastern Finland, Yliopistokatu 7, FI-80101 Joensuu, Finland</i> , ² <i>Department of Optoelectronics, Center for Physical Sciences and Technology (FTMC), Saulėtekio av. 3, LT-10257 Vilnius, Lithuania</i> , ³ <i>Physics and Astronomy, University of Exeter, Stocker Road, Exeter EX4 4QL, United Kingdom</i> | 17 |
| 14:30-15:15 | Single crystal diamond needles fabrication, characterization and application Alexander N. Obraztsov, <i>University of Eastern Finland, Joensuu 80101, Finland</i> | 18 |
| 15:15-15:30 | Fluorescent diamond needles in research and applications Sergei Malykhin, <i>Department of Physics and Mathematics, University of Eastern Finland, Joensuu, Finland</i> | 19 |
| 15:30-15:45 | Engineering the Surface of Nanodiamonds for Applications in Quantum Biosensing Filip Steiner ^{1,2} , Jakub Čopák ^{1,2} , Michal Gulka ¹ , Petr Cígler ¹ , ¹ <i>Institute of Organic Chemistry and Biochemistry, of the CAS, Prague, Czechia</i> , ² <i>Department of Physical and Macromolecular Chemistry, Faculty of Science, Charles University, Prague, Czechia</i> | 20 |
| 15:45-16:00 | Surface optimization of nanodiamonds using non-thermal plasma Michal Gulka ¹ , Priyadharshini Balasubramanian ² , Ekaterina Shagieva ³ , Jakub Copak ^{1,4} , Josef Khun ⁵ , Vladimir Scholtz ⁵ , Fedor Jelezko ² , Stepan Stehlik ³ , Petr Cigler ¹ , ¹ <i>Institute of Organic Chemistry and Biochemistry, of the CAS, Flemingovo nam. 2, Prague, Czechia</i> , ² <i>Institute of Quantum Optics, Ulm University, Ulm 89081, Germany</i> , ³ <i>Institute of Physics of the Czech Academy of Sciences, Cukrovarnická 10, 162 00 Prague 6, Czechia</i> , ⁴ <i>Department of Physical and Macromolecular Chemistry, Faculty of Science, Charles University in Prague, Czechia</i> , ⁵ <i>Department of Physics and Measurements, University of Chemistry and Technology in Prague, Czechia</i> | 21 |
| 16:30-17:15 | Diamond based quantum sensors Fedor Jelezko, <i>Institute of quantum optics, Ulm University, Germany</i> | 22 |
| 17:15-18:00 | On the optimal chemical interface of diamond for quantum biosensing Petr Cigler, <i>Institute of Organic Chemistry and Biochemistry, of the CAS, Flemingovo nam. 2, Prague, Czechia</i> | 23 |
| Wednesday, August 7 | | 25 |
| 17:30-18:00 | Realization of exciton-mediated optical spin-orbit interaction in organic microcrystalline resonators for circularly polarized electroluminescence Hongbing Fu, <i>Department of Chemistry, Capital Normal University, Beijing, 100048, P. R. China</i> | 27 |

| | | |
|-----------------------|--|-----------|
| 9:45-10:15 | Growth of two dimensional h-BN: Influence of the support on the electronic and optical properties Adrian Hemmi ¹ , Ari Paavo Seitsonen ² , Michael S. Altman ³ , Marcella Iannuzzi ⁴ , Thomas Greber ¹ , Huanyao Cun ¹ , ¹ Physik-Institut der Universität Zürich, Switzerland, ² Département de Chimie École Normale Supérieure, Paris, France, ³ Department of Physics, Hong Kong University of Science and Technology, Hong Kong, ⁴ Chemie-Institut der Universität Zürich, Switzerland | 28 |
| 10:15-10:30 | Terahertz meta-optics made with ultrashort pulse laser processing Haruyuki Sakurai, Kuniaki Konishi, <i>Institute for Photon Science and Technology, The University of Tokyo</i> | 29 |
| 11:00-11:45 | Optoelectronic and optomechanical properties of atomically thin inorganic nanosheets as revealed by in situ TEM Chao Zhang, Dmitri Golberg, <i>Centre for Materials Science and School of Chemistry and Physics, Queensland University of Technology (QUT), 2 George, Brisbane, QLD 4000, Australia</i> | 30 |
| 11:45-12:30 | Nanocarbon materials for sub-THz thermomechanical bolometry B. Bertoni ^{1,2} , L. Alborghetti ¹ , M. Cojocari ³ , L. Vicarelli ¹ , A. Tredicucci ^{1,2} , S. Roddaro ^{1,2} , S. Zanotto ² , G. Fedorov ³ , P. Kuzhir ³ , P. Lamberti ⁴ , A. Pitanti ^{1,2} , ¹ Dipartimento di Fisica, Università di Pisa, Largo B. Pontecorvo 3, 56127 Pisa – Italy, ² CNR – Istituto Nanoscienze, piazza San Silvestro 12, 56127 Pisa – Italy, ³ Department of Physics and Mathematics, Center of Photonic Sciences, University of Eastern Finland, Yliopistokatu 7, FI-80101 Joensuu - Finland, ⁴ Department of Information and Electrical Eng. and Applied Math., University of Salerno, via Giovanni Paolo II 132, Fisciano (SA) – Italy | 31 |
| 15:15-15:45 | Electro-optical terahertz modulators based on gallium nitride semiconductors Irmantas Kašalynas, Daniil Pashnev, Justinas Jorudas, Surya Revanth Ayyagari, Vytautas Janonis, Maxim Moscotin, Muhammad Sheraz, Liudvikas Subačius, <i>THz Photonics Laboratory, Center for Physical Sciences and Technology (FTMC), Saulėtekio av. 3, LT-10257 Vilnius, Lithuania</i> | 32 |
| 15:30-16:00 | Investigation of nanostructured TiO₂ Ildiko Peter, Gabriela Strnad, <i>George Emil Palade University of Medicine, Pharmacy, Science, and Technology of Targu Mures Faculty of Engineering and Information Technology Department of Industrial Engineering and Management Str. N. Iorga nr. 1, Târgu-Mureș, 540139, Romania</i> | 33 |
| 15:30-16:00 | 3D FDTD-LLG modelling of magnetisation dynamics in thin film ferromagnetic structures Feodor Y. Ogrin, <i>MaxLLG Ltd. Exeter, United Kingdom</i> | 34 |
| 16:30-17:15 | 3D-printed low-loss functional hollow waveguide devices for 200-400 GHz band Junji Yumoto, <i>Institute for Photon Science and Technology, The University of Tokyo, Japan</i> | 35 |
| 17:15-17:45 | Experimental activities on graphene in the sub-THz range G. Virone ¹ , F. Paonessa ¹ , M. U. Riaz ^{1,4} , G. V. Bianco ² , G. Bruno ² , A. D’Orazio ³ , L. Matekovits ^{1,4} , ¹ Consiglio Nazionale delle Ricerche, IEIIT, C.so Duca degli Abruzzi 24, 10129, Turin, Italy, ² Consiglio Nazionale delle Ricerche, NANOTEC, via Orabona, 4, 70125 Bari, Italy, ³ Politecnico di Bari, Dipartimento di Ingegneria Elettrica e dell’Informazione, Via Orabona 4, 70125 Bari, Italy, ⁴ Politecnico di Torino, DET, C.so Duca degli Abruzzi, 24 - 10129 Turin, Italy | 36 |
| 17:30-18:00 | High-Q Factor Dual-Layer Anapole Metamaterial for sub-THz range M. Cojocari ¹ , G. Matveev ¹ , L. Matekovits ² , Gianluca Dassano ² , P. Kuzhir ¹ , A. Basharin ¹ , ¹ Center for Photonics Sciences, Department of Physics and Mathematics, University of Eastern Finland, Yliopistonkatu, 80140, Joensuu, Finland ¹ Department of Electronics and Telecommunications, Politecnico di Torino, Corso Duca degli Abruzzi 24, 10129, Turin, Italy | 37 |
| Poster session | | 39 |

| | | |
|------|---|----|
| P.1 | Integration of 2D materials in suspended MEMS devices B. Bertoni ^{1,2} , L. Alborghetti ¹ , S. Zanotto ² , L. Vicarelli ¹ , A. Tredicucci ¹ , S. Roddaro ^{1,2} , A. Pitanti ¹ , ¹ <i>Dipartimento di Fisica, Università di Pisa, Largo B. Pontecorvo 3, 56127 Pisa – Italy</i> , ² <i>CNR – Istituto Nanoscienze, piazza San Silvestro 12, 56127 Pisa – Italy</i> | 41 |
| P.2 | Amorphous carbon nanoparticles obtained from anodic alumina/carbon composites Katsiaryna Chernyakova, Giedrė Grincienė, Renata Karpicz, <i>State Research Institute Center for Physical Sciences and Technology, Saulėtekio Ave. 3, LT-10257 Vilnius, Lithuania</i> | 42 |
| P.3 | Fabrication and characterization of THz metalens by ultraviolet femtosecond laser ablation Y. Hakamada ¹ , M. Matoba ² , H. Sakurai ² , K. Konishi ² , ¹ <i>Dept. of Phys, Univ. of Tokyo/ 7-3-1 Hongo, Bunkyo-ku, Tokyo, Japan 113-0033</i> , ² <i>nstitute for Photon Science and Technology, Univ. of Tokyo / 7-3-1 Hongo, Bunkyo-ku, Tokyo, Japan 113-0033</i> | 43 |
| P.4 | Fluorescence concentration quenching in Zinc-containing as well as non-containing phthalocyanines Ivan Halimski ¹ , Simona Streckaitė ¹ , Jevgenij Chmeliov ^{1,2} , Andrius Gelzinis ^{1,2} , Leonas Valkunas ¹ , ¹ <i>Center for Physical Sciences and Technology, Saulėtekio Ave. 3, Vilnius, LT-10257, Lithuania</i> , ² <i>Institute of Chemical Physics, Faculty of Physics, Vilnius University, Saulėtekio Ave. 9-III, Vilnius, LT-10222, Lithuania</i> | 44 |
| P.5 | Time-resolved phase imaging of femtosecond laser-induced air plasma with high spatial resolution Wataru Kimura, Shotaro Kawano, Ryohei Yamada, Haruyuki Sakurai, Kuniaki Konishi, Norikatsu Mio, <i>Graduate School of Science, The University of Tokyo, 7-3-1 Hongo, Bunkyo-ku, Tokyo 113-0033, Japan</i> | 45 |
| P.6 | Designing Bull’s eye structures for non-destructive inspection using GHz waves and carbon nanotube film Masakazu Konishi ¹ , Hiroki Okawa ² , Shun Hashiyada ³ , Yuto Matsuzaki ¹ , Qi Zhang ¹ , Kou Li ¹ , Yoshito Tanaka ¹ , Yukio Kawano ^{1,2,4} , ¹ <i>Department of Science and Engineering, Chuo University, 1-13-27 Kasuga, Bunkyo, Tokyo, Japan</i> , ² <i>Kanagawa Institute of Science and Technology, 705-1, Shimo-Imaizumi, Ebina, Kanagawa, Japan</i> , ³ <i>Research Institute for Electronic Science, Hokkaido University, Kita21, Nishi 10, Kita-ku, Sapporo, Hokkaido, Japan</i> ⁴ <i>National Institute of Informatics, 2-1-2 Hitotsubashi, Chiyoda, Tokyo, Japan</i> | 46 |
| P.7 | Fundamental limits to metalens critical dimensions N. Kossowski ¹ , E. Marinov ¹ , S. Khadir ¹ , P. Genevet ² , ¹ <i>Univeristé Côte d’Azur, CNRS-CRHEA, Rue Bernard Gregory, Valbonne, 06650, France</i> , ² <i>Physics department, Colorado School of Mines, 1523 Illinois Street, Golden, CO, 80401, USA</i> | 47 |
| P.8 | CNT film photo scanner for in-line pharma agent pills imaging in infrared–terahertz bands Miki Kubota ¹ , Yuya Kinoshita ¹ , Yuto Matsuzaki ¹ , Minami Yamamoto ¹ , Leo Takai ¹ , Yukio Kawano ^{1,2,3} , Kou Li ¹ , ¹ <i>Chuo University, 1-13-27 Kasuga, Bunkyo-ku, Tokyo, 112-8551, Japan</i> , ² <i>National Institute of Informatics, 2-1-2 Hitotsubashi, Chiyoda-ku, Tokyo, 101-8430, Japan</i> , ³ <i>Kanagawa institute of Industrial Science and Technology, 3-2-1, Sakado, Takatsu-ku, Kawasaki-shi, Kanagawa, 213-0012, Japan</i> | 48 |
| P.9 | Optical and spin properties of color centers in diamond needles Sergei Malykhin, Mariam Quarshie, Bo Xu, Elena Filonenko, <i>Department of Physics and Mathematics, University of Eastern Finland, Joensuu, Finland</i> | 49 |
| P.10 | Detection of dark plasmon modes of a single gold rod by radially polarized terahertz pulses Mizuho Matoba, Kuniaki Konishi, Norikatsu Mio, Junji Yumoto, Makoto Kuwata-Gonokami, <i>The University of Tokyo, 7-3-1 Hongo, Bunkyo-ku, Tokyo, Japan</i> | 50 |
| P.11 | Terahertz detection with optically gated vertical graphene nanowalls P. A. Obratsov ¹ , V. Papadakis ² , Y. Svirko ¹ , A. N. Obratsov ¹ , ¹ <i>Institute of Photonic Sciences,</i> | |

| | | |
|---------------------------|--|-----------|
| | <i>University of Eastern Finland, 80101 Joensuu, Finland, ²XpectralTEK, Av. da Igreja 7, 4705-732 Braga, Portugal</i> | 51 |
| P.12 | Physical and chemical composition optimization of CNT imagers for augmented reality non-destructive inspections Ryoga Odawara ¹ , Minami Yamamoto ¹ , Yukio Kawano ^{1,2,3} , Yoshihiro Watanabe ⁴ , Kou Li ¹ , ¹ Faculty of Science and Engineering, Chuo University, Tokyo, 112-8551, Japan, ² National Institute of Informatics, Tokyo, 101-8430, Japan, ³ Kanagawa institute of Industrial Science and Technology, 3-2-1, Sakado, Takatsu-ku, Kawasaki-shi, Kanagawa, 213-0012, Japan, ⁴ School of Engineering, Tokyo Institute of Technology, Tokyo, 152-8550, Japan | 52 |
| P.13 | Bound-state-In-the-Continuum effect in complementary metamaterial Anar Ospanova ¹ , Ladislau Matekovits ² , Alexey Basharin ¹ , ¹ Center of Photonics Sciences, University of Eastern Finland, Joensuu, Finland, ² Department of Electronics and Telecommunications, Politecnico di Torino, Torino, Italy | 53 |
| P.14 | Two-dimensional high-yield printable integration of carbon nanotube photo-thermal pixels for realtime, large-area, and broadband non-destructive testing camera applications Leo Takai ¹ , Yuto Matsuzaki ¹ , Minami Yamamoto ¹ , Yukio Kawano ^{1,2,3} , Kou Li ¹ , ¹ Chuo University, 1-13-27 Kasuga, Bunkyo-ku, Tokyo, 112-8551, Japan, ² National Institute of Informatics, 2-1-2 Hitotsubashi, Chiyoda-ku, Tokyo, 101-8430, Japan, ³ Kanagawa institute of Industrial Science and Technology, 3-2-1, Sakado, Takatsu-ku, Kawasaki-shi, Kanagawa, 213-0012, Japan | 54 |
| Thursday, August 8 | | 55 |
| 9:00-9:45 | Tailored growth of transition metal dichalcogenides monolayers for photonics and optoelectronics Andrey Turchanin, Friedrich Schiller University Jena, Jena, Germany | 57 |
| 9:45-10:15 | High-performance reconstructive spectrometers with van der Waals junctions Andreas C. Liapis ¹ , Faisal Ahmed ¹ , Md Gius Uddin ¹ , Yawei Dai ¹ , Xiaoqi Cui ¹ , Fedor Nigmatulin ¹ , Hoon Hahn Yoon ² , and Zhipei Sun ¹ , ¹ QTF Centre of Excellence, Department of Electronics and Nanoengineering, Aalto University, Finland, ² School of Electrical Engineering and Computer Science, Gwangju Institute of Science and Technology, Korea | 58 |
| 10:15-10:30 | Layered MoS2 for the enhancement of supercontinuum generation in photonic crystal fiber Xu Cheng ^{1,2} , Jin Xie ³ , Guodong Xue ³ , Hao Hong ³ , Zhipei Sun ² , Kaihui Liu ³ , Zhongfan Liu ^{4,5} , ¹ Group for Fibre Optics, École Polytechnique Fédérale de Lausanne (EPFL), Lausanne, Switzerland, ² QTF Center of Excellence, Department of Electronics and Nanoengineering, Aalto University, Espoo, Finland, ³ State Key Laboratory for Mesoscopic Physics, School of Physics, Peking University, Beijing, China, ⁴ Center for Nanochemistry, College of Chemistry and Molecular Engineering, Peking University, Beijing, China, ⁵ Beijing Graphene Institute (BGI), Beijing, China | 59 |
| 11:00-11:45 | Layered materials as a platform for quantum technologies Andrea C. Ferrari, University of Cambridge, UK | 60 |
| 11:45-12:15 | Relaxation pathways of excitations in semiconducting carbon nanotubes Leonas Valkunas, Department of Molecular Compounds Physics, Center for Physical Sciences and Technology, Suletekiu Ave. 3, 10257, Vilnius, Lithuania | 61 |
| 12:15-12:30 | Evidence of abnormal hot carrier thermalization at van Hove singularities of twisted bilayer graphene Nianze Shang ^{1,2} , Zhipei Sun ¹ , Kaihui Liu ² , Hao Hong ² , ¹ QTF Centre of Excellence, Department of Electronics and Nanoengineering, Aalto University, Espoo, Finland, ² State Key Laboratory for Mesoscopic Physics, School of Physics, Peking University, Beijing, China | 62 |

| | | |
|-------------|---|-----------|
| 14:30-15:15 | Electro-thermal and electromagnetic response of industrial-grade graphene materials based on quantum effects Antonio Maffucci, <i>Department of Electrical and Information Engineering, University of Cassino and Southern Lazio, Cassino, Italy</i> | 63 |
| 15:15-16:00 | Numerical modeling of cell membrane electromagnetic behaviour and nanoparticles interaction Patrizia Lamberti ¹ , Silvana Morello ² , Patrizia Gazzero ² , Elisabetta Sieni ³ , Maksim Shundalau ¹ , Vincenzo Tucci ¹ , ¹ <i>Department of Information and Electrical Eng. and Applied Math., University of Salerno, via Giovanni Paolo II 132, Fisciano (SA) – ITALY</i> , ² <i>Department of Pharmacy, University of Salerno, via Giovanni Paolo II 132, Fisciano (SA) – ITALY</i> , ³ <i>Department of Theoretical and Applied Science, University of Insubria, Varese, ITALY</i> . . . | 64 |
| 16:30-17:15 | High-precision observation and simulation of femtosecond laser ablation Kuniaki Konishi, <i>Institute for Photon Science and Technology, The University of Tokyo, Japan</i> | 65 |
| 17:15-18:00 | Recent advances in ultrafast laser nanostructuring of transparent materials P.G. Kazansky ¹ , Y. Lei ¹ , H. Wang ¹ , S. Shevtsov ¹ , M. Shribak ² , Y. Svirko ³ , ¹ <i>University of Southampton, Southampton, UK</i> , ² <i>University of Chicago and Marine Biological Laboratory, Woods Hole, USA</i> , ³ <i>Department of Physics and Mathematics, University of Eastern Finland, Joensuu, Finland</i> | 66 |
| | Author index | 67 |

Monday, August 5



©P.Obraztsov

Many-body effects on linear and nonlinear optical properties of low dimensional materials

Vasili Perebeinos

Electrical Engineering Department, University at Buffalo, Buffalo, New York, USA

E-mail: vasilipe@buffalo.edu

Atomically thin two-dimensional materials are direct bandgap semiconductors with a rich interplay of the valley and spin degrees of freedom, which offer the potential for electronics and optoelectronics. A strong Coulomb interaction leads to tightly bound electron-hole pairs or excitons and two-electron one-hole quasiparticles or trions. We solve the two-particle and three-particle problems for the wavefunctions for excitons and trions in the basis set of the model-Hamiltonian for single particles. The calculated linear and nonlinear absorptions, photoluminescence spectra, and polariton spectra as a function of doping and temperature explain the experimental data in 2D monolayers and predict novel spectroscopic features due to the many-body Coulomb interactions [1-5]. Exciton lifetime plays a crucial role in optoelectronic applications. I will also discuss the phonon-assisted Auger non-radiative decay mechanism of excitons in doped 2D materials. This material is based upon work supported by the Air Force Office of Scientific Research under award number FA9550-22-1-0312.

- [1] Y. V. Zhumagulov, A. Vagov, D. R. Gulevich, V. Perebeinos
Electrostatic and Environmental Control of the Trion Fine Structure in Transition Metal Dichalcogenide Monolayers
Nanomaterials 12, 3728 (2022)
- [2] V. D. Neverov, A. E. Lukyanov, Y. V. Zhumagulov, D. R. Gulevich, A. V. Krasavin, A. Vagov, V. Perebeinos
Non-linear spectroscopy of excitonic states in transition metal dichalcogenides
Phys. Rev. B 105, 239902 (2022)
- [3] Y. V. Zhumagulov, S. Chiavazzo, D. R. Gulevich, V. Perebeinos, I. A. Shelykh, O. Kyriienko
Microscopic theory of exciton and trion polaritons in doped monolayers of transition metal dichalcogenides
npj Comput Mater 8, 92 (2022)
- [4] Y.V. Zhumagulov, A. Vagov, N.Y. Senkevich, D.R. Gulevich, V. Perebeinos
Three-particle states and brightening of intervalley excitons in a doped MoS2 monolayer
Phys. Rev. B 101, 245433 (2020)
- [5] Y.V. Zhumagulov, A. Vagov, P.F. Junior, D.R. Gulevich, V. Perebeinos
Trion induced photoluminescence of a doped MoS2 monolayer
J. Phys. Chem. 153, 044132 (2020)

Moiré-induced Dirac cones replicas and minigaps opening in graphene/hBN superlattices

Simone Brozzesi¹, Alberto Zobelli², Maurizia Palumbo¹, Olivia Pulci¹

¹Department of Physics, University of Rome Tor Vergata, Rome, Italy

²Université Paris-Saclay, CNRS, Laboratoire de Physique des Solides, Orsay, France

Corresponding author: olivia.pulci@roma2.infn.it

Moiré pattern is a novel and extensive structure that emerges from the interference of multiple periodic templates. In condensed-matter physics, moiré patterns, also known as moiré superlattices, can be created by stacking two or more two-dimensional (2D) layered materials with a small twist angle and/or a slight lattice mismatch. The presence of moiré pattern results in the formation of a long range moiré potential, which interacts with the electrons of the system and affects the dispersion of the energy levels. In recent years, moiré superlattices have garnered significant attention due to their remarkable manifestation of previously unexplored phenomena and unique functionalities [1], like strongly correlated phases [2] and subsequent observation of superconductivity and topological states [3], and exotic excitonic states [4] arising from the interaction between excitons and moiré potential. The aim of this study is to demonstrate that the existence of a moiré pattern in a graphene/hBN heterostructure has a substantial influence on the energy levels dispersion of the system. In particular, there is the intention to show that this influence goes beyond the coupling between the planes and the rehybridization of levels that can be expected in van der Waals heterostructures, but significantly affects the energy levels dispersion of graphene within an energy range inside the hBN gap, where only contributions from C atoms are expected to be present. By means of DFT calculation based on a localized basis set approach, this study demonstrates that the presence of the long range moiré potential results in the formation of six replicas [5] of the graphene Dirac cones around the K-K' point of the 1BZ of graphene, which are separated by a reciprocal space superlattice vector G_m from the main cone. The intersection between the main cone and its replicas result in the opening of minigaps in the energy levels of graphene, without the direct interplay of the interaction with the hBN states. The relative positions of these minigaps is dependent on the moiré reconstruction of the system and can be tailored by tuning the rotation angle between the layers.

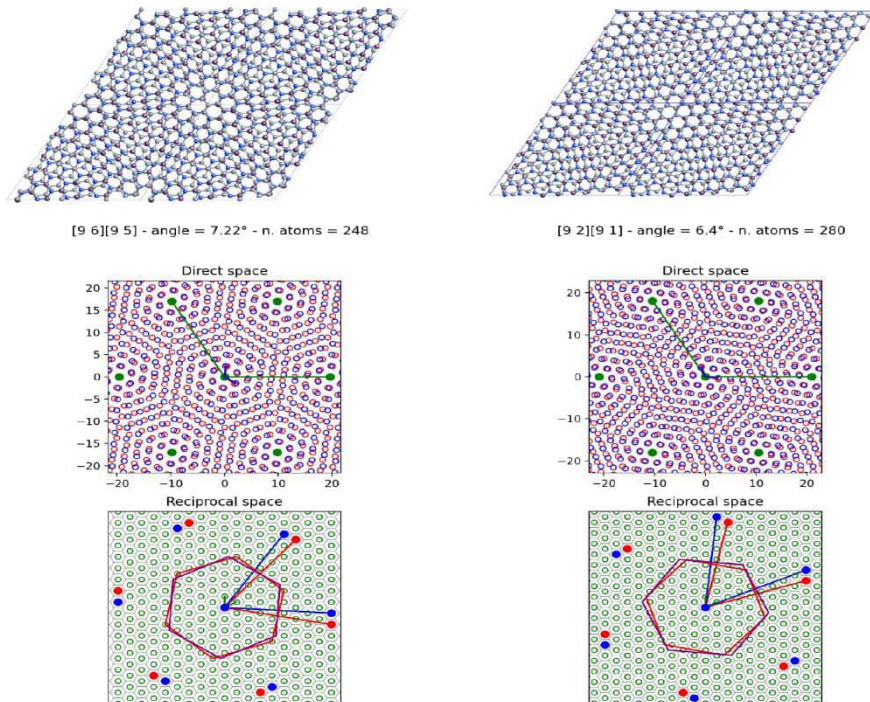
[1] Lifu Zhang, Ruihao Ni, and You Zhou, Journal of Applied Physics 133.8 (2023)

[2] Yuan Cao et al., Nature 556.7699 (2018), pp. 80–84

[3] Yuan Cao et al., Nature 556.7699 (2018), pp. 43–50

[4] Yuan Cao et al., Science advances 3.11 (2017), e1701696

[5] Ivo Pletikosić et al., Physical review letters 102.5 (2009), p. 0568088



THz, Raman, and fluorescence characterization of a weak-bound complex of *h*BN and *trans*-stilbene

Ivan Halimski¹, Daniil Pashnev^{1,2}, Martynas Talaikis¹, Andrej Dementjev¹, Renata Karpicz¹, Irmantas Kašalynas¹, Andžej Urbanovič^{1,2}, Patrizia Lamberti³, Maksim Shundalau³

¹Center for Physical Sciences and Technology, Saulėtekio Av. 3, Vilnius, LT-10257, Lithuania

²"Teravil" Ltd., Saulėtekio Av. 3, Vilnius, LT-10257, Lithuania

³University of Salerno, via Giovanni Paolo II 132, Fisciano (SA), Italy
mshundalau@unisa.it

1. Introduction

Hexagonal boron nitride (*h*BN) nanosheet is a 2D material, which is structural and isoelectronic analogue of graphene, but in contrast to the latter, *h*BN is an electrical insulator and does not absorb in the visible region [1]. Ultra-thin *h*BN is successfully applied as the dielectric layer in field effect transistors, protective cover in devices, buffer layer in film growth, etc. The properties of *h*BN nanosheets can be modified using the functionalization of their surface by molecular architectures. Non-covalent functionalization of 2D *h*BN provides a way to modify the physical properties without violating its structure. Adsorbed molecules interact with surfaces due to relatively weak van der Waals interactions. Downsizing of 2D *h*BN nanosheet allows to production of *h*BN quantum dots, which have unique photophysical properties and are biocompatible that determines their promising application in biomedicine for the diagnosis of various diseases, bioimaging and targeted drug delivery [2]. Apparently, the *h*BN surface can form π - π staggered stacking interactions with organic molecules containing aromatic rings. Both problems mentioned require an understanding of the strength of interaction and its manifestations in different spectral ranges and techniques including IR, Raman, and fluorescence (FL) spectra. The THz range has unique features because low-frequency deformation vibrations of fragments of complex relatively each other that characterize their weak interaction, manifest namely in the THz range. The *trans*-stilbene (TST) molecule serves as a suitable simple candidate to reveal the features of the formation of the *h*BN surface complexes with organic molecules using spectroscopic and theoretical methods.

2. Experimental

The TST molecules were adsorbed on the *h*BN surface by solvation in chloroform and evaporation of the solvent. Then samples of pure TST, the complex of TST and *h*BN, and a mix of *h*BN and polyethylene were pressed to obtain tablets 0.8 mm thick for THz and FL measurements. The THz spectra were measured at room and liquid nitrogen temperatures in the range of 0.4–3.5 THz. The Raman spectra were measured for powder samples.

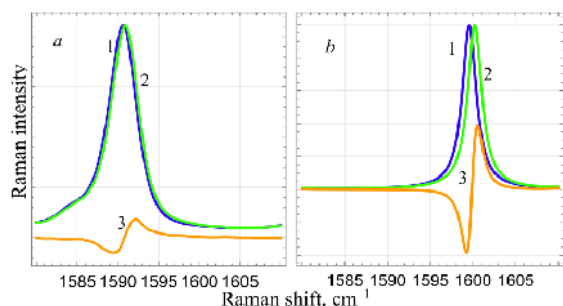


Fig. 1. Fragments of experimental (a) and theoretical (b) Raman spectra of TST (1), TST+*h*BN (2), and their difference (3).

complex demonstrates two additional weak bands at 0.7 and 1.1 THz compared to the spectrum of pure TST. These bands correspond to the librations of the TST molecules relative to the *h*BN surface. The formation of the complex also leads to a blue shift of mostly intensive Raman lines at 1639 (C=C stretching), 1591 (ring stretching), 1190 (C–ring stretching, Fig. 1), and 994 cm^{-1} (trigonal ring deformation) on $\sim 4 \text{ cm}^{-1}$. Both steady-state and time-resolved FL measurements also show the formation of the complex. The FL kinetic lifetime of the complex (0.917 ns) is shorter than pure TST (1.180 ns), but longer than pure *h*BN (0.440 ns).

5. Acknowledgements

This work was supported by Horizon 2020 RISE DiSeTCom (GA 823728) and Horizon Europe FLORIN (No. 101086142) projects.

6. References

- [1] L. Stagi, J. Ren, and P. Innocenzi, *Materials* **12** 3905 (2019).
- [2] X. Zhang, L. An, C. Bai, L. Chen, and Y. Yu, *Materials Today Chemistry* **20** 100425 (2021).

Three-dimensional fluctuation-based super-resolution bioimaging

Alexander Krupinski-Ptaszek¹, Paweł Szczypkowski¹, Adrian Makowski^{1,2}, Aleksandra Mielnicka³,
Monika Pawłowska¹, Ron Tenne⁴, Radek Lapkiewicz¹

1. *Institute of Experimental Physics, Faculty of Physics, University of Warsaw, Pasteura 5, Warsaw 02-093, Poland*
2. *Laboratoire Kastler Brossel, ENS-PSL Université, CNRS, Sorbonne Université, Collège de France, 24 rue Lhomond, Paris 75005, France*
3. *The Nencki Institute of Experimental Biology, PAS, 02-093 Warsaw, Poland*
4. *Department of Physics, University of Konstanz, Universitätsstraße 10, D-78457 Konstanz, Germany
radek.lapkiewicz@fuw.edu.pl*

Record-holding super-resolution microscopy (SRM) techniques, e.g. localization microscopy (LM) and stimulated-emission-depletion (STED) microscopy, require significant resources and effort from life-science researchers. In comparison with confocal microscopy, apart from relying on extensive sample-staining procedures and long acquisition times, applying LM for 3D and multicolor imaging poses a considerable experimental challenge. We provide a complete demonstration of an entry-level SRM technique – providing super-resolving capabilities with an experimental complexity level akin to that of confocal microscopy [1]. Exchanging the confocal pinhole with a small pixelated detector, we use the inherent fluctuations of dye molecules as contrast for SRM. This contrast is processed into a super-resolved image through a process of pixel reassignment, a robust and deterministic algorithm. Since the fluctuation contrast is ubiquitous to organic markers, it does not require engineering of the blinking statistics through the sample buffer. Together with the built-in capabilities for multi-color and 3D imaging, shown in our work [1], it can become a natural extension to confocal microscopy - a straightforward first step into the realm of SRM.

In our implementation we rely on a single photon avalanche diode (SPAD) array [2]. Its spatial resolution enables resolution enhancement through Image scanning microscopy (ISM [3]). The temporal resolution offers further improvements through the measurement of quantum [4] or classical [5] correlations in the emitted fluorescence, also extending the applications to fluorescence lifetime imaging (FLIM, [6]) and other methods based on time correlated single photon counting (TCSPC). TCSPC often requires significant measurement times, compromising spatial overlap of the color channels when sequential measurements are performed. Taking advantage of the intrinsic temporal resolution of SPADs, we utilize pulsed interleaved excitation to temporally multiplex fluorescence color channels, alleviating the need to measure one color at a time, and keeping the experimental setup simple. This enables multicolor TCSPC measurements yielding FLIM and correlation-based super-resolution, without the need for channel alignment in post processing — each position in the sample is measured simultaneously in available channels.

In the second experiment [7], we combine Super-resolution Optical Fluctuation Imaging (SOFI) [8] with temporal focusing two-photon excitation [9] – a wide-field microscopy method that is capable of excitation of a thin slice in a three-dimensional specimen. Both methods are straightforward to implement in a standard microscope, and by merging them, we obtain super-resolved 3D images of neurons stained with quantum dots. Our approach offers reduced bleaching of out-of-focus planes and an improved signal-to-background ratio that can be used when robust resolution improvement is required in thick, dense samples.

Acknowledgements

This work was supported by the Foundation for Polish Science under the FIRST TEAM project “Spatiotemporal photon correlation measurements for quantum metrology and super-resolution microscopy” co-financed by the European Union under the European Regional Development Fund (POIR.04.04.00-00-3004/17-00), by the National Science Centre, Poland, grant number 2022/47/B/ST7/03465, and Horizon Europe MSCA FLORIN project ID 101086142

References

- [1] A. Krupinski-Ptaszek et al. arXiv:2401.00261 (2023)
- [2] SPAD23 datasheet (<https://piimaging.com/product-spad23>)
- [3] C. B. Müller et al. Phys. Rev. Lett. 104, 198101 (2010)
- [4] R. Tenne et al. Nat. Photonics, 13, 116-122 (2019)
- [5] A. Sroda et al. Optica, 7, 1308-1316 (2020)
- [6] M. Costello et al. Nat. Meth. 16, 175–178 (2019)
- [7] P. Szczypkowski et al. arXiv:2402.19338 (2024)
- [8] R. Dertinger et al. Proc. National Acad. Sci. 106, 22287–22292 (2009)
- [9] D. Oron et al. Opt. Express 13, 1468–1476 (2005)

Luminescent Rare Earth Doped Nanoparticles – Light Based Theranostics

Fiorenzo Vetrone

*Institut National de la Recherche Scientifique (INRS), Centre Énergie, Matériaux et Télécommunications, Université du Québec, Varennes
(Montréal), QC, Canada
fiorenzo.vetrone@inrs.ca*

Since first reported, luminescent rare earth doped nanoparticles have attracted a great deal of interest. In the last decade, however, the field has rapidly taken off, progressing from the basic understanding of the photophysical properties governing their nanoscale luminescence, in particular upconversion, to their use in a plethora of applications, with considerable focus in biology and medicine. This interest stems primarily from the ability to stimulate these luminescent nanoparticles with near-infrared (NIR) light as well as their diverse emission wavelengths spanning the UV to the NIR. Therefore, with a single NIR excitation wavelength, it is possible to observe higher energy luminescence, known as upconversion, or single photon NIR emission (known as down-shifted luminescence). The former upconversion process proceeds through the sequential absorption of multiple NIR photons through the long-lived $4f$ electronic energy states of the tri-positive rare earth ions. As a result, upconversion is several of orders more efficient than conventional multiphoton absorption processes. This is especially interesting for applications in theranostics (**therapy + diagnostics** on the same platform) where the upconverted light can be used to trigger another light activated modality (therapy) while the NIR luminescence can be used for bioimaging and nanothermometry (diagnostics). Here, we present our work on the synthesis and development of various NIR excited (and emitting) core/shell rare earth doped nanostructures/nanoplatfoms and demonstrate how their various emissions could be harnessed for applications in biology and nanomedicine.

Super-resolution microscopy system for single-molecule tracking, including hardware and software, designed for bench-top use

Marijonas Tutkus^{1,2}, Mohammad Nour Alsamsam^{1,2}, Aurimas Kopustas^{1,2}, Meda Jureviciute¹, Juste Paksaitė¹

1 Vilnius University, Life Sciences Center, Institute of Biotechnology, Vilnius, Lithuania

2 Center For Physical Sciences And Technology, Vilnius, Lithuania

marijonas.tutkus@gmc.vu.lt, marijonas.tutkus@ftmc.lt

Fluorescence microscopy (FM), which uses molecule-specific fluorescent markers to measure and track the locations, and interactions of labelled biomolecules [1]. FM augmented with approaches such as super resolution microscopy (SRM) based on single-molecule (SM) localisation (SMLM) achieves nanometric resolution in 3D with SM sensitivity (2014 Nobel prize award) [2-4]. SMLM combined with SM tracking (SMT) reveals live-cell dynamics (e.g. diffusion) of individual biomolecules [5]. However, often the lack of user-friendly and inexpensive equipment forms a roadblock for many labs to use SMLM for their research.

In our previously published work on the miEye Bench-top super-resolution microscope system [6], we demonstrated exceptional performance using affordable equipment. This SRM systems is dedicated to SMLM technique, but also can be used to many other imaging applications such as single-molecule FRET. With this system, we achieved a lateral sample drift of approximately 10 nm over 5 minutes, while our autofocus system effectively controlled Z drift. Additionally, we achieved a ground-truth resolution of approximately 16 nm using DNA PAINT in vitro and less than 30 nm using dSTORM in fixated cells. The miEye system is an open-microscopy project, and we have made all information, including parts list, assembly guide, and software code "microEye" [7] for microscope control, data acquisition, and analysis/visualization, available as open-source [8].

In this presentation, we will unveil the latest updates to our microscope's hardware and software, which includes the installation of a dual-view emission path and 3D localization using astigmatism. We also will present results of extensive testing of various industrial-grade CMOS cameras for SMLM applications and compare them to our reference sCMOS camera performance. We will showcase our miEye system's capabilities through demonstration experiments, such as reliable tracking of HaloJF647-tagged Kinesin molecules in living eukaryotic cells on fluorescently labelled microtubules (while super-resolving and tracking microtubule network dynamics), highlighting the applicability our system. Our presentation will cover advancements in our SRM system and its use in exploring biological systems using SMLM and SMT techniques [9-10].

3. Acknowledgement.

This work was supported by European Regional Development Fund under grant agreement number 01.2.2-CPVA-V-716-01-0001 with the Lithuanian Central Project Management Agency (CPVA) for M.T and Horizon Europe HORIZON-MSCA-2021-SE-01 project FLORIN Grant agreement ID: 101086142. for M.T.

4. References

- [1] Brückner, D. B.; Chen, H.; Barinov, L.; Zoller, B.; Gregor, T. Stochastic Motion and Transcriptional Dynamics of Pairs of Distal DNA Loci on a Compacted Chromosome. *Science* 2023, 380 (6652), 1357–1362. <https://doi.org/10.1126/science.adf5568>
- [2] Hell, S. W. Nanoscopy with Focused Light (Nobel Lecture). *Angew. Chem. Int. Ed Engl.* 2015, 54 (28), 8054–8066. <https://doi.org/10.1002/anie.201504181>
- [3] Betzig, E. Single Molecules, Cells, and Super-Resolution Optics (Nobel Lecture). *Angew. Chem. Int. Ed Engl.* 2015, 54 (28), 8034–8053. <https://doi.org/10.1002/anie.201501003>
- [4] Moerner, W. E. W. E. Single-Molecule Spectroscopy, Imaging, and Photocontrol: Foundations for Super-Resolution Microscopy (Nobel Lecture). *Angew. Chem. Int. Ed Engl.* 2015, 54 (28), 8067–8093. <https://doi.org/10.1002/anie.201501949>
- [5] Cognet, L.; Leduc, C.; Lounis, B. Advances in Live-Cell Single-Particle Tracking and Dynamic Super-Resolution Imaging. *Curr. Opin. Chem. Biol.* 2014, 20, 78–85.
- [6] Alsamsam, M. N.; Kopūstas, A.; Jurevičiūtė, M.; Tutkus, M. The miEye: Bench-Top Super-Resolution Microscope with Cost-Effective Equipment. *HardwareX* 2022, 12, e00368. <https://doi.org/10.1016/j.ohx.2022.e00368>
- [7] <https://github.com/samhitech/microEye>
- [8] Tutkus, M., Alsamsam, M. N., Kopūstas, A., & Jurevičiūtė, M. (2022, September 26). The miEye: Bench-top super-resolution microscope with cost-effective equipment. <https://doi.org/10.17605/OSF.IO/J2FQY>
- [9] I. Baronaitė, D. Šulskis, A. Kopūstas, M. Tutkus, and V. Smirnovas. Formation of Calprotectin Inhibits Amyloid Aggregation of S100A8 and S100A9 Proteins. *ACS Chem. Neurosci.* 2024, 15, 9, 1915–1925, <https://doi.org/10.1021/acchemneuro.4c00093>
- [10] Š. Ivanovaitė, J. Paksaitė, A. Kopūstas, G. Karzaitė, D. Rutkauskas, A. Silanskas, G. Sasnauskas, M. Zaremba, S. K. Jones Jr., and M. Tutkus. smFRET Detection of Cis and Trans DNA Interactions by the BfiI Restriction Endonuclease. *J. Phys. Chem. B* 2023, 127, 29, 6470–6478, <https://doi.org/10.1021/acs.jpcc.3c03269>

Stability of Graphene/Carbon/Boron nitride Quantum Dots and Doxorubicin aggregates evaluated by optical methods

Katsiaryna Chernyakova, Martynas Zaleckas, Yaraslau Padrez, Lena Golubewa, Giedrė Grincienė, Renata Karpicz

Center for Physical Sciences and Technology, Saulėtekio Ave. 3, LT-10257 Vilnius, Lithuania.

Corresponding author e-mail Renata.karpicz@fmc.lt

Quantum dots (QDs), with advanced surface functionalization and luminescent properties that allow controlling the intracellular localization of nanocarrier-drug complexes, are promising nanostructured materials for theranostics, as they can simultaneously provide imaging and therapeutic effects. Theranostic agents must meet several requirements. The most important condition is that it delivers the medicine to the target. For this, it must be soluble in water and stable under physiological conditions. The nanocomplex must be biocompatible. It is highly desirable that it can be tracked optically to monitor its pharmacodynamics and accumulation in cancer tissue. In this study, we intend to investigate the stability, optical, and fluorescent properties of nanocomplexes of QDs and compounds with anticancer properties using spectroscopic methods.

The stability of blue and green luminescent graphene, carbon or boron nitride quantum dots, and doxorubicin aggregates was evaluated by optical methods. During this study, the absorption and fluorescence spectra of QDs and DOX, as well as the quenching kinetics, were measured in different pH environments using stationary spectrophotometry methods.

Different types of QDs forming a complex with doxorubicin have unique characteristics, but they also share a common feature. In all cases, doxorubicin's fluorescence quenching is observed, which can be a key indicator in determining the stability of QDs.

Acknowledgement.

Research partially supported by the Research Council of Lithuania (LMTLT) agreement No S-MIP-23-70, by Horizon Europe FLORIN Project No. 101086142 and by the Central Project Management Agency (CPMA) agreement No 10-038-T-0037.

Tuesday, August 6



©P.Obraztsov

Optical crystals of 2D materials

Kaihui Liu

School of Physics, Peking University, Beijing 100871, China

khliu@pku.edu.cn

Nonlinear optical crystals are the key components in advancing laser technology, offering the crucial functionalities of frequency conversion, signal modulation and parameter amplification. Over the last few decades, the utilization of well-established materials for nonlinear optical crystals like BBO, LiNbO₃, and KBBF has contributed to the fast development of quantum light sources, photonic integrated circuits and ultrafast lasers. The pursuit of suitable nonlinear optical crystals has led the exploration of the potential in two-dimensional (2D) materials, in which rhombohedral boron nitride (rBN) is particularly promising due to its high nonlinear susceptibility, broadband transparency, remarkable physicochemical stability, and compatibility with Si-based optical chips. However, the preparation of large-sized single-crystal rBN layers remains an extreme challenge. In this talk, I will introduce some recent progresses in the growth of large single-crystal rBN layers with both in-plane and out-of-plane controls[1-3], as well as the development of the twist-phase-matching theory for the design of 2D nonlinear optical crystals[4]. Twisted rBN will be a new useful optical crystal for future photonic and optoelectronic applications.

[1] Li Wang, Kaihui Liu*, et al. Epitaxial growth of a 100-square-centimetre single-crystal hexagonal boron nitride monolayer on copper. *Nature* 2019, 570, 91

[2] Zhibin Zhang, Kaihui Liu*, et al. Continuous epitaxy of single-crystal graphite films by isothermal carbon diffusion through nickel. *Nature Nanotechnology* 2022, 17, 1258.

[3] Jiajie Qi, Kaihui Liu*, et al. Stacking-controlled growth of rBN crystalline films with high nonlinear optical conversion efficiency up to 1%. *Advanced Materials* 2023, 2303122.

[4] Hao Hong, Kaihui Liu*, et al. Twist-phase-matching in two-dimensional materials. *Physical Review Letters* 2023, 131, 233801.

Ultrafast spectroscopy of a Dirac semimetal Cd_3As_2 driven by intense multi-terahertz pulses

Natsuki Kanda^{1,2}, Yuta Murotani², and Ryusuke Matsunaga²

¹ Ultrafast Coherent Soft X-ray Photonics Research Team, RIKEN Center for Advanced Photonics, RIKEN, 2-1 Hirosawa, Wako, Saitama 351-0198, Japan

²The Institute for Solid State Physics, The University of Tokyo, 5-1-5 Kashiwanoha, Kashiwa, Chiba 277-8581, Japan
Author e-mail address: n-kanda@riken.jp

Optical properties of topological Dirac semimetals are attracting growing interest because 3D massless electrons show unique electromagnetic responses with a large interaction volume with light, providing a fascinating platform for studying ultrafast control of matter and promising application in optoelectronics and nonlinear optics such as efficient harmonic generation [1]. Their unique infrared responses and large nonlinearity originate from the gapless band structure, where the interband and intraband transitions occur in the close energy scale and exert influences on each other. To thoroughly derive their novel functionalities, in-depth understanding of nonequilibrium broadband complex response functions is indispensable.

We have developed a phase-stable time-domain spectroscopy system in the multi-terahertz (10-50 THz) range [2] and studied ultrafast dynamics of the broadband response functions in a photoexcited Cd_3As_2 thin film with 30-fs time resolution. We found that photoexcited carriers largely suppress the multi-terahertz refractive index due to the elevated plasma frequency [3]. We also investigated the broadband response function in Cd_3As_2 under the formation of Floquet-Bloch state. Under 30-THz narrowband and linearly polarized pump, we found that the conductivity spectrum shows a highly dispersive line shape with net optical gain. The result is explained by the stimulated Rayleigh scattering, which corresponds to the transitions between the Floquet subbands and is remarkably enhanced by the elevated plasma frequency [4]. In addition, we performed 33-THz circularly polarized pump and THz polarization resolved probe experiments to study the light-induced anomalous Hall effect in Cd_3As_2 . Our comprehensive analysis clarified that the microscopic origins of the light-induced anomalous Hall current during and after the pump irradiation are accounted for by field-induced injection current [5] and inverse "isospin" Hall effect [6], respectively.

To manipulate the light-field driven states such as Floquet topological states, the control of the polarization states or the vector field waveforms of the pump pulse are important. We are developing the techniques for generation and detection of vector field shaping in multi-terahertz region. By using polarization modulated electro-optic sampling, the measurement of arbitrary trajectory of electric field vector was realized [7]. We also demonstrated the generation of the tailored counter rotating bicircular multi-THz pulses [8], which would be applied to ultrafast control of topological materials.

[1] B. Cheng *et al.*, Phys. Rev. Lett. **124**, 117402 (2020).

[2] N. Kanda *et al.*, Opt. Express **29**, 3479-3489 (2021).

[3] N. Kanda *et al.*, Nano Lett. **22**, 2358-2364 (2022).

[4] Y. Murotani, *et al.*, Phys. Rev. Lett. **129**, 207402 (2022).

[5] Y. Murotani *et al.*, Phys. Rev. Lett. **131**, 096901 (2023).

[6] Y. Murotani *et al.*, Nano Lett. **24**, 222 (2024).

[7] N. Kanda *et al.*, Opt. Express **32**, 1576 (2024).

[8] K. Ogawa *et al.*, arXiv:2312.04768 [physics.optics]

The dispersion energy strength of van der Waals interaction and absorption spectra of the two-dimensional stacked structures

Shuo Cao*, Changcheng Xu, Shaofeng Wang, Qing Wang, Jianjun Sun, Yong Ding

School of Physics, Liaoning University, Shenyang, P.R. China
E-mail: shuocao@lnu.edu.cn

Abstract: Stacking different two-dimensional (2D) materials together to form van der Waals (vdW) heterojunctions can effectively improve the performance of low-dimensional optoelectronic devices[1,2]. The stability of the vdW interaction is a key factor and challenge for practical application of 2D stacked material photoelectric devices, but the quantitative analysis of the weak interaction force between stacked 2D materials is less. Through energy decomposition analysis based on the force field (EDA-FF) method[3], we obtained the quantitative energy strength of the three components — electrostatic energy, exchange repulsion energy and dispersion energy of the total binding energy between bilayer graphene, graphene/MoS₂ and graphene/WS₂, shown in Figure 1.

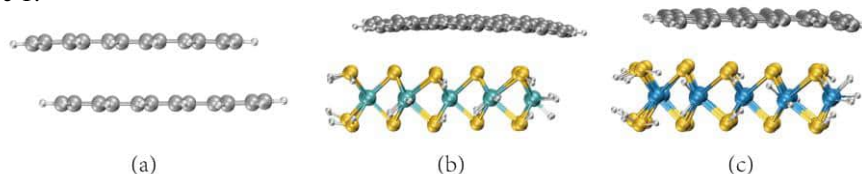


Figure 1, Stable configurations of the three 2D bilayer stacked structures: (a) bilayer graphene, (b) graphene/MoS₂ heterostructure, and (c) graphene/WS₂ heterostructure.

The dispersion energy of the vdW interaction accounts for more than 60% of the binding energy of the weak interaction between the 2D bilayer stacked structures, shown in Figure 2, which is useful for understanding the stabilization and reliability of 2D stacked material heterojunctions for practical applications.

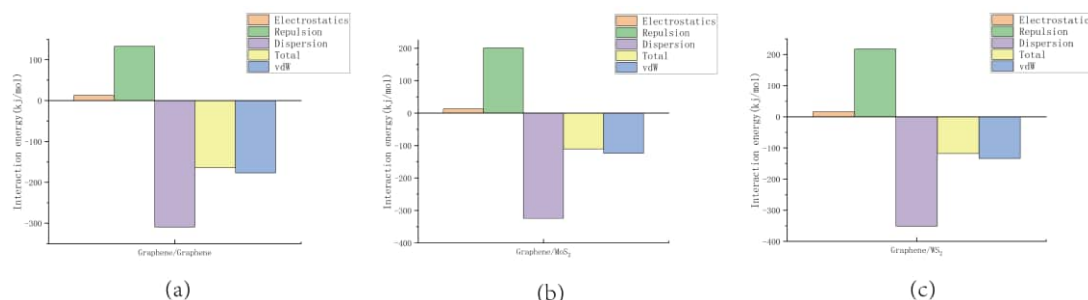


Figure 2, EDA-FF analysis result histograms: (a) bilayer graphene, (b) graphene/MoS₂, and (c) graphene/WS₂.

The two heterostructures of the graphene/MoS₂ and graphene/WS₂ have strong absorption peaks in the visible region, and the charge transfer forms at the strong absorption peak can be determined according to the charge transfer diagram, shown in Figure 3.

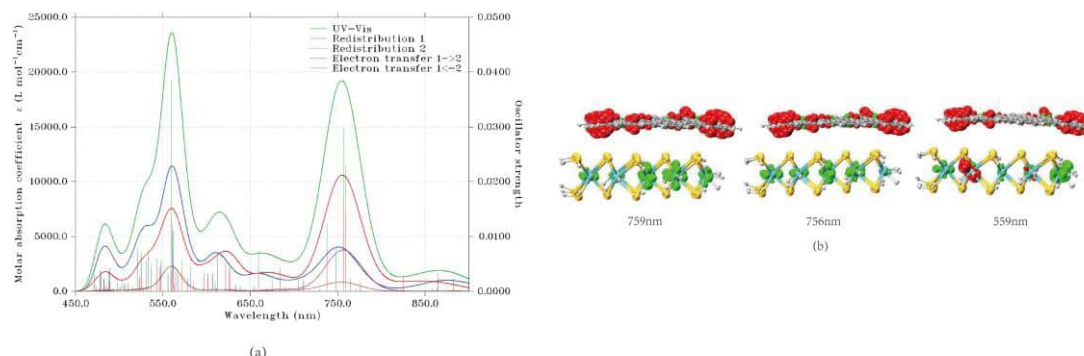


Figure 3, (a) Absorption spectrum of the graphene/MoS₂ heterostructure and (b) charge difference densities of the three excited states, where green and red represent holes and electrons, respectively.

References:

- [1] Ki Seok Kim, Doyoon Lee, Celesta S. Chang, Seunghwan Seo, Yaoqiao Hu, Soonyoung Cha, Hyunseok Kim, Jiho Shin, Ju-Hee Lee, Sangho Lee, Justin S. Kim, Ki Hyun Kim, Jun Min Suh, Yuan Meng, Bo-In Park, Jung-Hoon Lee, Hyung-Sang Park, Hyun S. Kum, Moon-Ho Jo, Geun Young Yeom, Kyeongjae Cho, Jin-Hong Park, Sang-Hoon Bae & Jeehwan Kim, Nature 614, 88 (2023).
- [2] Alberto Ciarrocchi, Fedele Tagarelli, Ahmet Avsar & Andras Kis, Nature Reviews Materials 7, 449 (2022).
- [3] Tian Lu, Zeyu Liu, Qinxue Chen, Materials Science and Engineering: B, 273, 115425 (2021).

Optical properties and terahertz applications of one-dimensional nanocarbons

R. R. Hartmann¹ and M. E. Portnoi²

¹Physics Department, De La Salle University, 2401 Taft Avenue, 0922 Manila, Philippines

²Physics and Astronomy, University of Exeter, Stocker Road, Exeter EX4 4QL, United Kingdom
m.e.portnoi@exeter.ac.uk

Carbon-based nanostructures are believed to be promising candidates for terahertz (THz) applications [1]. Following our earlier work on narrow-gap carbon nanotubes and graphene nanoribbons [2], as well as graphene bipolar waveguides [3] and double quantum wells [4], we are now considering dipole optical and terahertz transitions in two other types of nanocarbons – carbynes and cyclocarbons.

The technology for synthesizing carbynes (polyyne carbon chains) has rapidly evolved over the last few years, with stable long chains deposited on substrates now a reality [5]. We have recently demonstrated and explained a strong polarization dependence of photoluminescence from highly-aligned carbon chains terminated by gold clusters [6]. A prominent feature of long polyyne chains (chains with two alternating non-equal bonds) is the presence of topologically protected mid-gap edge states. For a finite-length chain, the two edge states form an even and odd combination with the energy gap proportional to the edge-state overlap due to tunneling. These split states of different parity support strong dipole transitions. We have shown [7] that for long enough carbyne chains, the energy separation between the HOMO and LUMO molecular orbitals formed by the edge states corresponds to the THz frequency range. There are several other allowed optical transitions in this system that can be used to maintain the inversion of population required for THz lasing. The frequency of THz transitions can be tuned by an external electric field [8].

Another recent achievement in nanocarbon technology is the demonstration of controlled synthesis of cyclocarbons, particularly the cyclocarbon allotropes C₁₈ [9] and more recently C₁₆ [10]. The properties of cyclocarbons in an external (lateral in the plane of the molecule) electric field differ drastically depending on the parity of the number of dimers in a polyyne ring. This is a direct consequence of breaking the inversion symmetry in a ring consisting of an odd number of dimers, including the famous C₁₈. Our estimates [11] show that adding just one extra carbon dimer to C₁₆ is equivalent to placing this molecule in an external magnetic field of over 1000 T. For an odd-dimer cyclocarbon, as a result of the absence of inversion symmetry, an experimentally attainable electric field should open a tunable gap between otherwise degenerate states, leading to two states with allowed dipole transitions between them in the THz range. Population inversion can be achieved again using optical pumping.

Acknowledgement

This work was supported by the EU H2020-MSCA-RISE projects TERASSE (H2020-823878) and CHARTIST (H2020-101007896), by the UK EPSRC grant EP/Y021339/1 and by the NATO Science for Peace and Security project NATO.SPS.MYP.G5860.

References

- [1] R. R. Hartmann, J. Kono and M. E. Portnoi, *Nanotechnology*, **25**, 322001 (2014).
- [2] R. R. Hartmann, V. A. Saroka and M. E. Portnoi, *J. Appl. Phys.*, **125**, 151607 (2019).
- [3] R. R. Hartmann and M. E. Portnoi, *Phys. Rev. B*, **102**, 155421 (2020).
- [4] R. R. Hartmann and M. E. Portnoi, *Phys. Rev. B*, **102**, 052229 (2020).
- [5] S. Kutrovskaia, A. Osipov, S. Baryshev, A. Zasedatelev, V. Samyshkin, S. Demirchyan, O. Pulci, D. Grassano, L. Gontrani, R. R. Hartmann, M. E. Portnoi, A. Kucherik, P. G. Lagoudakis and A. V. Kavokin, *Nano Lett.*, **20**, 6502 (2020).
- [6] A. Kucherik, A. Osipov, V. Samyshkin, R. R. Hartmann, A. V. Povolotskiy, M. E. Portnoi, *Phys. Rev. Lett.* **132**, 056902 (2024).
- [7] R. R. Hartmann, S. Kutrovskaia, A. Kucherik, A. V. Kavokin and M. E. Portnoi, *Physical Review Research*, **3**, 033202 (2021).
- [8] R. A. Ng, M. E. Portnoi and R. R. Hartmann, *arXiv:2309.00288* (2023).
- [9] K. Kaiser, L. M. Scriven, F. Schulz, P. Gawel, L. Gross and H. L. Anderson, *Science*, **365**, 1299 (2019).
- [10] Y. Gao, F. Albrecht, I. Rončević, I. Ettetdgui, P. Kumar, L. M. Scriven, K. E. Christensen, S. Mishra, L. Righetti, M. Rossmannek, I. Tavernelli, H. L. Anderson and L. Gross, *Nature*, **623**, 977 (2023).
- [11] R. A. Ng, M. E. Portnoi and R. R. Hartmann, *Phys. Rev. B*, **106**, L041403 (2022).

Terahertz emission from optically pumped carbon nanotube films

G. Fedorov¹, A. Saushin¹, D. Pashnev², I. Kašalynas², P. Kuzhir¹, M. Portnoi³

¹*Department of Physics and Mathematics, Center of Photonics Research, University of Eastern Finland, Yliopistokatu 7, FI-80101 Joensuu, Finland*

²*Department of Optoelectronics, Center for Physical Sciences and Technology (FTMC), Saulėtekio av. 3, LT-10257 Vilnius, Lithuania*

³*Physics and Astronomy, University of Exeter, Stocker Road, Exeter EX4 4QL, United Kingdom*

georgy.fedorov@uef.fi

Interband transitions in solids allow for the creation of room temperature operating emitters and detectors of radiation from mid infrared to ultraviolet optical ranges. Extending this approach to THz frequency range is yet to be attained. Quasimetallic carbon nanotubes (CNTs) that have curvature-induced bandgaps of several meV show great promise in this respect. It has been recently pointed out that the matrix element of dipole transitions in those 1D narrow-gap semiconductors has giant enhancement at the band edge and then decays quickly away from the band edge [1]. The transition matrix element enhancement is due to curvature effects – the same effects are responsible for gap opening in quasi-metallic nanotubes. Along with the van Hove singularity at the band edge this results in a giant enhancement of the probability of optical transitions near the band edges.

In this work we report on observation of THz room temperature emission from carbon nanotube film illuminated by visible range laser radiation. We show that this emission originates not only from thermal radiation of the CNT film heated by the optical excitation. Analysis of the polarization of emission of optically pumped CNT film and comparison to that of the same film heated above room temperature unambiguously shows that significant fraction of the emission in the former case occurs due to interband transitions in quasimetallic carbon nanotubes stimulated by optical excitation of charge carriers. This contribution is observed for frequencies up to 7 THz. The observed experimental data are analyzed within the analytical approach developed in the Ref. 1 and are found to be in good agreement with theoretical modeling. Our result opens a pathway for creation of novel terahertz radiation sources based on quasimetallic CNTs.

[1] Hartmann, R. R., V. A. Saroka, and M. E. Portnoi. "Interband transitions in narrow-gap carbon nanotubes and graphene nanoribbons." *Journal of Applied Physics* 125.15 (2019).

Single crystal diamond needles fabrication, characterization and application

Alexander N. Obratsov

University of Eastern Finland, Joensuu 80101, Finland
alexander.obratsov@uef.fi

Diamond is known as one of the most attractive material for the centuries. Nowadays its importance is greatly increasing due to demands in different areas from micromachining to quantum information processing. Crystalline structure and properties of diamond investigated in details and are deeply understood. In particular, shapes of the well-ordered diamond crystals are represented by cubic, octahedron and intermediate forms predetermined by the lattice symmetry. At the same time electronic and other properties are predetermined by strong covalent bonding of carbon atoms with sp^3 hybridized orbitals. The shapes of small-size crystallites may be drastically different from ideal bulky diamonds. With crystallite size decrease relative amount of atoms situated at surface in respect to total number of atoms is increased. Additionally, hybridization of atomic orbitals for the surface atoms is changed from sp^3 to sp^2 and to sp^1 leading to significant properties variations of nano-sized diamonds in comparison with the crystals of larger size.

Herein we present results of investigations on production, characterization and potential applications of pyramid-shaped needle-like diamond crystallites. These single-crystal diamond needles having dimensions of their rectangular base and length of micrometer size with apexes and cross-sections in nanometer scale possess unique combination of properties of bulky and nano-sized diamonds. The individual needles were extracted from a powdered material produced by oxidation of polycrystalline diamond film grown using chemical vapor deposition (CVD) method. Experimental investigations, modelling and computer simulations were used to reveal mechanisms of the needles formation.

We present results of needles characterization obtained with electron microscopy, electron emission, luminescent and Raman spectroscopy [1-3]. Developed methodologies allow manipulation by the individual needle crystallites and their assembling with the massive holders providing further applications. The potential applications of the needles include: probes for atomic force microscopy [4]; point electron beam source [5-8]; nano-dynamometer and electric field detector [9,10]; nano-thermometer [11]; optical sensing elements [11]; electro-mechanical devices [13]

- [1] Andrey S. Orekhov, Feruza T. Tuyakova, Ekaterina A. Obratsova, Artem B. Loginov, Andrey L. Chuvilin, Alexander N. Obratsov, *Nanotechnology* 27, 455707 (2016).
- [2] Feruza T. Tuyakova, Ekaterina A. Obratsova, Evgeny V. Korostylev, Dmitry V. Klinov, Kirill A. Prusakov, Andrey A. Alekseev, Rinat R. Ismagilov, Alexander N. Obratsov, *J. of Luminescence* 179, 539 (2016).
- [3] Sergey A. Malykhin, Rinat R. Ismagilov, Feruza T. Tuyakova, Ekaterina A. Obratsova, Pavel V. Fedotov, Anna Ermakova, Petr Siyushev, Konstantin G. Katamadze, Fedor Jelezko, Yury P. Rakovich, Alexander N. Obratsov, *Optical Materials* 75, 49 (2018).
- [4] Alexander N. Obratsov, Petr G. Kopylov, Boris A. Loginov, Mathew A. Dolganov, Rinat R. Ismagilov, and Natalia V. Savenko, *Rev. Sci. Instr.* 81, 013703 (2010)
- [5] Victor I. Kleshch, Stephen T. Purcell, Alexander N. Obratsov, *SCIENTIFIC REPORTS* 6, 35260 (2016).
- [6] V. Porshyn, V. I. Kleshch, E.A. Obratsova, A.L. Chuvilin, D. Lützenkirchen-Hecht, A. N. Obratsov, *Appl. Phys. Lett.* 110, 182101 (2017)
- [7] Victor I. Kleshch, Anton S. Orekhov, Alexandra E. Pishchulina, Ivan V. Sapkov, Dmitry N. Khmelenin, Artem B. Loginov, Rinat R. Ismagilov, Alexander N. Obratsov, *Carbon* 221, 118936 (2024).
- [8] Victor I. Kleshch, Vitali Porshyn, Pavel Serbun, Anton S. Orekhov, Rinat R. Ismagilov, Dirk Luetzenkirchen-Hecht, Alexander N. Obratsov, *Appl. Phys. Lett.* 120, 141601 (2022)
- [9] L. Rigutti, L. Venturi, J. Houard, A. Normand, E.P. Silaeva, M. Borz, S.A. Malykhin, A.N. Obratsov, A. Vella, *Nano Lett.* 17, 7401 (2017)
- [10] Olivier Torresin, Mario Borz, Julien Mauchain, Ivan Blum, Victor I. Kleshch, Alexander N. Obratsov, Angela Vella, Benoit Chalopin, *Ultramicroscopy* 202, 51 (2019).
- [11] L. Arnoldi, M. Spies, J. Houard, I. Blum, A. Etienne, R. Ismagilov, A. Obratsov, A. Vella, *Appl. Phys. Lett.* 112, 143104 (2018).
- [12] M. Borz, M. H. Mammez, I. Blum, J. Houard, G. Da Costa, F. Delaroche, S. Idlahcen, A. Haboucha, A. Hideur, V.I. Kleshch, A.N. Obratsov, A. Vella, *Nanoscale*, 11, 6852 (2019)
- [13] Victor I. Kleshch, Rinat R. Ismagilov, Vsevolod V. Mukhin, Anton S. Orekhov, Philippe Poncharal, Stephen T. Purcell, Alexander N. Obratsov, *Appl. Phys. Lett.* 122, 144101 (2023).

Fluorescent diamond needles in research and applications

Sergei Malykhin

*Department of Physics and Mathematics, University of Eastern Finland, Joensuu, Finland
sergeim@uef.fi*

Diamond, known for its exceptional hardness and optical clarity, is also highly valued for advanced technological applications due to its unique physical and chemical properties. Its excellent thermal conductivity, electrical insulation, and resistance to radiation damage make it indispensable in high-performance applications. In electronics, diamond enhances high-power and high-frequency devices with its wide bandgap, improving efficiency and durability. Its transparency to a broad spectrum of light makes it ideal for advanced optics and photonics, including high-power laser systems. Additionally, diamond's biocompatibility and chemical inertness are beneficial in biomedical applications, such as implantable medical devices and drug delivery systems.

Fluorescent diamonds exhibit fluorescence due to color centers in their crystal lattice, which absorb and emit light, resulting in visible fluorescence under certain conditions. These properties make fluorescent diamonds valuable for various advanced technological applications. They are used in bioimaging and medical diagnostics, where their biocompatibility and stable fluorescence allow for precise tracking and imaging of biological processes. The versatility of fluorescent diamonds with color centers continues to drive innovation in multiple scientific and technological fields.

Among diamond color centers, those exhibiting optically detected magnetic resonance (ODMR), such as NV [1], TR12 [2], and ST1 [3] centers, are particularly interesting. These centers' electronic spin states can be manipulated and read using optical methods. In quantum computing, they serve as stable qubits at room temperature, aiding the development of quantum processors [4]. In quantum sensing, they allow high-resolution detection of magnetic fields, electric fields and temperature [5].

Bulk diamonds, nanodiamonds, and diamond arrays represent different forms of diamond material, each with unique properties and applications across various technological fields. Bulk diamonds, prized for their optical purity and crystal quality, are ideal for advanced diamond-based optics. Nanodiamonds, with their high surface area, biocompatibility, and functionalization potential, are suitable for drug delivery and bioimaging [6]. Diamond arrays, consisting of patterned or ordered structures, leverage diamond's properties at micro and nanoscale, making them useful in quantum computing for hosting many qubits and in sensing technologies for high spatial resolution and sensitivity.

This work focuses on diamond needles, or single crystal diamond needles (SCDNs) [7], an alternative form of diamond. SCDNs are promising for both scientific research and technological applications. Their sharp tips and robustness make them ideal for high-resolution scanning probe microscopy. In quantum technology, SCDNs with embedded color centers [8], like NV centers, can serve as highly sensitive quantum sensors, capable of detecting magnetic fields, electric fields, and temperature variations with high precision. Their geometry is promising for efficient interaction with external quantum systems, suitable for quantum communication and computation. Additionally, their biocompatibility opens applications in medical diagnostics and treatment. The unique properties of diamond needles make them a powerful tool across various advanced technological and research domains.

This work was supported by Academy of Finland (Flagship Programme PREIN, decision 346518; research projects, decisions 340733, 357033; QuantERA project EXTRASENS, decision 361115), and Horizon Europe MSCA FLORIN Project 101086142.

- [1] M.W. Doherty, N.B. Manson, P. Delaney, F. Jelezko, J. Wrachtrup, L.C.L. Hollenberg, *Physics Reports*. 528 (2013) 1–45.
- [2] J. Foglszinger, A. Denisenko, T. Kornher, M. Schreck, W. Knolle, B. Yavkin, R. Kolesov, J. Wrachtrup, *NPJ Quantum Information*. 8 (2022).
- [3] P. Balasubramanian, M.H. Metsch, P. Reddy, L.J. Rogers, N.B. Manson, M.W. Doherty, F. Jelezko, *Nanophotonics*. 8 (2019) 1993–2002.
- [4] M.H. Abobeih, Y. Wang, J. Randall, S.J.H. Loenen, C.E. Bradley, M. Markham, D.J. Twitchen, B.M. Terhal, T.H. Taminiau, *Nature*. 606 (2022) 884–889.
- [5] J. Achard, V. Jacques, A. Tallaire, *Journal Physics D: Applied Physics*. 53 (2020) 313001.
- [6] J. Slegerova, I. Rehor, J. Havlik, H. Raabova, E. Muchova, P. Cigler, *Nanodiamonds as Intracellular Probes for Imaging in Biology and Medicine*, (Springer Netherlands, 2014)
- [7] S.A. Malykhin, J. Houard, R.R. Ismagilov, A.S. Orekhov, A. Vella, A.N. Obratsov, *Physica Status Solidi B*. 255 (2017).
- [8] S. Malykhin, Y. Mindarava, R. Ismagilov, F. Jelezko, A. Obratsov, *Diamond Related Materials*. 125 (2022) 109007.

Engineering the Surface of Nanodiamonds for Applications in Quantum Biosensing

Filip Steiner^{1,2}, Jakub Čopák^{1,2}, Michal Gulka¹, Petr Cígler^{1,*}

¹*Institute of Organic Chemistry and Biochemistry, of the CAS, Prague, Czechia*

²*Department of Physical and Macromolecular Chemistry, Faculty of Science, Charles University, Prague, Czechia*

**petr.cigler@uochb.cas.cz*

Nanodiamonds (NDs) with nitrogen-vacancy (NV) centers can serve as precise, target-specific, and localized quantum probes [1]. This capability arises from the quantum mechanical interactions between the NV electron spin and its environment, which can be subsequently detected optically. For their use in a range of applications, the ND surface modification is required. The most common surface modification is the oxidation of the ND surface. However, amination and azidation of the NDs are of interest as they provide wide possibilities for further functionalization tailored for quantum biosensing. For instance, strain-promoted [3+2] azide-alkyne cycloaddition (SPAAC) would provide a critical advancement in bioorthogonal chemistry, enabling the formation of triazole rings without the need for a metal catalyst [2].

In this work, we compared different strategies for ND surface amination and azidation, and we demonstrate a successful SPAAC covalent conjugation of modified oligonucleotides with azidated NDs. To prepare aminated NDs, we studied and optimized a high-temperature amination with ammonia gas [3]. The resulting NDs show excellent colloidal stability and contain a high load of amino groups on the surface. Azidated NDs were synthesized by nucleophilic substitution of brominated NDs [4] and by decarboxylative azidation [5] for comparison. We show that the nucleophilic substitution of brominated NDs is a valuable alternative for decarboxylative azidation. Further, we optimized the reaction conditions for conjugations of NDs with oligonucleotides modified by dibenzocyclooctyne (DBCO) or bicyclononyne (BCN) as clickable groups. We showed that the number of attached oligonucleotides can be tuned by the reaction conditions and by the selection of clickable groups.

Acknowledgement

The work was supported by the Czech Science Foundation project No. 23-04876S, the Ministry of Education, Youth, and Sports of the Czech Republic (project No. CZ.02.01.01/00/22_008/0004558, co-funded by the European Union), the European Union project C-QuENS (Grant No. 101135359), the Czech Academy of Sciences – Strategy AV21 – Research program VP29 (to P.C.), TACR project Nr. TH90010001 (QuantERA – ERA-NET Cofund, project EXTRASENS), and Horizon project No 101086142 (FLORIN).

References

- [1] Zhang T. et al.: ACS Sens., 2077-2107 (2021)
- [2] Bertozzi C. R. et. Al.: J. Am. Chem. Soc., 15046–15047 (2004)
- [3] Laube C. et al.: Mater. Chem. Front., 2527-2540 (2007)
- [4] Kennedy Z. et al., Langmuir, 2790-2798 (2017)
- [5] Melendrez C. et al.: Phys. Chem. Lett., 1147-1158 (2022)

Surface optimization of nanodiamonds using non-thermal plasma

Michal Gulka^{1,*}, Priyadharshini Balasubramanian², Ekaterina Shagieva³, Jakub Copak^{1,4}, Josef Khun⁵, Vladimir Scholtz⁵, Fedor Jelezko², Stepan Stehlik³, Petr Cigler¹

¹Institute of Organic Chemistry and Biochemistry, of the CAS, Flemingovo nam. 2, Prague, Czechia

²Institute of Quantum Optics, Ulm University, Ulm 89081, Germany

³Institute of Physics of the Czech Academy of Sciences, Cukrovarnická 10, 162 00 Prague 6, Czechia

⁴Department of Physical and Macromolecular Chemistry, Faculty of Science, Charles University in Prague, Czechia

⁵Department of Physics and Measurements, University of Chemistry and Technology in Prague, Czechia

*gulka.michal@gmail.com

Possibility of local sensitive monitoring of intracellular processes using quantum sensing with nitrogen-vacancy (NV) centers in nanodiamonds (NDs), would greatly advance cell biology and would enable numerous medical applications. Although such probes have been studied extensively [1], they are still limited in sensitivity. Whereas the NV center in bulk diamond holds record room-temperature electron spin coherence time among solid-state qubits, NVs in NDs exhibit much poorer relaxation times. As suggested in [2], prolongation of the NVs relaxation time should be possible by ND surface optimization creating mixed H/O termination.

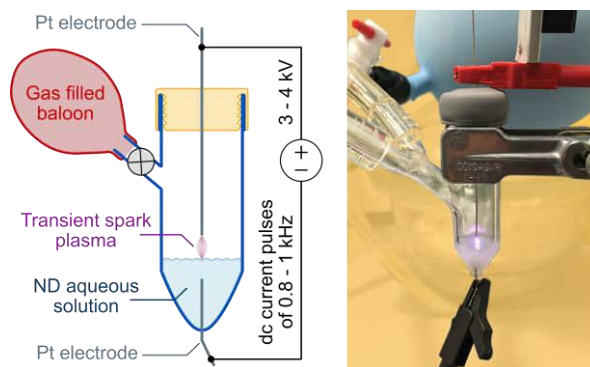


Fig. 1. Non-thermal plasma system for ND modifications

Here we employ a non-thermal plasma (NTP) [3], with the aim of prolongation of the NV electron spin relaxation times (Figure 1). We have used various nanodiamond samples (HPHT/detonation, H-/O-terminated surface) and ambient gases (air, O₂, He, and H₂). The NTP modification induces changes in C=O bonds, restructuring of C-H bonds, and differences in OH termination. Using hydrogen as the ambient gas results in the biggest changes in FTIR spectra. For oxidized HPHT NDs the zeta potential dropped from an initial ~ -40 mV to ~ -50 mV. Both T₁ and T₂ NV electron relaxation times improved significantly after the modification.

Acknowledgement

This project has received funding from the European Union's Horizon 2020 research and innovation program. The work was further supported by the Czech Science Foundation project No. 23-04876S, the Ministry of Education, Youth, and Sports of the Czech Republic (project No. CZ.02.01.01/00/22_008/0004558, co-funded by the European Union), the European Union project C-QuENS (Grant No. 101135359), the Czech Academy of Sciences – Strategy AV21 – Research program VP29 (to P.C.), TACR project Nr. TH90010001 (QuantERA – ERA-NET Cofund, project EXTRASENS), and Horizon project No 101086142 (FLORIN).

References

- [1] T. Zhang et al., ACS Sens. **6**, 2077–2107 (2021).
- [2] M. Kaviani et al., Nano Lett. **14**, 4772–4777 (2014).
- [3] J. Khun et al., Plasma Sources Sci. Technol. **27**, 065002 (2018).

Diamond based quantum sensors

Fedor Jelezko

*Institute of quantum optics, Ulm University
fedor.jelezko@uni-ulm.de*

Synthetic diamond has recently emerged as a candidate material for a range of quantum-based applications including quantum information processing and quantum sensing. In this presentation we will show how single nitrogen-vacancy (NV) colour centres can be created close to the diamond surface can be employed as nanoscale sensors of electric and magnetic fields. We will show nanoscale NMR enabled by single NV centres and discuss sensitivity and spectral resolution limits of nanoscale NMR. We will also discuss applications of NV centres for hyperpolarisation of nuclear spins and application of optical spin polarisation in MRI.

On the optimal chemical interface of diamond for quantum biosensing

Petr Cigler

*¹Institute of Organic Chemistry and Biochemistry, of the CAS, Flemingovo nam. 2, Prague, Czechia
cigler@uochb.cas.cz*

Non-perturbing sensing techniques applicable to biological systems are currently of central interest in the biosciences. Nanodiamond (ND) is a highly biocompatible nanomaterial for construction of nanosensors, which can accommodate nitrogen-vacancy (NV) centers. The NV spin properties can be read optically, which enables design of various probes based on quantum mechanical interactions. NDs can be exposed to biological environment and report sensitively on the spin-related processes occurring in a close vicinity of the particle employing for example the NV spin relaxometry measurements. ND relaxometry however reaches its limitations in terms of poor colloidal stability in physiological environment and non-specificity to detect only the magnetic field originated from the spins of interest.

To ensure colloidal stability in biologically-relevant environment we stabilize ND probes using thin polymer coatings that can be further modified to allow sensing of specific physical quantities or targeted molecules. To that end, we design molecular transducers for transposing the presence of particular analytes to a selective and unambiguous readout. Different types and concepts of surface architectures including those for selective measurements of pH, temperature, redox potential, and ascorbate concentration under physiological conditions will be discussed. Additionally, our recent developments of ND probes for detection of biomolecules using relaxometry together with a proof-of principle results will be presented.

Acknowledgement

This project has received funding from the European Union's Horizon 2020 research and innovation program. The work was further supported by the Czech Science Foundation project No. 23-04876S, the Ministry of Education, Youth, and Sports of the Czech Republic (project No. CZ.02.01.01/00/22_008/0004558, co-funded by the European Union), the European Union project C-QuENS (Grant No. 101135359), the Czech Academy of Sciences – Strategy AV21 – Research program VP29 (to P.C.), TACR project Nr. TH90010001 (QuantERA – ERA-NET Cofund, project EXTRASENS), and Horizon project No 101086142 (FLORIN).

Wednesday, August 7



©P.Obraztsov

Realization of exciton-mediated optical spin-orbit interaction in organic microcrystalline resonators for circularly polarized electroluminescence

Hongbing Fu

Department of Chemistry, Capital Normal University, Beijing, 100048, P. R. China

E-mail: hbfu@cnu.edu.cn

The ability to control the spin-orbit interaction (SOI) of light in optical microresonators is of fundamental importance for future photonics. Organic microcrystals, due to their giant optical anisotropy, play a crucial role in spin-optics and topological photonics. We demonstrated controllable and wavelength-dependent Rashba–Dresselhaus (RD) SOI, ascribed to the anisotropic excitonic response in an optical microcavity filled with an organic microcrystalline. We investigated the transition of the spin-splitting from twice winding caused by the splitting of the transverse-electric (TE) and transverse-magnetic (TM) modes to once winding caused by the RD effect. The interplay of the two allows engineering of the SOI of light in organic microcavities toward exploiting nonmagnetic and low-cost spin-photonics devices.

Circularly polarized (CP) electroluminescence from organic light-emitting diodes (OLEDs) has aroused considerable attention for their potential in future display and photonic technologies. Currently, the development of CP-OLEDs relies largely on chiral-emitters, which not only remain rare owing to difficulties in design and synthesis but also limit the performance of electroluminescence. Here, we demonstrate a chiral-emitter-free microcavity CP-OLED with a high dissymmetry factor (g_{EL}) and high luminance by embedding a thin two-dimensional organic single crystal (2D-OSC) between two silver layers which serve as two metallic mirrors forming a microcavity and meanwhile also as two electrodes in an OLED architecture. In the presence of the RD effect, the SOIs in the birefringent 2D-OSC microcavity result in a controllable spin-splitting with CP dispersions. Thanks to the high emission efficiency and high carrier mobility of the OSC, chiral-emitter-free CP-OLEDs have been demonstrated exhibiting a high g_{EL} of 1.1 and a maximum luminance of about 60000 cd/m², which places our device among the best performing CP-OLEDs.

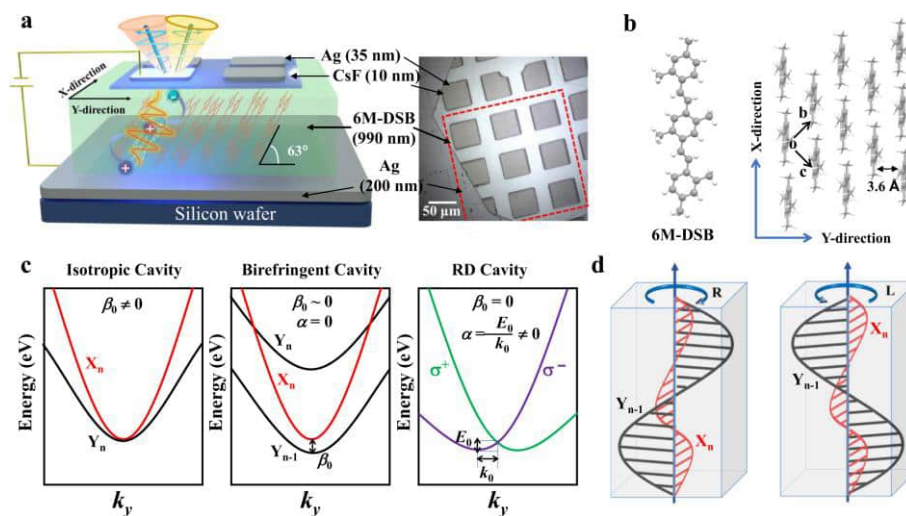


Figure 1. **a**, Schematic diagram of the microcavity CP-OLED device structure. **b** Left: Molecular structure of 6M-DSB. Right: brickwork molecular packing arrangement within the (001) crystal plane, viewed perpendicular to the microribbon top-facet. **c** Left: two orthogonally linearly polarized modes with the same parity in an isotropic microcavity. Middle: the dispersion of two orthogonally linearly polarized modes in an anisotropic microcavity. Right: RD SOI emerges when two orthogonally linearly polarized modes with opposite parity are resonant. **d** The resonant X- and Y-polarized cavity modes of opposite parity. The 6M-DSB crystal in the microcavity hence acts as a half-wave plate, and the intrinsic mode polarization of the light-emitting side of the mirror turns into a circle, corresponding to left-handed and right-handed circular polarizations, respectively..

References

- [1] J. H. Ren, Q. Liao, X. K. Ma, S. Schumacher, J. N. Yao, H. B. Fu, *Laser Photonics Rev.*, **16**, 2100252 (2022)
- [2] J. H. Ren, Q. Liao, F. Li, Y. M. Li, O. Bleu, G. Malpuech, J. N. Yao, H. B. Fu, D. Solnyshkov, *Nat. Commun.*, **12**, 689 (2021).
- [3] J. C. Jia, X. Cao, X. K. Ma, J. B. De, J. N. Yao, S. Schumacher, Q. Liao, H. B. Fu, *Nat. Commun.*, **14**, 31 (2023).

Growth of two dimensional *h*-BN: Influence of the support on the electronic and optical properties of the

Adrian Hemmi,¹ Ari Paavo Seitsonen,² Michael S Altman,³ Marcella Iannuzzi,⁴
Thomas Greber¹ and Huanyao Cun¹

¹Physik-Institut der Universität Zürich, Switzerland

²Département de Chimie École Normale Supérieure, Paris, France

³Department of Physics, Hong Kong University of Science and Technology, Hong Kong

⁴Chemie-Institut der Universität Zürich, Switzerland

Ari.P.Seitsonen@iki.fi

1. Growth of hexagonal boron nitride (*h*-BN) of high quality

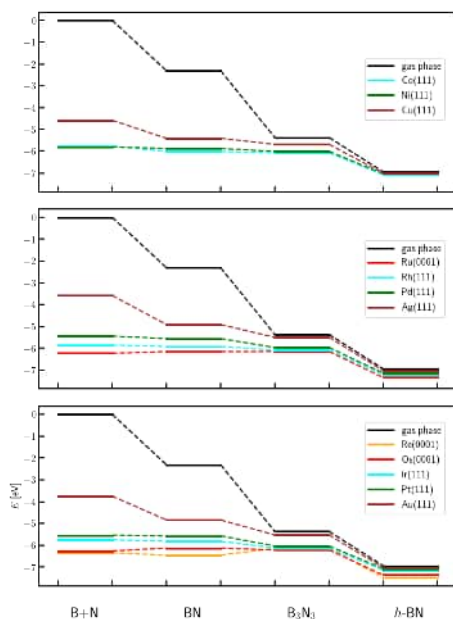


Fig. 1. Energy diagrams of formation of *h*-BN from single atoms to dimers to hexamers to full mono-layer; from Ref [3]

The single layer of the hexagonal boron nitride (*h*-BN) is an insulator that can be used to separate adsorbed species from the underlying substrate, both physically and electronically. The production of high-quality *h*-BN is essential for the ultimate performance of two dimensional (2D) materials-based devices, since it is the key 2D encapsulation material. We are working on the optimisation of the procedures to grow *h*-BN on surface of transition metals.

Our recent achievements include the enhanced quality of the *h*-BN on Rh(111) via 2D distillation [1], and a decisive guideline for fabricating high-quality *h*-BN on Pt(111) [2]. We have found that it is crucial to exclude carbon from the *h*-BN related process, otherwise carbon prevails over boron and nitrogen due to its larger binding energy, thereupon forming graphene on metals after high-temperature annealing. We introduce the pyrolysis temperature T_p as an important quality indicator for *h*-BN on transition metals.

In order to understand better the underlying physical trends, we have performed systematic density functional theory (DFT) calculations of fragments to the full mono-layer of *h*-BN on 12 different hexagonally oriented transition metals [3]. We further report corresponding studies carried out on graphene. We will also show results from DFT calculations of Moiré structures, where the *h*-BN sheet can be vertically bent.

2. Consequences of adsorption on the electronic and (linear) optical properties of *h*-BN

We are carrying out calculations of the electronic properties of the *h*-BN when supported on the various substrates. Also we report some preliminary results of the influence of the support on the linear optical properties of the *h*-BN. Further we will discuss the properties of adsorbed molecules on the supported *h*-BN that could be used for example as single molecule magnets, such as endo-fullerenes with lanthanide elements adsorbed inside the fullerene cage.

3. Acknowledgement.

We acknowledge financial support from the Swiss National Science Foundation (SNF project no. 200020_201086) and by the European Commission under the Graphene Flagship (contract no. CNECT-ICT-604391). We further acknowledge access to Piz Daint and Eiger@Alps at the Swiss National Supercomputing Centre (CSCS), Switzerland under the share of the Universität Zürich with the project ID uzh11.

4. References

- [1] Huanyao Cun, Zichun Miao, Adrian Hemmi, Yasmine Al-Hamdani, Marcella Iannuzzi, Jürg Osterwalder, Michael S Altman and Thomas Greber, "High-quality hexagonal boron nitride from 2D distillation", ACS Nano ACS Nano **15**, 1351-1357 (2021); doi: [10.1021/acsnano.0c08616](https://doi.org/10.1021/acsnano.0c08616)
- [2] Adrian Hemmi, Ari Paavo Seitsonen, Thomas Greber and Huanyao Cun, "The winner takes it all: Carbon supersedes hexagonal boron nitride with graphene on transition metals at high temperatures", Small **18**, e2205184 (2022); doi: [10.1002/smll.202205184](https://doi.org/10.1002/smll.202205184)
- [3] Ari Paavo Seitsonen and Thomas Greber, "Growing sp^2 materials on transition metals: Calculated atomic adsorption energies of hydrogen, boron, carbon, nitrogen, and oxygen atoms, C_2 and BN dimers, C_6 and $(BN)_3$ hexamers, graphene and *h*-BN with and without atomic vacancies", Nanoscale Advances **15**, 842 (2023); doi: [10.1039/D3NA00472D](https://doi.org/10.1039/D3NA00472D)
- [4] Roland Stania, Ari Paavo Seitsonen, Hyunjin Jung, David Kunhardt, Alexey A Popov, Matthias Muntwiler and Thomas Greber, "Correlation of Work Function and Conformation of C_{80} Endofullerenes on *h*-BN/Ni(111)", Advanced Materials Interfaces **11**, 2300935 (2024); doi: [10.1002/admi.202300935](https://doi.org/10.1002/admi.202300935)

Terahertz meta-optics made with ultrashort pulse laser processing

Haruyuki Sakurai, Kuniaki Konishi

*Institute for Photon Science and Technology, The University of Tokyo
kkonishi@ipst.s.u-tokyo.ac.jp*

The technology to control electromagnetic waves by using artificial structures of the same or smaller size as the wavelength is called metamaterials or metasurfaces, and by appropriately designing their shapes, it is possible to control their optical response in various ways. Electromagnetic waves in the frequency range of 0.1 to 10 THz are called terahertz waves, and in recent years, they have attracted attention not only for fundamental science but also for applications in sensing, wireless communications, and radio astronomy.

Although lithography techniques are generally used to fabricate micro-scale artificial structures, it is not easy to fabricate non-uniform structures in the height direction because the technique is good at fabricating structures in a two-dimensional plane. In addition, multiple micro-processing devices and clean-room environments are required to perform a series of processes, which are costly to maintain.

Recently, femtosecond laser processing technology has attracted attention as a new method for fabricating 3D structures. In a laser processing system using an ordinary galvanometer mirror, the focusing diameter of the beam is about 10 to 20 μm , which is sufficiently smaller than the typical wavelength of terahertz waves, which is several hundred μm . Therefore, it is possible to fabricate 3D microstructures below the terahertz wavelength by femtosecond laser processing, and it is expected to be a tool for fabricating terahertz metamaterials as an alternative to lithography.

In this talk, I will introduce the development of artificial microstructures such as large-area anti-reflective moth-eye structures and terahertz meta-lenses for terahertz wave control using ultrashort pulse laser processing, which is under study in our group. We have succeeded in fabricating an anti-reflective moth-eye structure with nearly 100% transmittance in the sub-terahertz region [1,2] (Fig. 1) and further enlarged it to 300 mm in diameter [3]. This structure has been implemented in a radio telescope for the first time and is currently in operation. It has also been reported that Huygens membrane metalens in the terahertz frequency region can be fabricated by using lithography to create appropriately designed holes in a thin silicon substrate [4]. We have successfully fabricated similar meta-lenses with femtosecond lasers.

Such laser fabrication techniques for meta-optics have the potential to fabricate large-area structures that could not be made with conventional lithography, and to dramatically simplify fabrication methods.

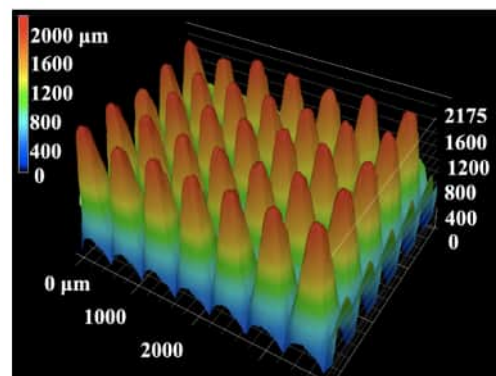


Fig. 1 Microscopic image of terahertz moth-eye structure fabricated by femtosecond laser processing.

References

- [1] Haruyuki Sakurai, Natsuki Nemoto, Kuniaki Konishi, Ryota Takaku, Yuki Sakurai, Nobuhiko Katayama, Tomotake Matsumura, Junji Yumoto, Makoto Kuwata-Gonokami, *OSA Continuum*, **2**, 2764 (2019).
- [2] R. Takaku, S. Hanany, H. Imada, H. Ishino, N. Katayama, K. Komatsu, K. Konishi, M. Kuwata-Gonokami, T. Matsumura, K. Mitsuda, H. Sakurai, Y. Sakurai, Q. Wen, N. Y. Yamasaki, K. Young, J. Yumoto, *Journal of Applied Physics* **128**, 225302 (2020).
- [3] Ryota Takaku, Qi Wen, Scott Cray, Mark Devlin, Simon Dicker, Shaul Hanany, Takashi Hasebe, Teruhito Iida, Nobuhiko Katayama, Kuniaki Konishi, Makoto Kuwata-Gonokami, Tomotake Matsumura, Norikatsu Mio, Haruyuki Sakurai, Yuki Sakurai, Ryohei Yamada, Junji Yumoto, *Optics Express* **29**, 41745-41765 (2021).
- [4] Yuki Hakamada, Mizuho Matoba, Haruyuki Sakurai, Kuniaki Konishi, "Fabrication of THz metalens by ultraviolet femtosecond laser ablation" SPIE Photonics West 2024 (San Francisco, USA)

Optoelectronic and optomechanical properties of atomically thin inorganic nanosheets as revealed by *in situ* TEM

Chao Zhang, Dmitri Golberg

Centre for Materials Science and School of Chemistry and Physics, Queensland University of Technology (QUT), 2 George, Brisbane, QLD 4000, Australia

dmitry.golberg@qut.edu.au

Free-standing few layered MoSe₂ nanosheet stacks' optoelectronic signatures were analyzed by using light compatible *in situ* transmission electron microscopy (TEM) utilizing an optical TEM holder allowing for the simultaneous mechanical deformation, electrical probing and light illumination of a sample [1]. Two types of deformation, namely (i) bending of nanosheets perpendicular to their basal atomic planes; and (ii) edge deformation parallel to the basal atomic planes, led to two distinctly different optomechanical performances of the nanosheet stacks. The former deformation induced a stable but rather marginal increase in photocurrent, whereas the latter mode was prone to unstable non-systematic photocurrent value changes and a red-shifted photocurrent spectrum. The experimental results were verified by *ab initio* calculations using density functional theory (DFT). The analogous experiments were continued on free-standing few-atomic-layer black phosphorus nanoflakes (Fig. 1) [2]. As compared to other 2-dimensional materials, the band gap of black phosphorus (BP) is related directly to multiple thicknesses and can be tuned by nanoflake thickness and strain. The photocurrent measurements with the TEM showed a stable response to infrared light illumination and change of nanoflakes band gap with deformation while pressing them between two electrodes assembled in the microscope. The photocurrent spectra of an 8-layer and a 6-layer BP nano-flake samples were then comparatively measured. DFT calculations were performed to identify the band structure changes of BP during deformations. The results provide useful pathways for BP smart band gap engineering *via* tuning the number of material atomic layers and programmed deformations to promote efficient optoelectronic applications.

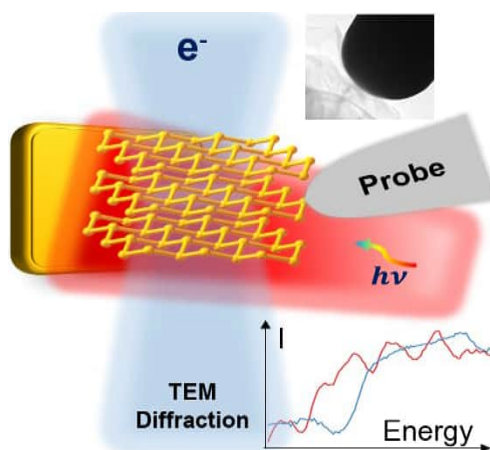


Figure 1. Schematic illustration of the *in situ* optoelectronic TEM setup for black phosphorus nanosheet optoelectronic response measurements. The inset is a low magnification TEM image illustrating the metal probe attached to the nanosheet in the microscope.

Acknowledgement

The authors are grateful to Prof. Dmitri Kvashnin of Emanuel Institute of Biochemical Physics, Russian Academy of Science, for supporting the regarded projects with Density Functional Theory (DFT) calculations. *In situ* TEM projects were supported by the Australian Research Council (ARC) in the frame of the Laureate Fellowship (D.G.) FL160100089.

References

- [1] C. Zhang, K. Larionov, K. Firestein, J.F.S. Fernando, C.-E. Lewis, P.B. Sorokin, D. Golberg *Nano Lett.* **22**, 673 (2022).
- [2] C. Zhang, A. Korovina, K.L. Firestein, J.F.S. Fernando, C.-E. Lewis, D.G. Kvashnin, D. Golberg *D. Small* (2023); doi: 10.1002/sml.202302455.

Nanocarbon materials for sub-THz thermomechanical bolometry

B. Bertoni^{1,2}, L. Alborghetti¹, M. Cojocari³, L. Vicarelli¹, A. Tredicucci^{1,2}, S. Roddaro^{1,2}, S. Zanotto², G. Fedorov³, P. Kuzhir³, P. Lamberti⁴, A. Pitanti^{1,2}

¹Dipartimento di Fisica, Università di Pisa, Largo B. Pontecorvo 3, 56127 Pisa – Italy

²CNR – Istituto Nanoscienze, piazza San Silvestro 12, 56127 Pisa – Italy

³Department of Physics and Mathematics, University of Eastern Finland, Yliopistonkatu 7, FI-80100, Joensuu – Finland

⁴Dept. of Information and Electrical Eng. and Applied Math., University of Salerno, via Giovanni Paolo II 132, Fisciano (SA) – Italy

alessandro.pitanti@unipi.it

1. Introduction

Imaging in the THz and sub-THz frequency range has been revealed as a strongly impacting technology to several fields ranging from security, quality control, in-vivo diagnostics and astrophysics [1]. In this research context, constraints for field applications and/or integration with existing technologies favour the use of uncooled (operating at room-temperature), fast detectors arranged in focal-plane arrays configuration, where an image “snapshot” can be acquired without the need for mechanical scanning.

Among the others, the concept of thermomechanical bolometers (TMB) has been recently introduced for far-infrared detection [2]. The basic concept of TMB devices relies on the frequency shift of the eigenfrequency of a mechanical resonator upon illumination-induced heating. Interesting metrics have been measured in preliminary trampoline resonator devices made of a 300/100nm Si₃N₄/Au bi-layer and measured with optical interferometry, with Noise-Equivalent-Power as low as 80 pW/sqrt(Hz) and roughly 20 Hz operating speed under a 140 GHz source illumination [2].

2. Advanced TMBs

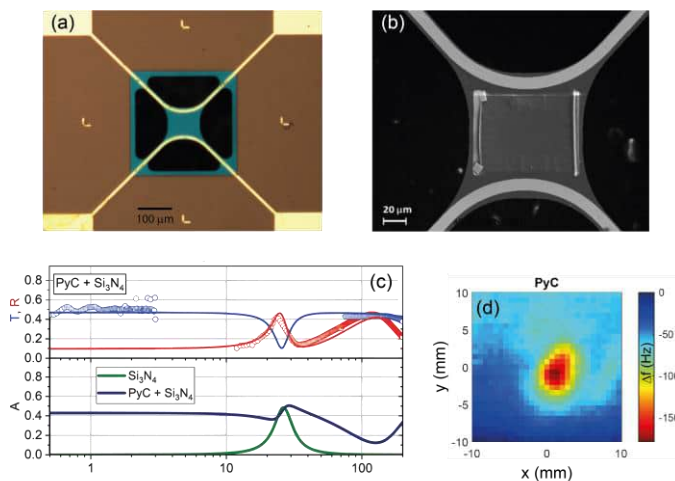


Fig. 1. (a): Microscope image of a typical TMB. (b): SEM of the PyC absorber integrated in the TMB. (c): Transmission and reflection spectra of a PyC film on Si₃N₄. Bottom panel shows estimated absorption obtained adding a 18 nm PyC film on the bare silicon nitride. (d): Beam profiling of the 140 GHz source using a PyC-TMB.

Micrograph of Fig. 1 (b). As expected, the presence of the PyC film greatly enhances the absorption in the range around 1 THz, as can be seen in the experimental data reported in Fig. 1 (c) and obtained for homogeneous coated and uncoated silicon nitride membranes [5]. Reaching a maximum absorption of 40 % with a minimally added mass, PyC films can benefit the sub-THz and THz TMBs performances, as can be seen by the sharp beam profiling image of Fig. 1 (d), obtained employed a PyC-TMB device.

3. Acknowledgement.

The authors acknowledge financial support of subproject H-Cube of EU ATTRACT phase 2 Research infrastructure H2020 (GA 101004462).

[1] *Fundamentals of Terahertz Devices and Applications*, edited by Dimitris Pavlidis, Wiley (2021)

[2] L. Vicarelli, A. Tredicucci and A. Pitanti, *ACS Phot.* **9**, 360 (2022)

[3] L. Gregorat et al., *submitted* (2024)

[4] P. Kuzhir et al., *J. Nanophotonics* **11**, 032504 (2017).

[5] J. Jorudas et al., *submitted* (2024)

Electro-optical terahertz modulators based on gallium nitride semiconductors

Irmantas Kašalynas, Daniil Pashnev, Justinas Jorudas, Surya Revanth Ayyagari,
Vytautas Janonis, Maxim Moscotin, Muhammad Sheraz, Liudvikas Subačius

THz Photonics Laboratory, Center for Physical Sciences and Technology (FTMC), Saulėtekio av. 3, LT-10257 Vilnius, Lithuania
irmantas.kasalynas@ftmc.lt

Semiconductors based on nitride and arsenide hold new promise for advancing custom-designed photonics and plasmonics, especially in the terahertz (THz) and infrared spectral ranges [1]–[3]. These materials are particularly attractive due to their potential applications in electro-optical modulation, where the control of electromagnetic wave amplitude and phase is essential. Such modulation finds uses in diverse fields such as wireless communications, quantum electronics, and spectroscopic imaging [4], [5].

In this presentation two types of electro-optical THz (EOT) modulators based on gallium nitride (GaN) semiconductors were investigated. The first modulator composed of high-quality n-GaN epilayers were used to operate under the regime of drifting space-charge (SC) domains [6]. The experiment revealed good polarization selectivity at test 0.6 THz frequency demonstrating amplitude modulation depth and maximum modulation speed values being up to 50% and 33 MHz, respectively. The maximum modulation amplitude was limited by an external electric field of about 1.65 kV/cm only. This value corresponded to the threshold at which the sample encountered electrical breakdown while operating within drifting SC domains. Notably, observed breakdown fields were significantly lower than the predicted critical electric field for GaN being of about 3.7 MV/cm [7].

Recent advancements in 2D plasmonics revealed their capability to modulate THz amplitude and phase at the temperature as high as 300 K, if one employs nano-grating-gate couplers with III-nitride group heterostructures providing high conductivity 2DEG layer [8], [9]. Near 2D plasmon resonance a significant modulation of the THz amplitude and phase retardation can be achieved; indeed, our group have demonstrated values of up to 50% and 25 degrees, respectively. The operation of such type of EOT can be efficiently controlled by gate voltage, that modify the resonant frequency of the 2D plasmon resonance, enabling precise control over the resonance characteristics of the device.

Both types of EOTs show potential for diverse applications in modulating THz waves for advanced communication and sensing systems [1]. However, devices employing 2D plasmon resonances offer rapid operation speeds, seamless integration possibilities with other semiconductor devices, and high modulation depth values reaching 100% in theory so far [10].

The authors acknowledge the Research Council of Lithuania (LMT) for the financial support under the "Hybrid plasmonic components for THz range (T-HP)" project GA 01.2.2-LMT-K-718-03-0096 and EU Research Council (ERC) for supporting the "Terahertz Photonics for Communications, Space, Security, Radio-Astronomy, and Material Science (TERAOPTICS)" project GA 956857 under the program H2020-EU.1.3.1. topic MSCA-ITN-2020.

References

- [1] A. Leitenstorfer et al., "The 2023 terahertz science and technology roadmap," *J. Phys. D: Appl. Phys.*, vol. 56, no. 22, p. 223001, Jun. 2023, doi: 10.1088/1361-6463/acbe4c.
- [2] V. Čižas et al., "Dissipative Parametric Gain in a $\text{GaAs}/\text{AlGaAs}$ Superlattice," *Phys. Rev. Lett.*, vol. 128, no. 23, p. 236802, Jun. 2022, doi: 10.1103/PhysRevLett.128.236802.
- [3] V. Janonis, J. Kacperski, A. Selskis, R. Balagula, and I. Kašalynas, "Directive and coherent thermal emission of hybrid surface plasmon-phonon polaritons in n-GaN gratings of linear and radial shapes," *Opt. Mater. Express*, vol. 13, no. 9, pp. 2662–2673, 2023, doi: 10.1364/OME.494777.
- [4] T. Kürner, D. M. Mittleman, and T. Nagatsuma, Eds., *THz Communications*, vol. 234. Cham: Springer International Publishing, 2022.
- [5] S. Boppel et al., "0.25- μm GaN TeraFETs Optimized as THz Power Detectors and Intensity-Gradient Sensors," *IEEE Trans. Terahertz Sci. Technol.*, vol. 6, no. 2, 2016, doi: x`.
- [6] R. M. Balagula, L. Subačius, P. Prystawko, and I. Kašalynas, "Electro-optical modulation of terahertz beam by drifting space-charge domains in n-GaN epilayers," *J. Appl. Phys.*, vol. 133, no. 20, May 2023, doi: 10.1063/5.0152661.
- [7] I. C. Kizilyalli, A. P. Edwards, O. Aktas, T. Prunty, and D. Bour, "Vertical power p-n diodes based on bulk GaN," *IEEE Trans. Electron Devices*, vol. 62, no. 2, pp. 414–422, 2015, doi: 10.1109/TED.2014.2360861.
- [8] P. Sai et al., "Electrical Tuning of Terahertz Plasmonic Crystal Phases," *Phys. Rev. X*, vol. 13, no. 4, p. 041003, Oct. 2023, doi: 10.1103/PhysRevX.13.041003.
- [9] D. Pashnev et al., "Experimental evidence of temperature dependent effective mass in AlGaIn/GaN heterostructures observed via THz spectroscopy of 2D plasmons," *Appl. Phys. Lett.*, vol. 117, no. 16, p. 162101, Oct. 2020, doi: 10.1063/5.0022600.
- [10] B. Sensale-Rodriguez et al., "Broadband graphene terahertz modulators enabled by intraband transitions," *Nat. Commun.*, vol. 3, no. 1, p. 780, Apr. 2012, doi: 10.1038/ncomms1787.

Investigation of nanostructured TiO₂

Ildiko Peter, Gabriela Strnad

George Emil Palade University of Medicine, Pharmacy, Science, and Technology of Targu Mures

Faculty of Engineering and Information Technology

Department of Industrial Engineering and Management

Str. N. Iorga nr. 1, Targu-Mures, 540139, Romania

Corresponding author e-mail (ildiko.peter@umfst.ro)

1. Abstract

Materials are very important in several fields. Nanostructured TiO₂ is a commonly investigated and employed material thanks to its some excellent properties related to its biocompatibility, non-toxic and semiconducting capacity and for the possibility to use it in dye-sensitized solar cells, biomedical fields, photocatalysis, etc. [1, 2]. At the end of 20th century some research reveals the viability to develop highly well-organized arrays of TiO₂ nanotubes employing a simple procedure, like electrochemical anodization on a metallic Ti surface and the investigation on such topic has been continued during the time. By exploring the possibility of developing and modifying the properties of such structures is possible to use them in a wide range of applications. Other studies confirmed that creating disorder into regular nanostructure specific optical behaviors are obtained [3]. Using electrochemical anodization (EA), where the interested material is introduced in an anodization cell, and by employing different procedure settings, as current parameters, electrolyte type, and anodization time, self-arranged nanotubular TiO₂ can be obtained. The mechanism of nanotubes development is complex and arises when the formation of oxide at the metal-oxide interface and its etching at the oxide-electrolyte interface are in competition.

Our study is integrated in this large research topic and here some results on the development and characterization of nanostructured TiO₂ layer on Ti alloys metallic substrates will be shortly presented. Even if such layers were developed for biomedical purposes, the same process can be used also for materials for photonics and/or optoelectronics applications. The experimental setup for electrochemical anodization (Fig. 1a) of the samples was of two electrode types. For each experiment the samples were positioned at the anode and the cathode was a 20 mm diameter disc in pure Cu. For the two types of electrolyte were employed, one of them aqueous electrolyte (1M H₃PO₄ + 0.5 wt% HF), and the other one organic electrolyte (0.5 wt% NH₄F + 2 wt% H₂O + ethylene glycol). The current was supplied by a programmable dual range DC power supply 9184B (BK Precision). Experiments in aqueous electrolyte were made at an anodization potential U = 20 V, applied with an initial ramp Ur = 0.2 V/s, for a duration T = 30 min. When using organic electrolyte anodization potential was U = 20, 40, and 60 V, Ur = 1 V/s, and duration T = 10, and 30 min. In house realized Nanosource2 software was used to supervise the anodization tests, and to check and record the process parameters. After anodization, the samples have been cleaned and investigated. Microstructural analysis confirms the nanostructured nature of the layers as reported in Fig.1b. More details on the results can be found in [4].

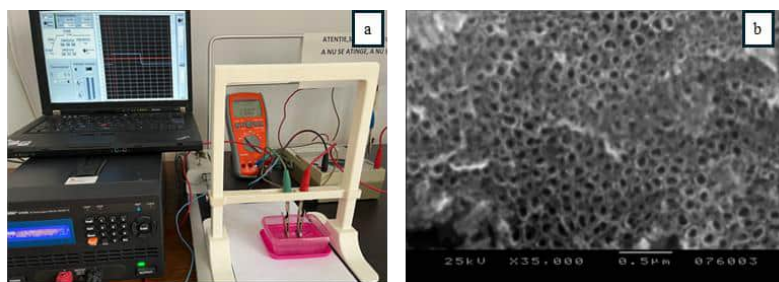


Fig. 1. The designed and built experimental setup and image (a) during the electrochemical anodization experiments and (b) SEM image of the nanostructured layer.

2. References

- [1] Cotton, J.D.; Briggs, R.D.; Boyer, R.R. et al. State of the Art in Beta Titanium Alloys for Airframe Applications, JOM, 2015, 67, 1281–1303. <https://doi.org/10.1007/s11837-015-1442-4>.
- [2] Sarimov, R.M.; Glinushkin, A.P.; Sevostyanov, M.A.; Konushkin, S.V.; Serov, D.A.; Astashev, M.E.; Lednev, V.N.; Yanykin, D.V.; Sibirev, A.V.; Smirnov, A.A.; Baimler, I.V.; Simakin, A.V.; Bunkin, N.F.; Gudkov, S.V. Ti-20Nb-10Ta-5Zr Is Biosafe Alloy for Building of Ecofriendly Greenhouse Framework of New Generation. Metals, 2022, 12, 2007. <https://doi.org/10.3390/met12122007>
- [3] Guo, M., Xie, K., Wang, Y. et al. Aperiodic TiO₂ Nanotube Photonic Crystal: Full-Visible-Spectrum Solar Light Harvesting in Photovoltaic Devices. Sci Rep 4, 6442 (2014). <https://doi.org/10.1038/srep06442>.
- [4] Strnad, G.; Jakab-Farkas, L.; Gobber, F.S.; Peter, I. Synthesis and Characterization of Nanostructured Oxide Layers on Ti-Nb-Zr-Ta and Ti-Nb-Zr-Fe Biomedical Alloys. J. Funct. Biomater. 2023, 14, 180. <https://doi.org/10.3390/jfb14040180>

3D FDTD-LLG modelling of magnetisation dynamics in thin film ferromagnetic structures.

Feodor Y. Ogrin

*MaxLLG Ltd. Exeter, United Kingdom
f.y.ogrin@maxllg.com*

There is a growing need in high frequency tunable microwave materials for applications in the areas of microwave electronics, transformation optics, photonics. Due to their intrinsic RF phenomena, such as FMR, ferromagnetic thin films have always been of great interest and led to a great amount of experimental research very often supported by numerical simulations. While purely magnetostatic solvers, such as OOMMF or Mumax, have always been the standard benchmark tools and usually provide a precise description of the magnetisation processes in thin-film ferromagnetic structures, these systems are however limited in applications where full electromagnetic solutions are required, especially when the material properties are extremely non-uniform (e.g. dielectric/metal interfaces). In such cases one needs to consider a modelling approach where a full solution of Maxwell equations is needed alongside the materialistic equations, such as e.g. Landau-Lifshits-Gilbert (LLG) providing the relation between the magnetisation and the magnetic field [1]. Here we propose such a model which uses 3D finite-difference-time-domain (FDTD) approach together with LLG to find the exact solutions for magnetisation dynamics in thin film ferromagnetic structures [2]. As a benchmark testing we demonstrate application of such model for different classical phenomena such as Faraday effect, and then explore the dynamic characteristics of thin films in magnetostatic applications. In particular we consider propagation of magnetostatic/spin waves in metallised magneto-dielectric thin films and magnetic structures and demonstrate their dispersion characteristics [3]. The results are compared with the standard analytical solutions and the simulations by using Mumax³. We also discuss the advantages of the model and its limitations for using in realistic prototype materials.

References

- [1] M. M. Aziz, Progress In Electromagnetics Research B 15, (2009) 1–29.
- [2] <https://www.maxllg.com/>
- [3] A.G. Gurevich and G.A. Melkov, "Magnetisation oscillations and waves", CRC press, 1996, R.W. Roberts et al. J. Appl. Phys. V33. (1962) 1267

3D-printed low-loss functional hollow waveguide devices for 200-400 GHz band

Junji Yumoto

Institute for Photon Science and Technology, The University of Tokyo
yumoto@ipst.s.u-tokyo.ac.jp

The use of electromagnetic waves in the sub-THz band (0.1–1 THz) is becoming increasingly important for future wireless communications, sensors, radio astronomy, and other applications. Research on elemental technologies and system demonstrations in the sub-THz band is advancing rapidly, contributing to the development of Beyond 5G and 6G technologies. To address the challenges of high-frequency signal transmission through cables, smaller cross-sectional metallic waveguides are employed to propagate wireless signals. As the frequency increases, the cross-sectional size of the waveguide decreases; for instance, the standardized size for the 300 GHz band is WR-3 (a cross-section of waveguides: $0.86 \times 0.43 \text{ mm}^2$). These structures are regarded known as sub-mm scale hollow structures with high aspect ratios (smsHS) in bulk metal, are increasingly difficult to fabricate using conventional machining.

3D printers facilitate the creation of hollow structures, including those with high aspect ratios, through their layering process. Despite numerous studies on 3D printing, fabricating smsHS structures for sub-THz waveguide devices remains a significant challenge. To address this, we developed a novel UV-curable resin type 3D printer, RECILS[1], which achieves palm-sized fabrication with the desired resolution of 20–30 μm . However, the objects fabricated with RECILS hinder the confinement of electromagnetic waves. A promising solution is to coat the surface of RECILS-printed objects with metal, thus enabling wave confinement.

This talk presents a novel fabrication technique for waveguide devices in the 200–400 GHz range. Our method integrates smsHS fabrication using RECILS with metal plating on the surfaces of hollow structures and flanges, a process we refer to as RECILS WG Fabrication Technology (RECILS WGFT) [2].

Figure 1 depicts a waveguide with standardized UG387 flanges fabricated by RECILS WGFT. This straight waveguide has a cross-section of $0.86 \times 0.43 \text{ mm}^2$ and measures 25.4 mm in length. Its hollow structure and flanges are coated with nickel (Ni) and copper (Cu). The measured insertion losses for these straight waveguides range from 0.5 to 0.8 dB per inch in the 200–400 GHz frequency band, comparable to those of bulk metal waveguides.

Bandpass filter (BPF) waveguide devices, fabricated using RECILS WGFT, incorporate five internal resonators interconnected by a cavity iris, as shown in Fig. 2(a), which presents an X-ray CT image. Fig. 2(b) displays the performance characteristics of three BPFs with resonator lengths L of 410, 440, and 490 μm . The insertion loss in the passband and the extinction ratio were approximately 1 dB and over 30 dB, respectively.

Waveguide devices in the sub-THz band fabricated with RECILS WGFT demonstrate low-loss and lightweight properties, showing significant promise in this domain. The ability to produce twisted, bent or spiral waveguides further underscores the potential of this technology. Continued advancements are expected to usher in a new era of 3D integrated waveguide circuits in the sub-THz band.

[1] Kentaro Soeda, Hirosuke Suzuki, Shuichi Yokobori, Kuniaki Konishi, Hiroharu Tamaru, Norikatsu Mio, Makoto Kuwata-Gonokami and Junji Yumoto, Lasers in Manufacturing Conference 2021 Proceedings, https://wlt.de/sites/default/files/2021-10/system_technology_process_control/Contribution_322.pdf, (2021).

[2] Kentaro Soeda, Kazunori Naganuma, Yoshinori Yamaguchi, Kuniaki Konishi, Hiroharu Tamaru, Norikatsu Mio, Hiroshi Itoh and Junji Yumoto, SPIE Photonics West, Paper 12885-45, January 2024.



Fig. 1 RECILS-printed straight waveguide for 200–400 GHz

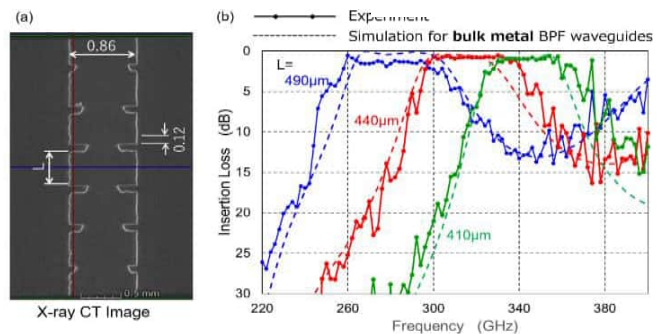


Fig. 2 (a) X-ray CT image of BPF waveguide. (b) Insertion loss of 3 BPF waveguides with L of 490 μm (blue), 440 μm (green), and 410 μm (green). Broken lines represent simulations assuming bulk metal BPF waveguides having the same structures.

Experimental activities on graphene in the sub-THz range

G. Virone^a, F. Paonessa^a, M. U. Riaz^{ad}, G. V. Bianco^b, G. Bruno^b, A. D'Orazio^c, L. Matekovits^{ad}

^aConsiglio Nazionale delle Ricerche, IEIIT, C.so Duca degli Abruzzi 24, 10129, Turin, Italy

^bConsiglio Nazionale delle Ricerche, NANOTEC, via Orabona, 4, 70125 Bari, Italy

^cPolitecnico di Bari, Dipartimento di Ingegneria Elettrica e dell'Informazione, Via Orabona 4, 70125 Bari, Italy

^dPolitecnico di Torino, DET, C.so Duca degli Abruzzi, 24 - 10129 Turin, Italy

giuseppe.virone@cnr.it

1. Introduction

The main challenges for future wireless communications are terabit-per-second data rate and coverage everywhere. Such performance could be achieved by exploiting the sub-THz frequency regime (100 GHz – 1 THz) [1], in both Terrestrial and Non-Terrestrial Networks. One of the key-enabling subsystems to operate in the sub-THz frequency range is the antenna. In modern communication environments, the antenna system generally consists of antenna arrays and reflective/refracting surfaces. The present research activities on these topics require advanced materials with good electrical properties (to achieve efficient devices) and a high degree of reconfigurability [2]. These challenges motivate the research line on graphene at sub-THz.

2. The experimental activity

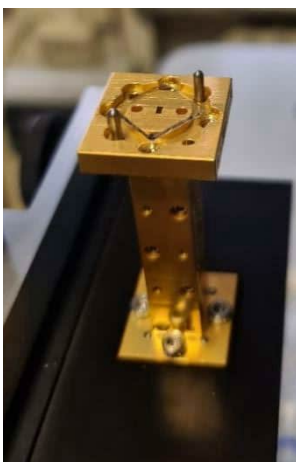


Fig. 1. Example of waveguide-based experimental setup in the 110-170 GHz frequency band

Previous studies demonstrated that reconfigurable absorbers [2], and screens [3], can be obtained in X-band (7-13 GHz) with properly designed graphene layers. Ongoing projects aim at extending these results in the millimeter-wave range (above 30 GHz) [4], and beyond (sub-THz). Such activities require a complete characterization of the properties of the adopted advanced material(s). To this end, we are developing a set of experimental setups to characterize multilayer Chemical Vapor Deposition, CVD, graphene samples in the 65-750 GHz frequency range. An example is shown in Fig. 1. The gold-plated metal waveguide is connected to a millimeter-wave extender (black surface) which is then connected to a Vector Network Analyzer (not visible). The square-shaped glass sample (of edge length of 8.5 mm) is placed on top of the waveguide interface/flange. The graphene layers are transferred on one side of the glass sample. The electromagnetic field is excited/probed through the rectangular aperture (open-ended waveguide 1.6 mm x 0.8 mm) at the center of the top metal flange. This measurement configuration is simpler than the one reported in [5], where lens-based horns were adopted. Consequently, it will allow for an accurate modeling of the electromagnetic environment, leading to a more precise estimation of the material parameters. Moreover, the present measurement setup can be easily calibrated by connecting known devices to the upper waveguide flange.

The results of a measurement campaign carried out on multilayer graphene samples will be presented at the workshop along with possible device configuration that could be developed accordingly.

3. Acknowledgement.

This work was supported by the European Union under the Italian National Recovery and Resilience Plan (NRRP) of NextGenerationEU, partnership on "Telecommunications of the Future" (PE00000001 - RESTART).

The measurement setup is part of the PNRR Infrastructure named Earth-Moon-Mars (EMM), IR0000038 – CUP: C53C22000870006.

4. References

- [1] Wei Jiang, Qiheng Zhang, Jiguang He, et al., Terahertz Communications and Sensing for 6G and Beyond: A Comprehensive View. TechRxiv. June 22, 2023.
- [2] Grande, M., Bianco, G.V., Perna, F.M. et al., Reconfigurable and optically transparent microwave absorbers based on deep eutectic solvent-gated graphene. Sci Rep 9, 5463 (2019). <https://doi.org/10.1038/s41598-019-41806-w>
- [3] M. Grande, G. V. Bianco, M. A. Vincenti, D. de Ceglia, P. Capezzuto, V. Petruzzelli, M. Scalora, G. Bruno, and A. D'Orazio, Optically transparent microwave screens based on engineered graphene layers, Opt. Express 24, 22788-22795 (2016)
- [4] Magno, G., Caramia, L., Bianco, G.V. et al., Design of optically transparent metasurfaces based on CVD graphene for mmWave applications. Sci Rep 13, 4920 (2023). <https://doi.org/10.1038/s41598-023-31298-0>
- [5] Ehsan Dadrasnja, Sujitha Puthukodan, Vinod V. K. Thalakkatukalathil, Horacio Lamela, Guillaume Ducournau, Jean-Francois Lampin, Frédéric Garet, Jean-Louis Coutaz, Sub-THz Characterisation of Monolayer Graphene, Journal of Spectroscopy, vol. 2014, Article ID 601059, 6 pages, 2014. <https://doi.org/10.1155/2014/601059>

High-Q Factor Dual-Layer Anapole Metamaterial for sub-THz range

M. Cojocari⁽¹⁾, G. Matveev⁽¹⁾, L. Matekovits⁽²⁾, Gianluca Dassano⁽²⁾, P. Kuzhir⁽¹⁾, and A. Basharin⁽¹⁾

(1) Center for Photonics Sciences, Department of Physics and Mathematics, University of Eastern Finland, Yliopistonkatu, 80140, Joensuu, Finland

(2) Department of Electronics and Telecommunications, Politecnico di Torino, Corso Duca degli Abruzzi 24, 10129, Turin, Italy
maria.cojocari@uef.fi

Simulation results and experimental study are presented for a dual-layer metamaterial displaying a resonance with a Q-factor of 4000 in the sub-THz frequency range, achieved by combining resonances from two complementary planar metamaterials. The initial layer, constituting the original metamaterial, is comprised of metallic unit-cells shaped like epsilon letters and is based on a high Q-factor planar toroidal metamaterial [1]. This metamaterial exhibits significant localization of electromagnetic energy in the near field region rather than in the radiation zone due to the interference of toroidal and electric dipole moments with identical radiation patterns in the far zone. The second layer, which complements the first one, is composed of a metallic layer with cutouts in the epsilon letter shape [2]. Individually, the original metamaterial depicts a high Q-factor resonance and confines the electric field of the incident wave. Conversely, the inverted structure does not respond to the incident wave but is instead stimulated by near-field interaction with the original metamaterial. The observed low losses can be ascribed to the interaction between the two most significant multipoles excited within the metamaterials [3]. In the case of the original metamaterial, this interaction entails interference between toroidal and electric dipole moments, resulting in an anapole formation. Conversely, the properties of the inverted metamaterial arise from the interaction between toroidal dipole and magnetic quadrupole moments. Both metamaterials are manufactured as free-standing to evade dielectric losses from the substrate, which could considerably reduce the Q-factor of the resonance. The simulated metamaterial (Fig.1a) is stimulated with the wave polarized along the wires of the metamolecules of the original type, enabling the support of dual loops of currents along the voids, leading to toroidal excitation. The inverted structure, rotated to complement the original one, does not exhibit excited currents with the wave's set polarization; instead, it is activated by near-field interaction with the original metamaterial. Transmission spectra of the metamaterials at varying distances are depicted in Fig. 1b, with optimal outcomes attained at a distance of 0.8 mm. The metamaterials were created using a xTool laser cutter on a 50nm brass film, with the original and inverted structures comprising 10x10 metamolecules of 1.3 mm radius and periods of 2.60 mm and 2.55 mm, respectively. Experimental transmission spectra (Fig.1c) were gauged utilizing a Keysight PNA Network Analyzer with VNA Extenders WR-12. The layers were contained in 3D-printed holders separated by spacers ranging from 0.6 to 2 mm in thickness. The most prominent resonance, with a Q-factor close to 4000, was noted at a distance of 0.8 mm, similar to the simulation.

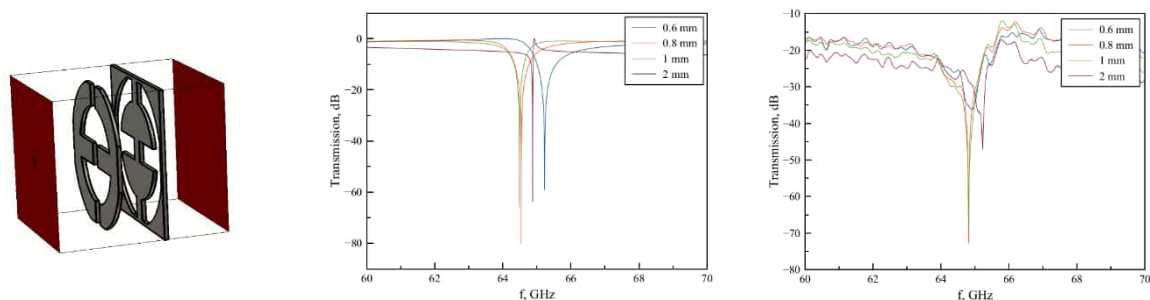


Figure 1.: a) metamaterial model, b) simulated and c) experimental metamaterial transmission spectra for different distances between the layers.

In conclusion, a new dual-layer metamaterial configuration with a high Q-factor resonance in the sub-THz frequency range has been introduced. Through simulations and experiments, the efficacy of this configuration combining responses from two complementary planar metamaterials has been illustrated.

[1] A. Basharin, V. Chuguevsky, N. Volsky, M. Kafesaki, E. N. Economou, "Extremely high Q-factor metamaterials due to anapole excitation", *Phys. Rev.B* 95 (3), 035104, 2017.

[2] M. V. Cojocari, A. K. Ospanova, V. I Chichkov, M. Navarro-Cia, A. Gorodetsky, A. A. Basharin, "Pseudo-anapole regime in terahertz metasurfaces" *Phys. Rev. B*, 104(7), 075408, 2021.

[3] M. V. Cojocari, A. A. Basharin, "Spatial Separation Of Electric And Magnetic Fields In Toroidal Metamaterial", In *Novel Optical Materials and Applications* (pp. NoW1D-4). Optica Publishing Group, 2018

Poster session



©P.Obraztsov

Integration of 2D materials in suspended MEMS devices

B. Bertoni^{*1,2}, L. Alborghetti¹, S. Zanotto², L. Vicarelli¹, A. Tredicucci¹, S. Roddaro^{1,2} and A. Pitanti¹

¹Dipartimento di Fisica, Università di Pisa, Largo B. Pontecorvo 3, 56127 Pisa – Italy

²CNR – Istituto Nanoscienze, piazza San Silvestro 12, 56127 Pisa – Italy

*benedetta.bertoni@nano.cnr.it

1. Introduction

Micro-electromechanical system (MEMS) resonators are small suspended structures, typically ranging in size from 10 to 1000 μm , that vibrate at specific resonant frequencies. Their peculiar frequency response has been used as the key mechanism for sensing applications of , among others, temperature [1], position [2] and mass.

The possibility of achieving high measurements sensitivity is mainly due to a large Q factor, that can be tailored employing innovative mechanical solutions such as soft clamping and dissipation dilution.

An interesting route sees the combination of MEMS with weightless and stiff 2D materials (2DM) which can be used to enhance the device functionalities or exploit its existing capabilities to tune and investigate the material itself. Transferring the 2DM after the whole MEMS has been fully fabricated offers a large degree of flexibility and an optimal conservation of the 2DM quality, being essentially unexposed to any wet/dry etching process.

This combined platform offers several interesting advantages; for instance, the tunable thermal conductivity of MEMS can be exploited to investigate the 2DM properties under local heating. Furthermore, the MEMS mechanical motion can be used to impart a dynamic stress on the material, which would be of interest for photoluminescent transition metal dichalcogenides, such as MoS₂ and WS₂, where strain-dependent photoluminescent has been demonstrated at room temperature [3]. Finally, the 2DM can be employed as ultra-thin absorbers in broadband thermomechanical microbolometers (TB) [4].

2. 2DM as absorbers in TBs

In our work, we integrated ultra-thin (almost 2D) graphitic materials in silicon nitride (SiN) trampoline TBs in order to boost the overall absorbance, hence the detection responsivity, without impacting on the mechanical quality of the resonator. We chose graphene, specifically multi-layer graphene (MLG) due to its tunable conductivity, which is strongly linked to its absorption spectra.

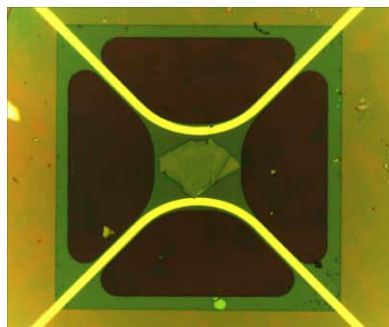


Figure 1: Optical microscope image of a MLG flake deposited at the center of the trampoline membrane.

The transfer technique is based on a multilayer PPMA-PVA vector, which allows us to precisely place the exfoliated MLG on a device region where it is enhancing its properties without impacting its operation, see Figure 1.

Measuring the absorbance in the mid-IR range we found an average value of 30%, while SiN is basically transparent over a broad spectrum region.

Showing a substantial absorption enhancement over the bare TB trampoline, our approach offers interesting possibilities for material investigation and enhanced devices.

3. Acknowledgement

The authors acknowledge financial support of subproject H-Cube of EU ATTRACT phase 2 Research infrastructure H2020 (GA 101004462).

[1]X. Song, H. Liu, Y. Fang, C. Zhao, Z. Qu, Q. Wang and L. Tu, *Sensors* 2020, 20(13), 3652

[2] M. Chien, J. Steurer, P. Sadeghi, N. Cazier, and S.Schmid, *ACS Phot* 7,8, 2197–2203 (2020)

[3]X. He, H. Li, Z. Zhu, Z. Dai; Y. Yang,P.Yang,Q.Zhang, P.Li, U. Schwingschlogl, X.Zhang, *Appl. Phys. Lett.* 109, 173105 (2016)

[4] L. Vicarelli, A. Tredicucci and A. Pitanti, *ACS Phot.* 9, 360 (2022)

Amorphous carbon nanoparticles obtained from anodic alumina/carbon composites

Katsiaryna Chernyakova, Giedrė Grincienė, Renata Karpicz

State Research Institute Center for Physical Sciences and Technology, Saulėtekio Ave. 3, LT-10257 Vilnius, Lithuania
Corresponding author e-mail katsiaryna.charniakova@ftmc.lt

Carbon nanoparticles (CNPs) are a new class of carbon nanomaterials suitable for biological applications due to their chemical stability, non-toxicity, biocompatibility, low cost, and well-defined luminescence signal with tunable wavelength options. In this study, we synthesized and characterized fluorescent amorphous carbon nanoparticles obtained by dissolving anodic alumina/carbon composites. Anodic alumina/carbon composites were obtained by electrochemical oxidation of pure Al foil (100 μm , AlfaAesar) in a complex electrolyte containing formic acid, ammonium heptamolybdate, and oxalic acid at 60 V and 80 V (constant voltage mode), 18 °C for 120 min. The Pt grid was used as a counter electrode. Then, Al was etched, and the resulting films were dissolved in a hot aqueous solution of 0.1 M HCl. The resulting solutions were dialyzed (to wash away Al^{3+} ions), centrifugated, and filtrated. The pH of the final solutions was ca. 5–6.

The morphology, composition, and fluorescence (FL) properties of CNPs were characterized. According to the TEM studies, CNPs were 20–25 nm in diameter. The zeta potential of the CNP solutions showed a single negative peak at -29.2 mV with a width of 8.20 mV. The value and sign of potential indicate that CNPs are stable in water solutions, and the surface of CNPs has negatively charged moieties, such as C=O, C–O, and O–H. Surface-enhanced Raman spectroscopy confirmed the amorphous nature of CNPs: two predominant peaks observed at 1365 cm^{-1} and 1600 cm^{-1} can be attributed to the D-band and G-band, respectively. The intensity ratio of the G- to D-band peak was 2.20, indicating that the synthesized CNPs mainly comprise sp^2 graphitic carbons with sp^3 carbon defects originating from oxygen-containing groups. CNPs exhibited an excitation-dependent emission behavior at 280–450 nm excitation wavelengths with average lifetimes of 7.25–8.04 ns. In our case, average lifetimes are longer than in the case of CNPs synthesized electrochemically and solvothermally and comparable with those of hydroxyl-coated CNPs (9.5 ns). The origin of the FL of CNPs can be explained by the presence of two different FL centers, namely the core of CNPs and various emission centers on the CNP surface: carbonyl, carboxyl, and hydroxyl groups. As CNPs could be exceptional candidates for detection technologies, the biocompatibility assays were performed with living COS-7 mammalian cells, showing a minimal negative impact on the living cells.

Acknowledgments

Research partially supported by the Research Council of Lithuania (LMTLT) agreement No S-MIP-23-70, by Horizon Europe FLORIN Project No. 101086142 and by the Central Project Management Agency (CPMA) agreement No 10-038-T-0037.

Fabrication and characterization of THz meta-lens by ultraviolet femtosecond laser ablation

Y. Hakamada^a, M. Matoba^b, H. Sakurai^b, K. Konishi^b

^aDept. of Phys, Univ. of Tokyo/7-3-1 Hongo, Bunkyo-ku, Tokyo, Japan 113-0033; ^bInstitute for Photon Science and Technology, Univ. of Tokyo/7-3-1 Hongo, Bunkyo-ku, Tokyo, Japan 113-0033
kkonishi@ipst.s.u-tokyo.ac.jp

In recent years, various applications of terahertz (THz) waves have been proposed, including high-speed communication and imaging [1]. THz optical elements are essential to realize these applications.

Metasurfaces are optical elements which achieve a designed functionality by tailoring the optical response of wavelength-scale structures. Metasurfaces have made it possible to design optical elements which are not limited by bulk material properties. In particular, meta-lenses, or metasurfaces tailored for light-focusing performance, have attracted much attention for their potential to realize ultimately thin lenses [2]. Recently, it has gained attention that highly efficient meta-lenses can be designed by using Mie resonance in subwavelength dielectric structures [3]. In particular, a THz membrane meta-lens realized by forming through-holes several hundred micrometers in diameter in a Si thin film was proposed, demonstrating impressive focusing performance and efficiency [4]. Typically, the fabrication of such meta-lenses necessitates the utilization of lithography technology. This involves the operation of various specialized devices and chemicals in a cleanroom environment. Consequently, the processing procedure becomes costly and complicated; to improve the practicality of meta-lens technology, a simplified fabrication method is desired.

Femtosecond laser processing is capable of micrometer-order, high-precision processing and has been shown to be applicable to the fabrication of THz optics [5]. Using such technology, we reported on the fabrication of a free-standing membrane meta-lens with a 20 mm diameter and 30 mm focal distance for a design frequency of 0.8 THz [6]. An optical microscope image of the laser fabricated meta-lens is shown in Fig.1(a). The focusing performance of this meta-lens was found to be comparable to that of commercial polymer-type THz lenses, and was able to focus THz light to a spot diameter of approximately 1 mm in diameter, as measured by a THz camera (Fig.1 (b)). In this work, we compare the performance of this lens with that of a 3D simulation model. By considering both the spectral width of the evaluating THz wave and the camera spectral sensitivity, we find good agreement in the focus profile between both simulation and experimental results, showing that the lens has high potential designability (Fig.1 (c)). This result demonstrates that laser processing is available option for THz meta-lens fabrication and establishes a simple meta-lens fabrication technique.

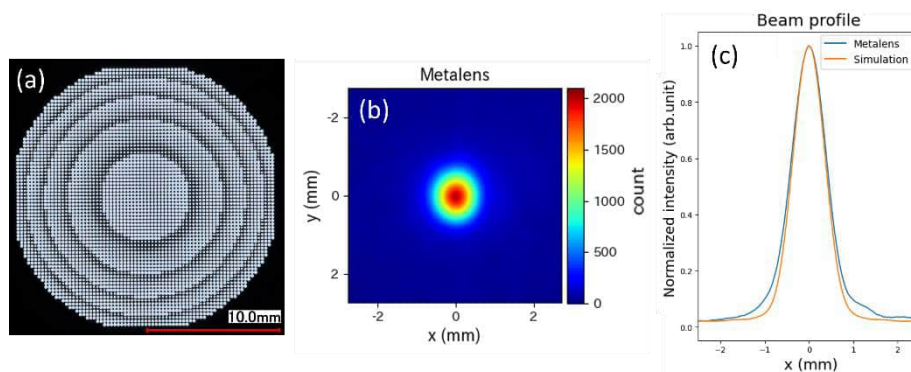


Fig.1 (a) Microscopic images of the fabricated THz metalens. (b) The profile at the focal point achieved by the membrane meta-lens, observed by a THz camera. (c) Full width at half maximum of meta-lens and simulation results at the focal point

References

- [1] Huang, Y., Shen, Y. and Wang, J., "From Terahertz Imaging to Terahertz Wireless Communications," Proc. Est. Acad. Sci. Eng. 22, 106–124 (2023).
- [2] Moon, S.-W., Kim, Y., Yoon, G. and Rho, J., "Recent Progress on Ultrathin Metalenses for Flat Optics," iScience 23(12), 101877 (2020).
- [3] Liu, W. and Kivshar, Y. S., "Generalized Kerker effects in nanophotonics and meta-optics [Invited]," Opt. Express 26(10), 13085–13105 (2018).
- [4] Yang, Q., Kruk, S., Xu, Y., Wang, Q., Srivastava, Y. K., Koshelev, K., Kravchenko, I., Singh, R., Han, J., Kivshar, Y. and Shadrivov, I., "Mie - resonant membrane Huygens' metasurfaces," Adv. Funct. Mater. 30(4), 1906851 (2020).
- [5] Sakurai, H., Nemoto, N., Konishi, K., Takaku, R., Sakurai, Y., Katayama, N., Matsumura, T., Yumoto, J. and Kuwata-Gonokami, M., "Terahertz broadband anti-reflection moth-eye structures fabricated by femtosecond laser processing," OSA Contin. 2(9), 2764 (2019).
- [6] Hakamada, Y., Matoba, M., Sakurai, H., Konishi, K., "Fabrication of THz metalens by ultraviolet femtosecond laser ablation," Proc. SPIE 12885, 48-51 (2024).

Fluorescence concentration quenching in Zinc-containing as well as non-containing phthalocyanines

Ivan Halimski¹, Simona Streckaitė¹, Jevgenij Chmeliov^{1,2}, Andrius Gelzinis^{1,2}, Leonas Valkunas¹

¹Center for Physical Sciences and Technology, Saulėtekio Ave. 3, Vilnius, LT-10257, Lithuania

²Institute of Chemical Physics, Faculty of Physics, Vilnius University, Saulėtekio Ave. 9-III, Vilnius, LT-10222, Lithuania
ivan.halimski@ftmc.lt

Concentration quenching (CQ) [1,2] of fluorescence (FL) is a phenomenon of FL quantum yield decreasing with molecular concentration increasing. CQ is observed in various systems—from synthetic dyes to natural systems, e.g., chlorophylls. Since CQ results in loss of energy, it is important to understand how it can be controlled.

CQ can be observed both in thin films and in liquids. However, it is difficult to observe CQ of high concentrated solutions due to reabsorption effects [3], which affects both steady-state and time-resolved fluorescence. Using cuvettes as thin as possible could be a solution to avoid reabsorption.

In this work CQ is investigated in solutions (prepared in chloroform in thinnest commercially available borosilicate glasses) of Zinc 2,9,16,23-tetra-tert-butyl-29H,31H-phthalocyanine (ZnTTB; see Fig. 1a) and 2,9,16,23-tetra-tert-butyl-29H,31H-phthalocyanine (TTB; see Fig. 1b). The materials are of their own interest. They could be used as good model systems of close chlorophyll-containing systems, or as a model of artificial photosynthetic antenna; also, phthalocyanines themselves are used in organic solar cells and for photodynamic therapy.

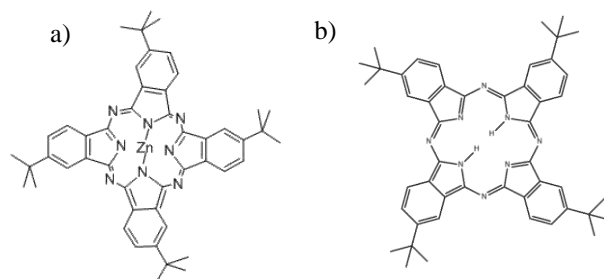


Fig. 1. Molecular structures of ZnTTB (a) and TTB (b).

We studied CQ by varying concentration of phthalocyanine by two orders of magnitude, from 0.1mM up to 10mM, and recoding FL decay kinetics (see Fig. 2a) together with FL spectrum (Fig. 2b). While FL spectra remain the same, FL kinetics clearly exhibit faster non-exponential decay at higher concentration. Each kinetics is analyzed with single- and double-exponential decay and stretched-exponential decay $\exp[-(t/\tau)^b]$, where parameter b indicates the deviation from single-exponential kinetics. CQ is explained in the terms of donor–trap model, where a single donor molecule is surrounded by an infinite number of acceptors. For this reason, all the kinetics are additionally fitted with $\exp[-t/\tau_D - (t/\tau_2)^{1/2}]$ function (called ‘DAC’), where τ_D is the decay rate of excited donor molecule in the absence of acceptors and τ_2 represents quenching due to acceptors. A detailed analysis and supporting information will be provided during the conference.

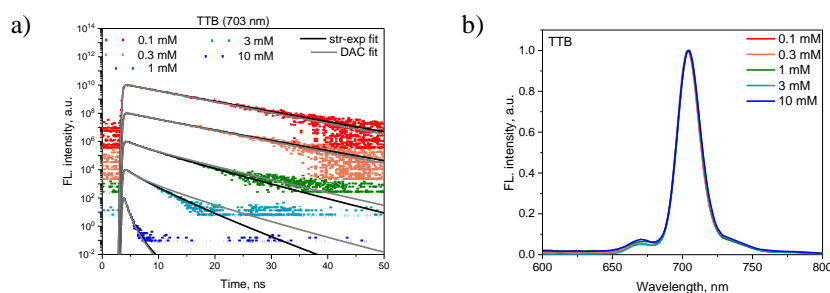


Fig. 2. FL kinetics (a) and spectrum (b) of TTB.

References

- [1] J. Tamošiūnaitė, S. Streckaitė, J. Chmeliov, L. Valkunas and A. Gelzinis, *Chemical Physics*, **572**, 111949 (2023).
- [2] S. Barysaitė, J. Chmeliov, L. Valkunas and A. Gelzinis, *The Journal of Physical Chemistry B*, In Press, 2024.
- [3] S. Dhami, A.J. De Mello, G. Rumbles, S.M. Bishop, D. Phillips and A. Beeby. *Photochemistry and Photobiology*, **61** (4), 341–346 (1995).

Designing Bull's eye structures for non-destructive inspection using GHz waves and carbon nanotube film

Masakazu Konishi¹, Hiroki Okawa², Shun Hashiyada³, Yuto Matsuzaki¹, Qi Zhang¹, Kou Li¹, Yoshito Tanaka³, and Yukio Kawano^{1,2,4}

¹Department of Science and Engineering, Chuo University, 1-13-27 Kasuga, Bunkyo, Tokyo, Japan

²Kanagawa Institute of Science and Technology, 705-1, Shimo-Imaizumi, Ebina, Kanagawa, Japan

³Research Institute for Electronic Science, Hokkaido University, Kita21, Nishi 10, Kita-ku, Sapporo, Hokkaido, Japan

⁴National Institute of Informatics, 2-1-2 Hitotsubashi, Chiyoda, Tokyo, Japan
a19.wdtg@g.chuo-u.ac.jp

1. Introduction

Corrosion of metals in concrete due to aging is an important problem in reinforced concrete buildings. Recently, we have developed a method to measure metal corrosion inside concrete using GHz wave [1]. We have also demonstrated that our carbon nanotube (CNT) sensor can detect GHz waves, enabling its applications in non-destructive inspection [2]. This sensor detects electromagnetic wave using the electromotive force generated by the thermal gradient between the wave-irradiated area and the rest of the region, and thus the detection efficiency depends on the beam size. However, it is difficult to reduce the beam size of GHz waves, which have a wavelength of around 10 cm. This is because the beam size is limited to the wavelength due to the diffraction limit. Therefore, generating a significant thermal gradient with GHz waves is challenging. Here we use the Bull's eye (BE) structure including one aperture with a bowtie shape, where the shorter gap width is 0.6 mm, to achieve GHz wave confinement beyond the diffraction limit.

2. Experiment

Figure 1a shows the designed BE structure modeled by a perfect electric conductor in air. A linearly polarized plane wave along the y-axis is used as an incident wave. The energy density of the electromagnetic fields was calculated at plane 200 μm below the aperture using electromagnetic simulation based on the finite-difference time-domain (FDTD) method. We defined the energy density enhancement as the ratio of the energy density with the structure to that without the structure.

3. Results and Discussions

As shown in Fig. 1b, the BE structure exhibits resonance at around 14.16 GHz, where the energy density enhancements exceeding 1600 are achieved. Figure 1c shows the line profile of the energy density enhancements along the shorter gap at the resonant frequency (14.16 GHz). Despite the incident GHz wave with a wavelength of about 2.1 cm, the waves with strong energy density enhancement were confined within a gap of 0.6 mm. This result can be considered as sufficient energy concentration because the length of the CNT sensor is more than 10 times larger than the gap width.

4. Conclusion

We have demonstrated through electromagnetic field calculations that focusing GHz waves beyond the diffraction limit is possible using a BE structure with a tiny aperture gap. Combining this BE structure with a CNT sensor could potentially improve the response voltage of the sensor from the conventional few μV range to several mV. This enhancement enables wireless non-destructive inspection through the antenna using a simple microcontroller with Wi-Fi functionality and an amplifier circuit.

5. Acknowledgements

This work was supported by JST-Mirai Program Grant No. JPMJMI23G1, JST, ACT-X Grant No. JPMJAX23KL, Japan, Grants-in-Aid for Scientific Research (KAKENHI) (Nos. JP21H01746, JP21H05809, JP22H01553, JP22H01555, JP22H05470, JP23H00169, JP23K19125, JP24K01288, JP24K17325) from the Japan Society for the Promotion of Science, and the Kanagawa Institute of Industrial Science and Technology.

6. References

[1] H. Okawa, T. Oohashi, T. Tanabe, I. Sato, and Y. Kawano, the 2023 Autumn Meeting of the Japan Inst. Metals (2023).

[2] K. Li, Y. Kinoshita, D. Shikichi, M. Kubota, N. Takahashi, Q. Zhang, R. Koshimizu, R. Tadenuma, M. Yamamoto, L. Takai, Z. Zhou, I. Sato, and Y. Kawano, Adv. Optical Mater. 2302847 (2023).

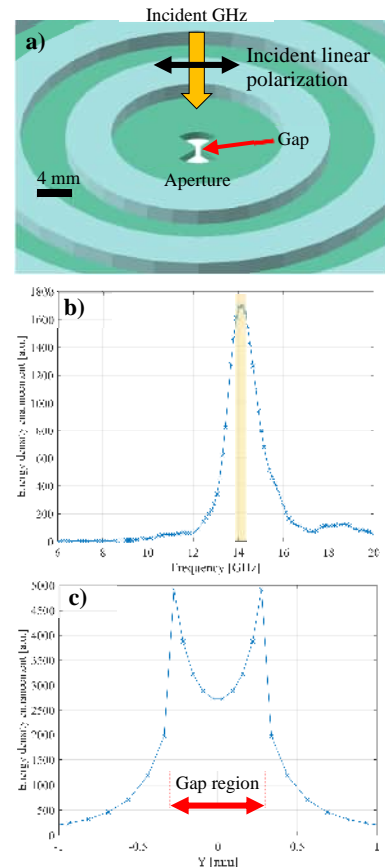


Figure 1. (a) Designed BE structure. (b) The energy density enhancement spectrum of BE at point 200 μm below the center of the aperture. (c) Line profile of the energy density enhancement of BE at 200 μm below of the aperture.

Fundamental limits to metalens critical dimensions

N. Kossowski^{1*}, E. Marinov¹, C. Majorel¹, S. Khadir¹ and P. Genevet²

¹Univeristé Côte d'Azur, CNRS-CRHEA, Rue Bernard Gregory, Valbonne, 06650, France

²Physics department, Colorado School of Mines, 1523 Illinois Street, Golden, CO, 80401, USA

*corresponding author: Nicolas.kossowski@crhea.cnrs.fr

Arrays of microlenses have been integrated to imaging system to increase their spatial resolution of by tackling both electronic and optical crosstalk between pixels [1]. For practical applications, microlenses requires to have the size of the pixels, thus few microns, reaching the diffraction limits. It becomes increasingly difficult to fabricate with refractive lenses [2], therefore metasurfaces have been investigated as a promising solution compatible with traditional semiconductor processes.

Here, we studied the fundamental limits to micro-metalens design by considering a diffraction theory framework based on Stratton-Chu integral [3]. We identified two limits for which the metasurface is operating. The first limit is defined by the aperture of the metasurface itself while the second limit is defined by the period of the metasurface. Inside these limits, we identified two domains of operations: (i) high numerical aperture with full control of the wavefront and narrow bandwidth operation, (ii) low numerical aperture with partial control of the wavefront with ‘‘focal shift’’ [4] and broadband behavior. We verified our theory with 10 μ m diameter metalenses fabricated in GaN and operating at 617nm. Each metalens has a different focal length, thus probing the different regime of operations.

Our study presents guidelines in the design of small metalenses and explicit fundamental limits to their applications.

NK, EM, CM, SK, and PG acknowledges financial support from the French National Research Agency ANR Project Millesime 2 (ANR-21-ASTR-0014).

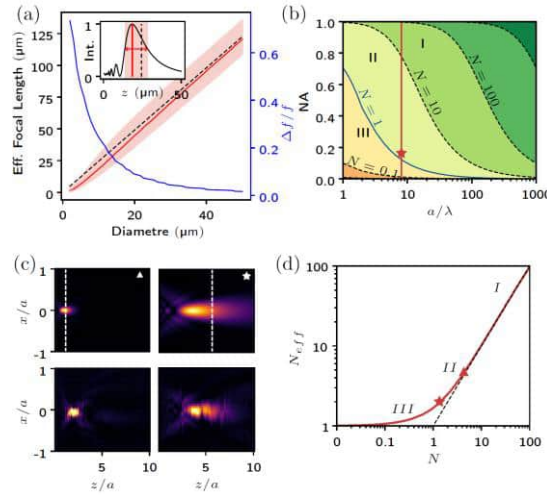


Figure 1: (a) In red, variation of the effective distance focal (maximum of amplitude) in function of the diameter of the metalenses with fix numerical aperture $NA = 0.2$. In blue (right y-axis), variation of the focal shift with regards to the designed focal length. (b) Mapping of the Fresnel number $N = a^2/\lambda f$, in function of the numerical aperture and the size of the aperture (in wavelength). The green color shows $N > 1$ and the yellow colors $N < 1$. (c) Comparison between numerical simulations and measurements for GaN metalenses of $2a = 10\mu m$ at $\lambda = 617nm$, with focal length $f = 10\mu m$ and $f = 30\mu m$, represented by the with dashed line. (d) Evolution of the effective Fresnel number in function of the Fresnel number. Red line corresponds to the simulations and the symbols refer to (c).

[1] Rogalski, A., Martyniuk, P. & Kopytko, M. Challenges of small-pixel infrared detectors: a review. *Rep. Prog. Phys.* **79**, 046501 (2016).

[2] Cai, S. *et al.* Microlenses arrays: Fabrication, materials, and applications. *Microscopy Research and Technique* **84**, 2784–2806 (2021).

[3] Stratton, J. A. & Chu, L. J. Diffraction Theory of Electromagnetic Waves. *Phys. Rev.* **56**, 99–107 (1939).

[4] Li, Y. Focal shifts in diffracted converging electromagnetic waves. I. Kirchhoff theory. *J. Opt. Soc. Am. A, JOSAA* **22**, 68–76 (2005).

CNT film photo scanner for in-line pharma agent pills imaging in infrared–terahertz bands

Miki Kubota^{1*}, Yuya Kinoshita¹, Yuto Matsuzaki¹, Minami Yamamoto¹, Leo Takai¹,
Yukio Kawano¹⁻³, Kou Li¹

¹ Chuo University, 1-13-27 Kasuga, Bunkyo-ku, Tokyo, 112-8551, Japan

² National Institute of Informatics, 2-1-2 Hitotsubashi, Chiyoda-ku, Tokyo, 101-8430, Japan

³ Kanagawa Institute of Industrial Science and Technology, 3-2-1, Sakado, Takatsu-ku, Kawasaki-shi, Kanagawa, 213-0012, Japan
a20.7c7e@g.chuo-u.ac.jp

1. Introduction

Pharmaceuticals are essential in modern society, and high-quality management is essential. Therefore, it is desirable to conduct full and detailed inspections in the manufacturing process. However, such an inspection system is still insufficient, which potentially causes the supply of defective products. The above situation indicates that establishing additional inspection methods is indispensable. In recent years, the demand for non-destructive inspection has grown, not only for pharmaceuticals. In every inspection method, optical measurements in infrared (IR) and terahertz (THz) bands have gathered attention as transmissive properties of materials differ with wavelength and composition [1, 2]. Regarding photo-detection, carbon nanotubes (CNT) film is also adequate in the above ultrabroad IR–THz bands with the photo-thermoelectric (PTE) effect [3, 4]. To this end, this work integrated IR–THz multi-wavelength imaging systems to the line with the CNT film photo scanner and performed imaging measurements of the pharma agent pills (Fig. 1a).

2. Experiment

This work constructed an in-line transmissive imaging system with multi-wavelength irradiation: short wavelength infrared (SWIR, λ - 4.33 μm), long wavelength infrared (LWIR, λ - 6.33 μm), and sub-THz (λ - 909 μm). Fig. 1b shows the presenting CNT film imager and its function. The PTE response of the pixel differs with external photo-irradiation intensity. This device detects the optical transmissive signal to the target under a one-axis scan imaging.

3. Results

Fig. 1c shows the multi-wavelength imaging results of sedative pills containing plastic, glass, and metal inside. In a monochrome color scale, the darker and brighter range refers to the higher and lower intensity of the transmissive PTE responses. The local reduction of the transmittance in the pill corresponds to the foreign substance, which is visually indistinguishable. The above PTE image indicates that the two-wavelength irradiation of SWIR and LWIR visualises the plastic. Then, the obtained result detects the glass with LWIR irradiation. Finally, all three-wavelength irradiation in this work visualizes the metal. These tendencies that visibilities differ with irradiation bands reflect broad changes in transmittance of the various materials with composition and wavelength in IR–THz regions. The above situation leads to composition identification of foreign substances by combining the database of material and transmittance in IR–THz bands. In this way, this work focused on optical properties in IR–THz bands and demonstrated a basic system for pharma inspection with the CNT film photo scanner.

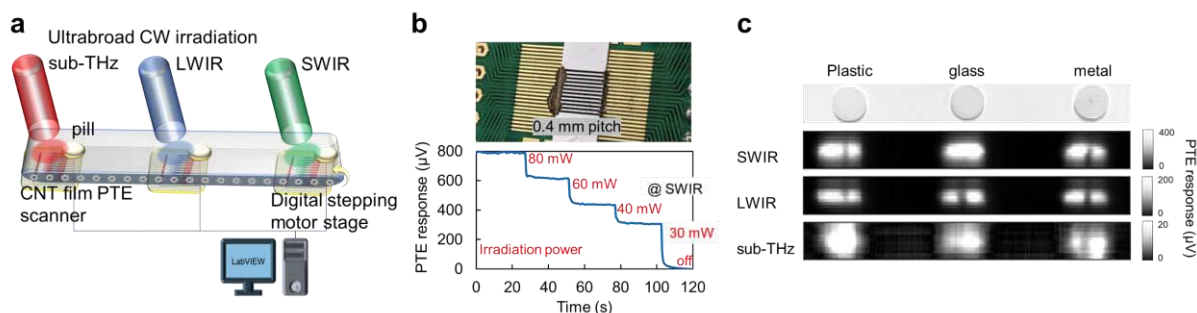


Fig. 1. a, In-line multi-wavelength imaging system in this work. b, CNT film photo scanner and its change in PTE response with external photo-irradiation intensity. c, Material composition identification of the samples with different concealed foreign substances.

4. References

- [1] K. Li, *et al.* *Advanced Optical Materials*, early view (2023)
- [2] K. Li, *et al.* *Micromachines*, **14**, 1, 61 (2023)
- [3] D. Suzuki, *et al.* *Sensors and Actuators A: Physical*, 354 (2023)
- [4] T. Araki, *et al.* *Advanced Materials*, early view (2023)

Optical and spin properties of color centers in diamond needles

Sergei Malykhin, Mariam Quarshie, Bo Xu, Elena Filonenko

*Department of Physics and Mathematics, University of Eastern Finland, Joensuu, Finland
sergeim@uef.fi*

Diamonds, the hardest natural material, have unique properties that are essential for industrial and scientific applications. Made of carbon atoms arranged in a crystalline structure, diamonds also exhibit remarkable optical clarity and high thermal conductivity. Beyond their use in jewelry, diamonds are crucial for cutting, grinding, and drilling tools. Additionally, fluorescent point defects, known as color centers, have been actively researched in recent decades, enhancing diamond's value for advanced technological applications. These color centers exhibit bright, stable fluorescence even at room temperature, making them ideal for imaging and optical sensing. High-precision optical registration of pH [1] and temperature [2] using color centers has been demonstrated. Combined with diamond's biocompatibility, the unique optical properties of color centers hold promise for bioimaging and medical diagnostics at the cellular level. Moreover, color centers often function as single molecules with quantum features, making diamond a promising solid-state platform for quantum applications. Leveraging these properties, diamonds have shown potential in various quantum fields. In quantum sensing, diamonds serve as nano-thermometers [3] and sensors for magnetic and electric fields [4,5] and mechanical stress [6]. In quantum computing, diamonds have enabled the creation of quantum processors with 27 nuclear-spin qubits [7]. In quantum communication, diamond color centers have introduced single-photon emitters [8] and multi-qubit quantum network nodes [9]. In quantum imaging, nitrogen-vacancy (NV) centers in diamonds have allowed the imaging of current flow in graphene [10].

This work focuses on single crystal diamond needles (SCDNs) as a promising material to enhance the technological implementation of diamond color centers. SCDNs, with a pyramidal shape and square base, are produced using a combination of chemical vapor deposition (CVD) and selective oxidation from methane and hydrogen gases [11]. Optimization of experimental procedures and post-processing techniques allows for the production of SCDNs with tip sizes down to a few nanometers, length control from hundreds of nanometers to hundreds of micrometers, and color centers distributed with sub-micrometer precision along the SCDN [12].

We present the results of our recent research on the optical and spin properties of color centers typically forming in SCDNs during synthesis. We discuss fluorescence lifetimes, photoluminescence excitation (PLE), and spin properties, highlighting the potential of fluorescent diamond needles in quantum sensing, computing, and other applications.

This work was supported by Academy of Finland (Flagship Programme PREIN, decision 346518; research projects, decisions 340733, 357033; QuantERA project EXTRASENS, decision 361115), and Horizon Europe MSCA FLORIN Project 101086142.

- [1] H. Raabova, D. Chvatil, P. Cigler, *Nanoscale*, 11, 18537–18542 (2019).
- [2] L. Golubewa, Y. Padrez, S. Malykhin, T. Kulahava, E. Shamova, I. Timoshchenko, M. Franckevicius, A. Selskis, R. Karpicz, A. Obratsov, Y. Svirko, P. Kuzhir, *Advanced Optical Materials*, 10 (2022).
- [3] G. Kucsko, P.C. Maurer, N.Y. Yao, M. Kubo, H.J. Noh, P.K. Lo, H. Park, M.D. Lukin, *Nature*, 500, 54–58 (2013).
- [4] S. Hong, M.S. Grinolds, L.M. Pham, D. Le Sage, L. Luan, R.L. Walsworth, A. Yacoby, *MRS Bulletin*, 38, 155–161 (2013).
- [5] F. Dolde, H. Fedder, M.W. Doherty, T. Nöbauer, F. Rempp, G. Balasubramanian, T. Wolf, F. Reinhard, L.C.L. Hollenberg, F. Jelezko, J. Wrachtrup, *Nature Physics*, 7, 459–463 (2011).
- [6] L. Rigutti, L. Venturi, J. Houard, A. Normand, E.P. Silaeva, M. Borz, S.A. Malykhin, A.N. Obratsov, A. Vella, *Nano Letters*, 17, 7401–7409 (2017).
- [7] M.H. Abobeih, Y. Wang, J. Randall, S.J.H. Loenen, C.E. Bradley, M. Markham, D.J. Twitchen, B.M. Terhal, T.H. Taminiu, *Nature*, 606, 884–889 (2022).
- [8] I. Aharonovich, S. Castelletto, D.A. Simpson, C.-H. Su, A.D. Greentree, S. Praver, *Reports on Progress in Physics*, 74, 076501 (2011).
- [9] P.-J. Stas, Y.Q. Huan, B. Machielse, E.N. Knall, A. Suleymanzade, B. Pingault, M. Sutula, S.W. Ding, C.M. Knaut, D.R. Assumpcao, Y.-C. Wei, M.K. Bhaskar, R. Riedinger, D.D. Sukachev, H. Park, M. Lončar, D.S. Levonian, M.D. Lukin, *Science*, 378, 557–560 (2022).
- [10] J.-P. Tetienne, N. Dontschuk, D.A. Broadway, A. Stacey, D.A. Simpson, L.C.L. Hollenberg, *Science Advances*, 3 (2017).
- [11] S.A. Malykhin, A.M. Alexeev, E.A. Obratsova, R.R. Ismagilov, V.I. Kleshch, A.N. Obratsov, *Materials Today Proceedings*, 5, 26146–26152 (2018).
- [12] S. Malykhin, Y. Mindarava, R. Ismagilov, F. Jelezko, A. Obratsov, *Diamond and Related Materials*, 125, 109007 (2022).

Detection of Dark Plasmon Modes of a Single Gold Rod by Radially Polarized Terahertz Pulses

Mizuho Matoba, Kuniaki Konishi, Norikatsu Mio, Junji Yumoto and Makoto Kuwata-Gonokami

The University of Tokyo, 7-3-1 Hongo, Bunkyo-ku, Tokyo, Japan
matoba@ipst.s.u-tokyo.ac.jp

1. Introduction

Radial beams have radially symmetric polarization distribution and generate longitudinal electric fields oscillating along the propagation direction at the focal point [1]. This characteristic electric field distribution can couple with modes that are difficult to couple with uniformly linearly polarized light, such as dipole-forbidden dark modes of plasmon resonance, and has been used for their excitation and detection [2, 3]. However, in previous reports, the optical response caused by the interaction between radial beams and matter has been observed through the detection of intensity of the light, which makes it difficult to separate the response of the longitudinal electric field from that of the transverse electric field. If direct observation of longitudinal electric fields of radial beams is performed with terahertz time-domain spectroscopy (THz-TDS) using broadband terahertz radial beams, it may be possible to selectively observe the optical response of dark modes as changes in the longitudinal electric field component [4]. In this study, we demonstrate the detection of dipole-forbidden modes by longitudinal electric fields.

2. Results

We performed THz-TDS measurement using terahertz radial beams. Figure (a) illustrates a schematic of the experimental configuration. A gold rod was placed at the first focal point of the confocal system in which terahertz radial beams generated using a half waveplate mode converter and a nonlinear crystal with threefold rotational symmetry [5]. The longitudinal electric fields at the second focal point were measured with electro-optic (EO) sampling using a (100) ZnTe crystal to investigate the changes brought by the interaction between the rod and the beams. Experiments with linearly polarized beams were also carried out for comparison, in which transverse electric fields were measured.

Figure (b) shows the experimental results for a rod of 1010 μm length and 100 μm diameter. These spectra show the relative electric field amplitude, the electric fields measured with the rod divided by the electric fields measured without the rod. When linearly polarized beams were irradiated, dips were observed only at the frequencies of the bright mode (0.38, 0.68, 0.96 and 1.24 THz), whereas when radial beams were irradiated, dips were also observed at the frequencies of the dark mode (0.50, 0.76, 1.07 and 1.38 THz), which cannot be excited by waves with uniform linear polarization. This shows that the dark modes can be excited by radial beams and detected by observing the longitudinal electric fields after propagation. Our results demonstrate that the electric field distribution generated by focusing radial beams is able to achieve non-contact excitation and detection of the dipole-forbidden modes. This technique has the potential to realize non-contact detection of plasmon modes, including non-radiant modes used for sensing and other applications.

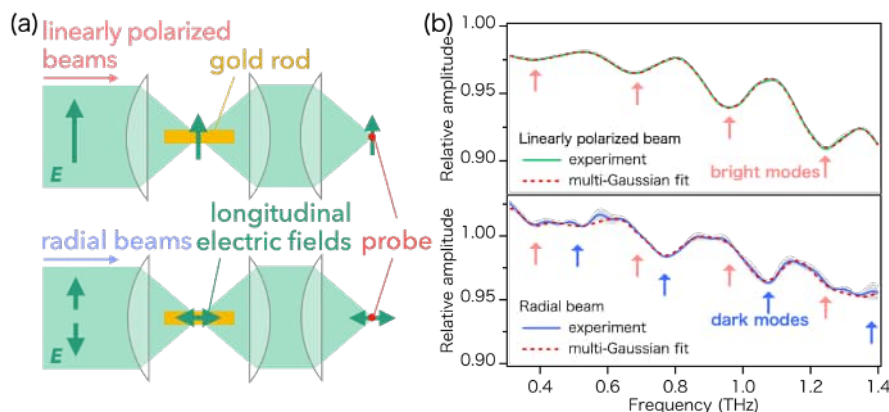


Fig. (a) The schematic of the optical system used in the simulation and the experiment. Green arrows indicate the direction of the polarization. (b) The relative electric field intensity, shown with the error width. Blue (Red) arrows indicate the frequencies corresponding to dark (bright) modes of the rod.

3. References

- [1] Q. Zhan, *Advances in Optics and Photonics* **1**, 1 (2009).
- [2] D. E. Gómez, Z. Q. Teo, M. Altissimo, T. J. Davis, S. Earl and A. Roberts, *Nano Letters* **13**, 3722 (2013).
- [3] T.-S. Deng, J. Parker, Y. Yifat, N. Shepherd and N. F. Scherer, *The Journal of Physical Chemistry C* **122**, 27662 (2018).
- [4] M. Matoba, K. Konishi, N. Mio, J. Yumoto and M. Kuwata-Gonokami, 2022 47th International Conference on Infrared, Millimeter and Terahertz Waves (IRMMW-THz), Tu-AM-3-4, (2022).
- [5] Z. Zheng, N. Kanda, K. Konishi and M. Kuwata-Gonokami, *Optics Express* **21**, 10642 (2013).

Terahertz detection with optically gated vertical graphene nanowalls

Petr A. Obraztsov¹, Vassilis Papadakis², Yuri Svirko¹, Alexander N. Obraztsov¹

¹*Institute of Photonics, University of Eastern Finland, 80101 Joensuu, Finland*

²*XpectralTEK, Av. da Igreja 7, 4705-732 Braga, Portugal*

petr.obraztsov@uef.fi

Efficient terahertz (THz) photoconductive detection demands an active medium with high absorptivity, ultrashort carrier lifetime, and high mobility of photo-excited charge carriers. Graphene, with its ballistic charge carriers, offers mobilities up to $15,000 \text{ cm}^2 \cdot \text{V}^{-1} \cdot \text{s}^{-1}$ at room temperature and ultrafast carrier relaxation times. Its gapless Dirac-cone electron band structure allows 2.3% optical absorption across a broad spectral range, enabling excitation with low-energy photons. These properties make graphene competitive with conventional materials used for THz photoconductive antennas, such as low-temperature grown or Cr-doped GaAs.

Despite various approaches for measuring THz radiation power with graphene, including bolometric response, photovoltaic and photothermoelectric effects, and graphene-based field-effect transistors, only on-chip coherent pulse detection and generation have been demonstrated so far. However, graphene's application for THz detection is hindered by two main limitations: low responsivity due to limited absorption in atomically thin layers and moderate lateral dimensions restricting scalability.

In this work, we report on the time-domain detection of THz radiation using optically gated vertical graphene nanowalls (VGNs) [1]. VGNs, also known as nanographite (NGF), consist of vertically oriented graphene-containing carbon nanosheets with few-layer basal graphene layers, chemically active defect sites, and edges. NGF's properties, including excellent electrical and thermal conductivity, chemical stability, and large specific surface area, are advantageous for various applications. Tailoring the NGF microstructure through growth process adjustments ensures high optical absorption efficiency, making it suitable for applications such as photodetectors and thermal sensors.

We fabricated and evaluated a set of THz photoconductive detectors using VGNs grown on Si substrates via the CVD method. A direct comparison of the coherent photocurrent response of these optically gated devices with those of graphene and widely used electro-optic detectors demonstrates VGNs' strong potential for THz time-domain detection. The mesoporous 2D material's enhanced sensitivity and robustness surpass those of single-layer graphene, paving the way for the mass production of ultrafast photoconductive detectors.

This research was funded by H2020 Programme (RISE project Chartist (101007896) and Academy of Finland (decision numbers 340831 (UPHYPE project)).

[1] Obraztsov, P. A.; Chizhov, P.; Kaplas, T.; Bukin, V.; Silvennoinen, M.; Hsieh, C.-F.; Konishi, K.; Nemoto, N.; Kuwata-Gonokami, M., *ACS Photon.*2019, 6, 1780–1788.

Physical and chemical composition optimization of CNT imagers for augmented reality non-destructive inspections

Ryoga Odawara^{1*}, Minami Yamamoto¹, Yukio Kawano^{1,2,3}, Yoshihiro Watanabe⁴, Kou Li¹

¹Faculty of Science and Engineering, Chuo University, Tokyo, 112-8551 (Japan)

²National Institute of Informatics, Tokyo, 101-8430 (Japan)

³Kanagawa institute of Industrial Science and Technology, Kanagawa, 213-0012 (Japan)

⁴School of Engineering, Tokyo Institute of Technology, Tokyo, 152-8550 (Japan)

Corresponding Autor E-mail: a20.b5bw@g.chuo-u.ac.jp

1. Foreword

In the field of non-destructive inspection, ultra-broadband electromagnetic wave imaging measurements using carbon nanotube (CNT) film photo-thermal (PTE) sensors have been attracting attention in recent years[1]. This sensor can detect ultrabroadband photo-irradiation in infrared, THz, and millimetre waves regions at room temperature. Furthermore, the sensor has flexible characteristics. Therefore, the sensor has the potential to inspect for any shape. The vital matter of non-destructive inspections is speed and accuracy. In higher-speed operations, the integration time of signal readout is shorter. As a result, the normal mode noise increases. In addition, 2D integration of the sensor is necessary to realize higher-speed imaging rather than single elements or 1D integration setups. Therefore, it is essential to select device materials that can withstand the noise of higher-speed operations and integrate optical sensors in higher density for achieving superior performances of CNT film imagers. This study reports the physical and chemical composition optimization of CNT film broadband imagers beyond the speed-sensitivity trade-off for augmented reality non-destructive inspection.

2. Experiment and result

Fig. 1 shows a comparison of PTE images (target: metallic pattern marked as "10") obtained by the CNT film PTE sensor. In the conventional study, the noise in PTE images increased significantly as the operation speed became faster. This tradeoff between noise and speed is a critical problem for an image sensor. For this reason, this study adopts the high conductivity of the CNT film to solve this tradeoff. As a result, this study succeeds in decreasing the noise at higher-speed operation time. It turns out the CNT film utilized in this study can reduce noise more than that in the conventional study. Thus, the operation speed of the sensor is available at over five times faster than that of the conventional study.

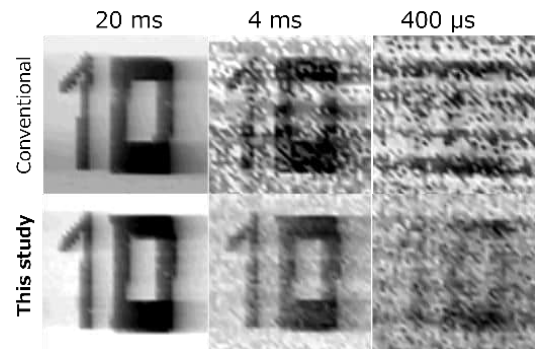


Fig. 1 Comparison of imaging results.

In Fig. 1, this work employed the single element CNT film PTE sensor for those images. Owing to the single-element configuration, the imaging time is extended. Hence, this study focused on the imager design of 2D integration to reduce imaging time. Fig. 2 shows the design of the CNT film imager and the imaging result with that device. This design succeeds in an 8×8 integration by the original design. Image sensor pixels consist of the interface portion between CNT films and electrodes. As shown in Fig. 2, the successful integration of pixels maintained 2.4 mm spacing. The CNT solution printing technique produced this design. This imager achieved five times shorter imaging time rather than that of the single element.

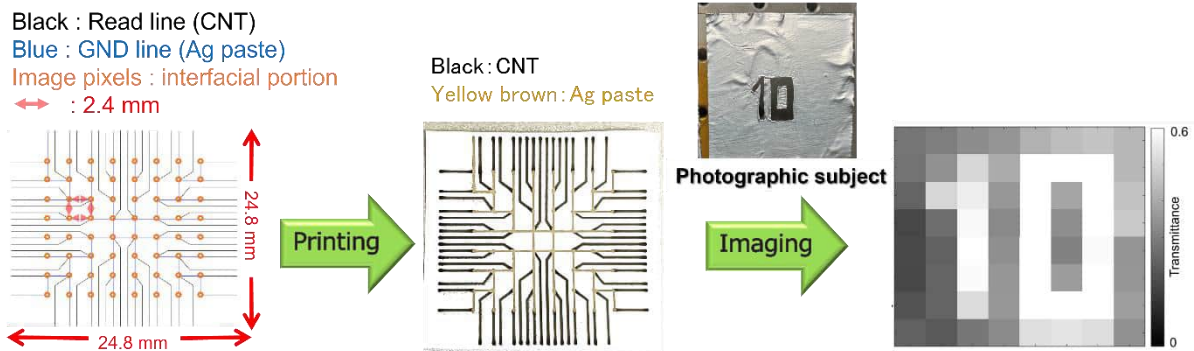


Fig. 2 Design of the CNT film imager and imaging result by that camera

[1] K. Li, et. al., *Adv. Mater. Interface*, **2023**, 10, 2300528.

Anar Ospanova¹, Ladislau Matekovits², Alexey Basharin¹

¹ Center of Photonics Sciences, University of Eastern Finland, Joensuu, Finland

² Department of Electronics and Telecommunications, Politecnico di Torino, Torino, Italy

Contact: anar.ospanova@uef.fi

Keywords: metamaterial, GHz, microwaves, Bound State in Continuum, transmission, high Q resonance

Bound State In the Continuum – BIC – is an effect anticipated for its high quality and excitation method. BICs are typically characterized by the complete confinement of electromagnetic wave within the continuous spectrum, as well as coexisting with radiating waves that continuously support energy leakage [1, 2]. Another feature is that in highly symmetric structures the effect can manifest itself due to the smallest change in symmetry.

Here we show self-complementary metamaterial comprising two layers resembling chessboard to show BIC effect appearing due to small change on symmetry of the structure. This metamaterial has already shown an ultrabroadband transparency in microwave range [3]. Therefore, we demonstrate that the slightest tilt of the angle of the incident wave results in BIC excitation.

Experimental results demonstrate the appearance of BIC resonance at ~ 6.5 GHz when impinging wave is tilted by 0.5 degree (Figure 1 a). The effect measured by two-horn antenna method perfectly matches previously simulated results [3]. The measured samples have shown Q-factor ~ 1000 .

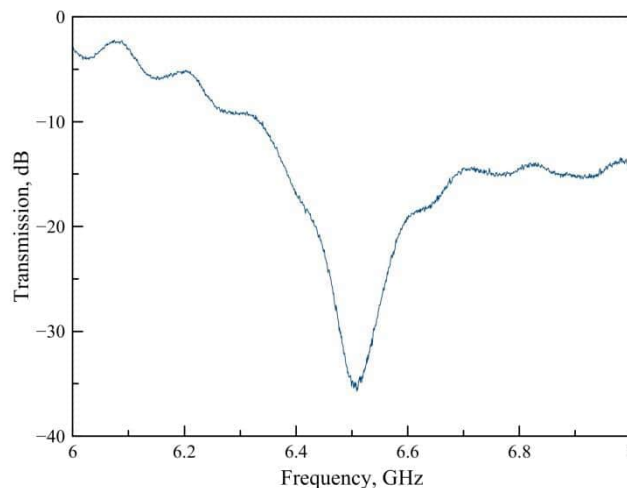


Fig. 1: Experimental results of metamaterial in the range of 6-7 GHz.

BIC engineered structure supports highly localized electromagnetic field that is extremely sensitive to changes in the environment, thus, allows for the confinement and manipulation of light within subwavelength structures. This enables the creation of highly efficient optical devices that are highly demanded in nanophotonics for various applications, including sensing and communication technologies. Nanophotonic sensors based on the BIC effect can be fabricated on a small scale, allowing for integration into compact and portable devices for on-site or real-time monitoring applications.

1. V. I. Kukulin, V. Krasnopolsky, and J. Horacek, “Theory of resonances: Principles and Applications”, (Springer Science & Business Media, 2013)
2. C. W. Hsu, B. Zhen, A. D. Stone, J. D. Joannopoulos, and M. Soljacic, “Bound states in the continuum”, *Nature Reviews Materials* **1**, 1, 2016
3. A. Ospanova, M. Cojocari, P. Lamberti, A. Plyushch, L. Matekovits, Yu. Svirko and P. Kuzhir, A. Basharin, “Broadband transparency of Babinet complementary metamaterials”, *Appl. Phys. Lett.* **122**, 231702, 2023

Two-dimensional high-yield printable integration of carbon nanotube photo-thermal pixels for realtime, large-area, and broadband non-destructive testing camera applications

Leo Takai¹, Yuto Matsuzaki¹, Minami Yamamoto¹, Yukio Kawano^{1,2,3}, Kou Li¹

¹Chuo University, Tokyo 1-13-27, Japan

²National Institute of Informatics, Tokyo 2-1-2, Japan

³Kanagawa Institute of Industrial Science and Technology, Kanagawa 705-1, Japan
a20.ymc3@g.chuo-u.ac.jp

1. Introduction

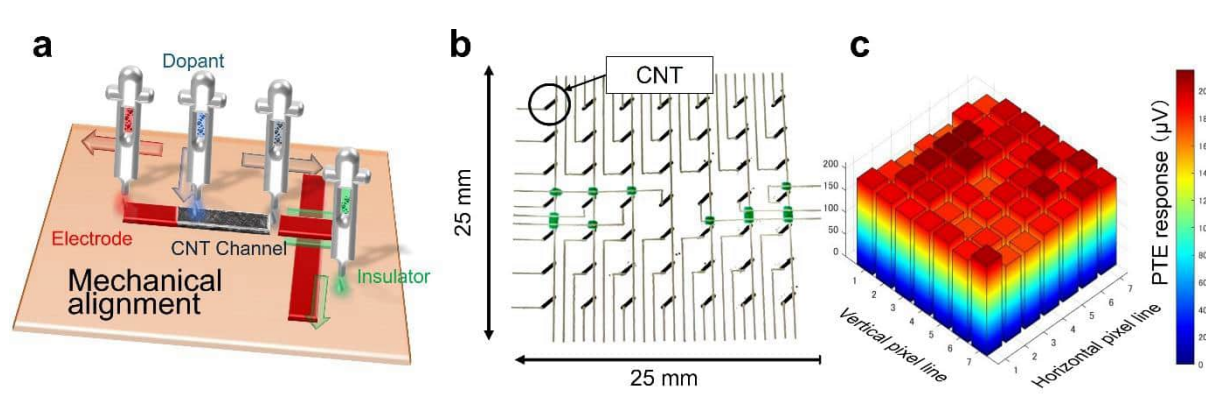
This study aims to develop a photo-thermoelectric broadband imaging camera sheet and apply it to non-destructive testing technology by taking advantage of the optical and mechanical properties of carbon nanotube (CNT) thin films [1]. The presenting device has ultra-broadband absorption properties and flexibility compared to existing solid-state detectors. The principle of this device is the photo-thermoelectric effect (PTE). First, certain electromagnetic waves irradiated on CNTs are absorbed into local heating. Then, heat generates the electromotive force by the Seebeck effect. This work employed a desktop auto dispenser (available in uncooled atmospheric conditions) to print the entire structure on a flexible/stretchable thin substrate for fabricating the above imaging sheet. This study succeeded in developing a high yield photo-thermoelectric 2D camera device and real-time, large area, and broadband non-destructive imaging by mechanical alignment of each pixel.

2. Method

This study employed the mechanical auto dispenser (Fig. 1a) as the printing equipment. All materials used, including electrodes and insulators, are in ink form. The device materials used are SWCNTs and n-type chemical carrier dopants (for forming pn junctions). These liquid materials show high compatibility with existing printing technology, and the dispenser enables high-yield micro-integration and three-dimensional wiring structures, leading to the realization of a two-dimensional camera sheet.

3. Results and Discussion

Figure. 1b illustrates the fabricated 2D camera sheet in this study. This camera sheet has 49 pixels. The n-type dopant applies to the upper right half of the CNT film. This camera sheet uses the PTE effect as its operating principle [2]. The device is able to perform ultra-broadband optical detection with low noise at room temperature due to the PTE operation of the CNT film. Measurement of the PTE response value by irradiating a near-infrared laser ($\lambda=1.55 \mu\text{m}$) at the pn junction of each pixel showed that this camera device is high yield (Figure. 1c). This represents that the camera printing is highly accurate.



[李恒1]

Fig. 1a. In-line multi-wavelength imaging system in this work. b. The black lines are CNTs with n-type doping in the upper right. c. PTE response of each element.

4. References [李恒2]

- [1] K. Li, et al., *Nature Communications*, 12, 3009 (2021).
[2] K. Li, et al., *Science Advances*, 8, 19, eabm4349 (2022).

Thursday, August 8



©P.Obraztsov

Tailored growth of transition metal dichalcogenides monolayers for photonics and optoelectronics

Andrey Turchanin

Friedrich Schiller University Jena, Jena, Germany
Abbe Center of Photonics (ACP), Jena, Germany

Two-dimensional materials (2D), their van der Waals and lateral heterostructures possess a manifold of unique electronic, optoelectronic, and photonic properties which make them highly interesting for fundamental studies and technological applications. To realize this potential, their tailored synthesis by chemical vapor deposition (CVD, MOCVD) as well as understanding the role of their intrinsic defects and 2D-material/substrate interactions are decisive. In this talk I will present an overview of our recent progress on the synthesis, characterization and studying of fundamental photonic and optoelectronic phenomena in various 2D material systems including some device applications. A particular focus will be on the transition metal dichalcogenides monolayers (TMDs), their engineered variants like Janus TMDs and lateral heterostructures as well as their integration with other low dimensional and 3D materials like, e.g., optical fibers and wave guides.

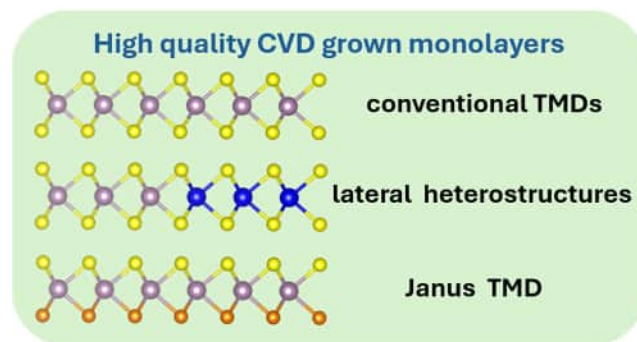


Fig. 1. Schematic representation of some 2D materials to be presented.

Acknowledgement

EU-DFG FLAG-ERA Project “H2O”, TMWWDG FGR 0088 “2D-Sens”, DFG SFB 1375 „NOA“ Project B2, SPP 2244/1 “2DMP” Project TU149/13-1 and TU149/21-1, DFG Project TU 149/16-1.

References

- [1] A. George et al., Controlled growth of transition metal dichalcogenides monolayers using Knudsen-type cells for the precursors *J. Phys. Mater.* **2**, 016001 (2019).
- [2] S. Shree et al., High optical quality of MoS₂ monolayers grown by chemical vapor deposition. *2D Mater.* **7**, 015011 (2020).
- [3] I. Paradeisanos et al., Controlling interlayer excitons in MoS₂ layers grown by chemical vapor deposition. *Nat. Commun.* **11**, 2391 (2020).
- [4] G. Q. Ngo et al., Scalable functionalization of optical fibers using atomically thin semiconductors. *Adv. Mater.* **32**, 2003826 (2020).
- [5] A. George et al., Giant persistent photoconductivity in monolayer MoS₂ field-effect transistors. *npj 2D Mater. Appl.* **5**, 15 (2021).
- [6] S. B. Kalkan et al., Wafer scale synthesis of organic semiconductor nanosheets for van der Waals heterojunction devices. *npj 2D Mater. Appl.* **5**, 92 (2021).
- [7] E. Najafidehaghani et al., 1D p-n junction electronic and optoelectronic devices from transition metal dichalcogenide lateral heterostructures grown by one-pot chemical vapor deposition synthesis *Adv. Funct. Mater.* **31**, 2101086 (2021).
- [8] Z. Gan et al., Chemical vapor deposition of high-optical quality large-area monolayer Janus transition metal dichalcogenides. *Adv. Mater.* **34**, 2205226 (2022).
- [9] Z. Gan et al., Patterned growth of transition metal dichalcogenides monolayers for electronic and optoelectronic device applications. *Small Methods* **6**, 2200300 (2022).
- [10] D. Beret et al., Exciton spectroscopy and unidirectional transport in MoSe₂-WSe₂ lateral heterostructures encapsulated in hexagonal boron nitride. *npj 2D Mater. Appl.* **6**, 84 (2022).
- [11] G. Q. Ngo et al., In-fiber second-harmonic generation with embedded two-dimensional materials. *Nat. Photonics* **16** 769-776 (2022)
- [12] S.B. Kalkan, High-performance monolayer MoS₂ field-effect transistors on cyclic olefin copolymer-passivated SiO₂ gate dielectric. *Adv. Opt. Mater.* **11**, 2201653 (2023).
- [13] R. Rosati et al., Interface engineering of charge-transfer excitons in 2D lateral heterostructures. *Nat. Commun.* **14**, 2438 (2023).
- [14] H. Lamsaadi et al., Kapitza-resistance-like exciton dynamics in atomically flat MoSe₂-WSe₂ lateral heterojunction. *Nat. Commun.* **14**, 5881 (2023).
- [15] J. Picker et al., Structural and electronic properties of MoS₂ and MoSe₂ monolayers grown by chemical vapor deposition on Au(111). *Nanoscale Adv.* **6**, 92-101 (2024).

High-performance reconstructive spectrometers with van der Waals junctions

Andreas C. Liapis^{1*}, Faisal Ahmed¹, Md Gius Uddin¹, Yawei Dai¹,
Xiaoqi Cui¹, Fedor Nigmatulin¹, Hoon Hahn Yoon², and Zhipei Sun¹

¹*QTF Centre of Excellence, Department of Electronics and Nanoengineering, Aalto University, Finland.*

²*School of Electrical Engineering and Computer Science, Gwangju Institute of Science and Technology, Korea.*

andreas.liapis@aalto.fi

1. Main text

Conventional spectrometers rely on bulk optical components such as gratings or filters to separate colors from one another, and therefore cannot be miniaturized without sacrificing their performance. Recently, a new class of ‘ultra-miniaturized reconstructive spectrometers’ has emerged that overcomes this limitation by not requiring that colors be separated prior to detection [1]. Instead, such spectrometers combine the spectral sensitivity and photodetection in a single component element whose spectral responsivity can be electrically modulated. A computational algorithm is then used to reconstruct the spectral content of unknown input light from variations in the photocurrent as the applied modulation signal is swept. Nanometer-level spectral resolutions are possible even though the footprint of the device is on the order of a few tens of micrometers.

Layered 2D materials are ideal candidates for producing such miniaturized spectrometers. They exhibit strong light-matter interaction, and their bandgap can be modulated (e.g. via the Stark effect), leading to an electrically-tunable optical response [3]. Moreover, they naturally possess dangling-bonds-free surfaces, and can be assembled in van der Waals (vdW) structures without taking into consideration lattice mismatch. This allows us to engineer the energy band alignment at the heterostructure interface by choosing the appropriate combination of materials.

Previously, we reported a miniaturized spectrometer based on a locally-gated vdW junction between MoS₂ and WSe₂, operating in the spectral range of 400 – 850 nm [2]. Here, we further simplify the device architecture while simultaneously extending its operating range to cover both the visible and NIR [4]: we construct a simple vdW heterostructure diode using multilayer MoS₂, which possesses a relatively wide bandgap of 1.2 eV, and multilayer black phosphorus (BP), whose bandgap is only 0.3 eV (Fig 1a, b). The resulting vdW junction exhibits an efficient modulation of band alignment between staggered-gap and broken-gap, which changes the character of charge carrier transport from thermionic emission to band-to-band tunneling, merely by controlling the source-to-drain bias voltage (V_{DS}), without requiring gate modulation. The modulation of optical responsivity observed is sufficient to reconstruct spectra with nm-scale peak accuracy in both the visible and NIR (Fig 1c–f).

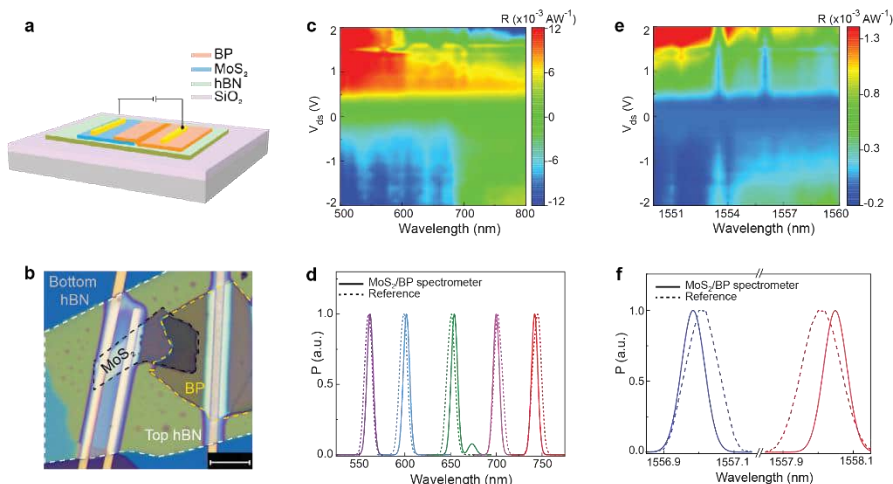


Fig. 1. **a** Schematic of the vdW junction computational spectrometer. **b** The fabricated MoS₂/BP vdW diode seen under an optical microscope. To protect the device, the heterostructure is encapsulated with hBN on either side. Scale bar 10 μm . **c** Responsivity as a function of wavelength and applied V_{DS} in the visible range. **d** Comparison of reconstructed and reference spectra in the visible range. **e** and **f** Responsivity matrix and benchmarking of reconstructed spectra in the NIR region.

2. Acknowledgement

This work was supported by Business Finland (R2B A-gate), Academy of Finland (314810, 333982, 336144, 352780, 352930, and 353364), the Academy of Finland Flagship Programme (320167, PREIN), the EU H2020-MSCA-RISE-872049 (IPN-Bio), the Jane and Aatos Erkkö foundation and the Technology Industries of Finland centennial foundation (Future Makers 2022), and ERC (834742).

3. References

- [1] X. Cui, Y. Zhang, A. C. Liapis, and Z. Sun, *Light: Science & applications*, **12**(1), 142 (2023).
- [2] H. H. Yoon, H. A. Fernandez, F. Nigmatulin, *et al.*, *Science*, **378**(6617), 296 (2022).
- [3] Chaves, A., Azadani, J.G., Alsaman, H. *et al.*, *npj 2D Mater Appl* **4**, 29 (2020).
- [4] Md G. Uddin, S. Das, A. M. Wang, *et al.*, *Nature Communications* **15**(1), 571 (2024).

Layered MoS₂ for the enhancement of supercontinuum generation in photonic crystal fiber

Xu Cheng^{1,2}, Jin Xie³, Guodong Xue³, Hao Hong³, Zhipei Sun², Kaihui Liu³, Zhongfan Liu^{4,5}

¹Group for Fibre Optics, École Polytechnique Fédérale de Lausanne (EPFL), Lausanne, Switzerland

²QTF Center of Excellence, Department of Electronics and Nanoengineering, Aalto University, Espoo, Finland

³State Key Laboratory for Mesoscopic Physics, School of Physics, Peking University, Beijing, China

⁴Center for Nanochemistry, College of Chemistry and Molecular Engineering, Peking University, Beijing, China

⁵Beijing Graphene Institute (BGI), Beijing, China

khliu@pku.edu.cn

1. Introduction

Decorating the silica-based photonic crystal fibre (PCF) to enhance its nonlinearity and expand its spectrum range is a significant research topic in supercontinuum laser optics [1]. Previously, methods such as filling nonlinear gases or liquids into the hollow core PCFs have been explored and made great progress [2], yet these hybrids are plagued by mode instability, leakage risk and environmental fluctuation. The emergence of two-dimensional (2D) layered materials offers a unique opportunity. The integration of 2D robust crystals could ensure the stability and portability of PCF for table-top laser sources. Here, we report the first realization of integrating solid-state 2D nonlinear optical layers with commercial nonlinear PCF to boost its supercontinuum generation (SCG) efficiency.

2. Result and discussion

For SCG in the PCF, the transmission loss, dispersion profile and nonlinear coefficient are the three most important parameters. In principle, 2D layered MoS₂, with the merits of atomic-level flatness and relative large bandgap (with low scattering loss and absorption), extremely thin thickness (hardly damage the transmission mode and dispersion profile of optical fiber), ultra-high optical nonlinear response (n_2 is about 5 orders of magnitude higher than that of silica at 1550 nm), and facile integration with silica-based waveguides, is an ideal partner to combine with PCF for its SCG enhancement [3,4]. Guided by these inspirations, here we directly grow solid-state thin-layer 2D MoS₂ into the air-holes of nonlinear PCF (MoS₂-PCF) and investigate its SCG performance (Figure 1). As expected, the SCG of the MoS₂-PCF exhibits a significantly enhancement compared with that of the bare-PCF. Specifically, the threshold power to reach one octave broadening in the MoS₂-PCF is reduced by 30% compared to that of the bare-PCF. This improvement of SCG efficiency mainly originates from the enhancement of the nonlinear coefficient by the interaction of the optical field with MoS₂.

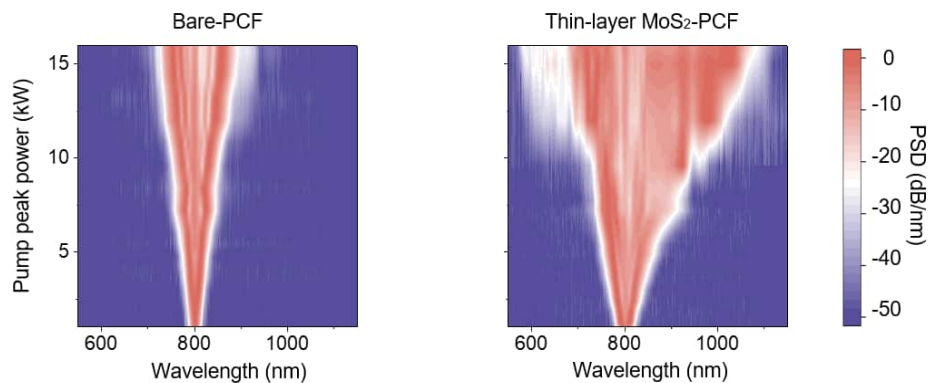


Fig. 1 SCG spectral evolution profiles of the bare-PCF (left) and thin-layer MoS₂-PCF (right) under 800 nm pulsed laser pump. The embedded thin MoS₂ film enhances the SCG broadening significantly.

3. Conclusions

To the best of our knowledge, our work should be the only feasible route of integrating a solid-state nonlinear optical crystal with PCF to enhance its SCG. Given the large library of 2D materials with diverse physical properties, this non-destructive, portable and easy-to-integrate solution will greatly promote the development of fiber-based table-top light sources with different functionalities.

4. References

- [1] R. R. Alfano, *The supercontinuum laser source: the ultimate white light* (Springer, 2022).
- [2] J. M. Dudley, G. Genty, S. Coen, Review of Modern Physics, **78**, 1135 (2006).
- [3] A. Autere, H. Jussila, Y. Y. Dai, Y. D. Wang, H. Lipsanen, Z. P. Sun, Advanced Materials **30**, 1705963 (2018).
- [4] Y. G. Zuo, W. T. Yu, C. Liu, X. Cheng, R. X. Qiao, J. Liang, X. Zhou, J. H. Wang, M. H. Wu, Y. Zhao, P. Gao, S. W. Wu, Z. P. Sun, K. H. Liu, X. D. Bai, Z. F. Liu, Nature Nanotechnology **15**, 987 (2020).

Layered materials as a platform for quantum technologies

Andrea C. Ferrari

University of Cambridge, UK

Layered materials are taking centre stage in the ever-increasing research effort to develop material platforms for quantum technologies. We are at the dawn of the era of layered quantum materials. Their optical, electronic, magnetic, thermal and mechanical properties make them attractive for most aspects of this global pursuit. Layered materials have already shown potential as scalable components, including quantum light sources, photon detectors and nanoscale sensors, and have enabled research of new phases of matter within the broader field of quantum simulations. I will discuss opportunities and challenges faced by layered materials within the landscape of material platforms for quantum technologies, with focus on applications that rely on light–matter interfaces [1].

[1] A. R. P. Montblanch et al. *Nature Nano* 18, 555 (2013)

Relaxation Pathways of Excitations in Semiconducting Carbon Nanotubes

Leonas Valkunas

*Department of Molecular Compounds Physics, Center for Physical Sciences and Technology, Suletekio Ave. 3, 10257, Vilnius, Lithuania
Leonas.valkunas@fmf.lt*

Experimental studies of the excitation relaxation dynamics in single-walled semiconducting carbon nanotubes indicate changes of the observable signals on a very fast timescale [1, 2]. We present a thorough analysis of one- and two-color transient absorption measurements performed on single- and double-walled semiconducting carbon nanotubes. By combining the currently existing models describing exciton–exciton annihilation—the coherent and the diffusion-limited ones—we are able to simultaneously reproduce excitation kinetics following both E11 and E22 pump conditions. Our simulations revealed the fundamental photophysical behavior of one-dimensional coherent excitons and non-trivial excitation relaxation pathways. In particular, we found that after non-linear annihilation a doubly-excited exciton relaxes directly to its E11 state bypassing the intermediate E22 manifold, so that after excitation resonant with the E11 transition, the E22 state remains unpopulated. A quantitative explanation for the observed much faster excitation kinetics probed at E22 manifold, comparing to those probed at the E11 band, is also provided.

[1] M. W. Graham, J. Chmeliov, Y.-Z. Ma, H. Shinohara, A. A. Green, M. C. Hersam, L. Valkunas and G. R. Fleming, *J. Phys. Chem. B*, **115**, 5201–5211 (2011).

[2] J. Chmeliov, J. Narkeliunas, M. W. Graham, G. R. Fleming and L. Valkunas, *Nanoscale*, **8**, 1618-1626 (2016).

Evidence of abnormal hot carrier thermalization at van Hove singularities of twisted bilayer graphene

Nianze Shang^{1,2}, Zhipei Sun¹, Kaihui Liu² and Hao Hong²

¹ QTF Centre of Excellence, Department of Electronics and Nanoengineering, Aalto University, Espoo, Finland
² State Key Laboratory for Mesoscopic Physics, School of Physics, Peking University, Beijing, China

In the past decades, hot carriers in graphene have been exhaustively studied in many ways. From the broadband ultrafast photoluminescence (PL)[1, 2], to the ultrafast and efficient hot carrier harvesting among graphene and various semiconducting materials. These intriguing carrier dynamic behaviours and the diverse ultrafast phenomena have addressed graphene an excellent platform for advanced optoelectronics and photonics.

As a unique engineering method for two-dimensional (2D) materials, interlayer twisting brings new opportunities in both fundamental physics and applications into graphene. The emergence of van Hove singularities (VHSs) endows graphene enhanced density of states, intensified light absorption and strongly bound excitons[3, 4]. Strong correlation of electrons in magic-angle TBG can further lead to more intriguing phenomena like correlated insulating states, superconductivity et al[5]. With all these fascinating optical and electronic properties, TBG-like 2D material systems have infused new vitality to the research frontiers of materials science and condensed matter physics. However, research until now on TBG is limited to the ground state, and the photoexcited state dynamical properties of TBG, representing one of the irreplaceable aspects of its physical picture and cornerstone for its application design, are still little studied.

Here, we propose the time-resolved PL autocorrelation method to unveil the ultrafast hot carrier dynamics in TBG. As ultrafast PL intensity is linearly correlated with the transient hot carrier density, time-resolved PL autocorrelation should be a faithful reflection to the carrier dynamics[6]. By extracting the peak components from PL spectra which represent the pure VHS contribution, we can recover the VHS carrier dynamics from the carrier mixture. Ultrafast hot carriers on the linear bands of TBG behave similarly to MLG, while the carriers captured by VHS possess a decelerated dynamic, which is 4-time longer than that of MLG. Further time-dependent density functional theory (TDDFT) suggests that the prolonged lifetime is attributed to the abnormal hot carrier thermalization brought by bottleneck effect at mini-gaps and interlayer charge redistribution process in real space.

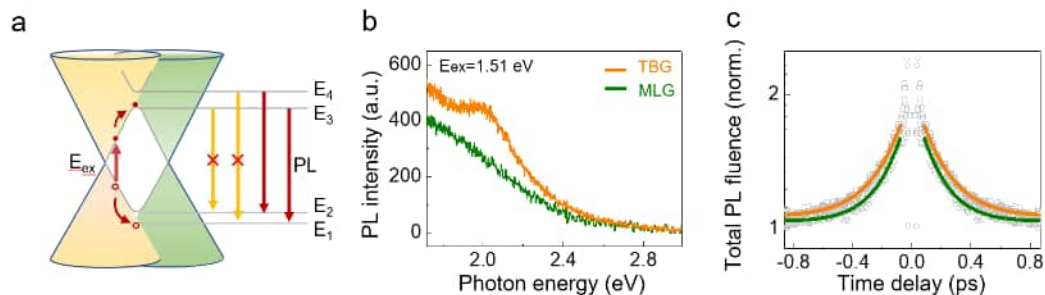


Figure 1 Ultrafast PL and PL autocorrelation of TBG. a. Bandgap opening at VHS of TBG and its optical transition selection rules. b. the ultrafast PL spectra of TBG and MLG. c. ultrafast PL autocorrelation of TBG and MLG, where TBG shows a longer lifetime.

Our exploration should have important implications for the design of TBG-based ultrafast photonics and optoelectronics devices, such as light-harvesting, light-sensing or light-emitting devices. Meanwhile, our technique should be a unique spectroscopy method to investigate the fundamental element interaction in TBG at small twist angles, when the system lies in a strong-correlation regime at a cryogenic environment. We expect that the abnormal dynamics at VHS will bring more intriguing physics to TBG and its family.

References

- [1] C. H. Lui, K. F. Mak, J. Shan and T. F. Heinz *Phys. Rev. Lett.* **105**, 127404 (2010)
- [2] W.-T. Liu, S. W. Wu, P. J. Schuck, M. Salmeron, Y. R. Shen and F. Wang *Phys. Rev. B* **82**, 081408 (2010)
- [3] R. W. Havener, Y. Liang, L. Brown, L. Yang and J. Park *Nano Lett.* **14**, 3353 (2014)
- [4] H. Patel, R. W. Havener, L. Brown, Y. Liang, L. Yang, J. Park and M. W. Graham *Nano Lett.* **15**, 5932 (2015)
- [5] Y. Cao, V. Fatemi, S. Fang, K. Watanabe, T. Taniguchi, E. Kaxiras and P. Jarillo-Herrero *Nature* **556**, 43 (2018)
- [6] T. C. O'Haver and J. D. Winefordner *Anal. Chem.* **38**, 1258 (1966)

Electro-thermal and electromagnetic response of industrial-grade graphene materials based on quantum effects

Antonio Maffucci

Dept. of Electrical and Information Engineering, Univ. of Cassino and Southern Lazio, Cassino, Italy
maffucci@unicas.it

1. Response of industrial-grade graphene nanoplatelets films.

This work summarizes some of the results obtained in the frame of the Horizon 2020 project TERASSE (Terahertz Antennas with Self-amplified Spontaneous Emission) [1]. Specifically, the work focuses on the study of novel graphene-based materials and on their electrical and thermal properties.

Materials based on graphene are extensively researched because to exceptional mechanical, thermal, and electrical properties. However, due to its high cost, the substance that is formally denoted as graphene is not very interesting for practical uses. As a result, in recent times, interest has been drawn to what is known as "industrial graphene," which refers to substitute, less expensive materials that are simple to manufacture on an industrial scale. The materials based on so-called graphene nanoplatelets (GNPs) among these offer a good trade-off between improved physical qualities, large-scale production, and affordable costs [2].

This work examines the electro-thermal and electromagnetic response of commercial graphene films based on graphitic nanoparticles (GNPs), which are produced using an inexpensive graphitic precursor (intercalated expandable graphite) using an industrial procedure.

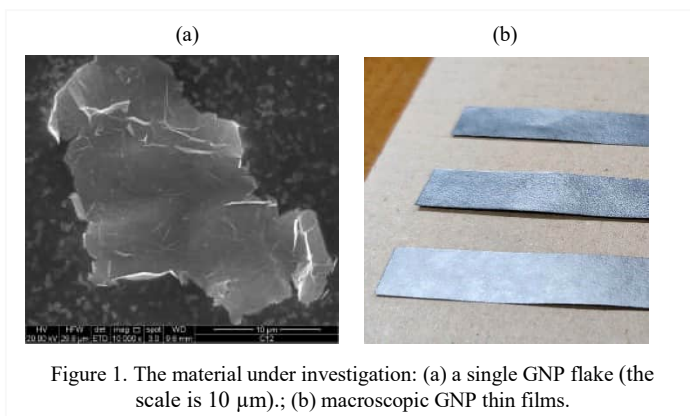


Figure 1. The material under investigation: (a) a single GNP flake (the scale is 10 μm); (b) macroscopic GNP thin films.

A picture of a single GNP and of the final strip analyzed in this paper is provided in Fig.1. The GNP flakes have an average lateral dimension of about 30 μm , and thickness of about 14 nm, Fig.1a. In this paper, two types of films have been investigated, differing from the percentage of GNPs and of the binders, in the following denoted as G-Preg 95/5 and G-Preg 70/30, see Fig.1b.

The equivalent electrical resistivity and thermal conductivity are studied by means of models and experimental characterization.

The temperature dependence of the electrical

resistance shows an unusually negative temperature coefficient of the resistance, which is a favorable feature for heat management in electronic systems. A theoretical explanation of this behavior is based on quantum effects related to the electrical transport in these materials [3].

As for the thermal conductivity, a novel procedure has been assessed as an alternative to the laser-flash characterization usually adopted for thin films. The procedure proposed here is based on the analysis of the time evolution of the thermal transients after the strip is heated to the target temperature. The measured values of these parameters for the commercial graphene strips under investigation ranged from 200 to 400 W/mK [4].

Finally, this material has been characterized in terms of its electromagnetic shielding effectiveness, with the idea of using it as an innovative coating for electronics cases. A shielding effectiveness of about 40–50 dBs has been demonstrated in a wide frequency range.

2. Acknowledgement.

This work was partially supported by the Project "TERASSE", funded by EU under H2020-MSCA-RISE Programme, grant # 823878.

3. References

- [1] www.terasse.org
- [2] A. Kovtun, et al. "Benchmarking of graphene-based materials: real commercial products vs. ideal graphene," *2D Materials*, **6**, p.025006, (2019).
- [3] S. Sibilia, F. Bertocchi, S. Chiodini, F. Cristiano, L. Ferrigno, G. Giovinco, A. Maffucci, "Temperature-dependent electrical resistivity of macroscopic graphene nanoplatelet strips," *Nanotechnology* **32** 275701 (2021).
- [4] G. Giovinco, S. Sibilia, A. Maffucci, "Characterization of the thermal conductivity and diffusivity of graphene nanoplatelets strips: a low-cost technique," *Nanotechnology*, **34**, p. 345703 (2023).

Numerical modeling of cell membrane electromagnetic behaviour and nanoparticles interaction

Patrizia Lamberti¹, Silvana Morello², Patrizia Gazzero², Elisabetta Sieni³, Maksim Shundalau¹ and Vincenzo Tucci¹

¹Dept. of Information and Electrical Eng. and Applied Math., University of Salerno, via Giovanni Paolo II 132, Fisciano (SA) – ITALY

²Dept. of Pharmacy, University of Salerno, via Giovanni Paolo II 132, Fisciano (SA) – ITALY

³Dept. of Theoretical and Applied Science, University of Insubria, Varese, ITALY

*plamberti@unisa.it

1. Summary

Computational modelling and analysis in biology and medicine have received major attention in recent years.. Multi-scale and Multiphysics computational modeling and analysis, capable to capture biological and physiological interdependencies across multiple observational scales –not only in time and space, but also in physico-chemical modality– could be very useful. In particular models can be employed to address the basic interaction mechanisms between electromagnetic (EM) fields, nanoparticles and biological cells, and to study biophysical phenomena occurring on spatiotemporal scales that cannot be observed with experimental methods. Starting from the circuitual model of cell membranes, the possibility to have the EM cell membrane field distribution will be presented and used to perform in silico analysis of eukaryotic and excitable cells subjected to electromagnetic stimuli.

2. Description of the problem and proposed approaches

Computational modelling and analysis in biology and medicine have received major attention in recent years. The interdisciplinary efforts developed so far aimed at elucidating structures and functions of living systems with major challenges in computational modelling to understand, analyze and predict the complex mechanisms of biological systems [1-2]. Researchers are now beginning to address the grand challenge of multi-scale computational modeling and analysis, such as in the case of carbon-based nanoparticles presence [3] used to interact with cells: effectively capturing biological and physiological interdependencies across multiple observational scales –not only in time and space, but also in physico-chemical modality– and doing so in a computationally efficient manner [4]. In this scenario analytical and numerical models can be employed to address the basic interaction mechanisms between EM fields, nanoparticles and biological cells, and to study biophysical phenomena occurring on spatiotemporal scales that cannot be observed with experimental methods. Starting from a circuitual model of cell membranes [5-6], the use of equivalent medium theory is exploited in order to derive a field model of cell membrane EM behaviour taking in to account the presence of voltage controlled ionic channels and the field induced membrane non linearity [4,7]. The systems of equations to be solved is obtained by coupling suitable differential equations describing these two phenomena with the Electroquasistatic formulation of Maxwell equations. A finite element solution of the system in a commercial software (Comsol multiphysics) is here reported and used to perform in silico analysis of excitable cells and of agglomerate of eukaryotic cells subjected to electromagnetic stimuli in presence of nanoparticles [8].

3. Acknowledgement.

The work was carried out within the framework of the European Union's Horizon Europe research and innovation programme under the Marie Skłodowska Curie grant agreement No 101086142 and it was partially supported by the European Union under the Italian National Recovery and Resilience Plan (NRRP) of NextGenerationEU, Mission 4, Component 2, Investment 1.1, Call for tender No. 1409 of 14.9.2022 of the Italian Ministry of University and Research (MUR), Project Title DEEPEST (Digging into rEversible and irreversible ElectroPoration: in vitro and in silico multiphysical analyses on cEll models for cancer Treatment) CUP B53D23002500006 - Grant Assignment Decree No. 960 of 30/06/2023.

4. References

- [1] P. Lamberti, et al., "nsPEF-induced effects on cell membranes: use of electrophysical model to optimize experimental design," IEEE Transactions on Dielectrics and Electrical Insulation, vol. 20, no. 4, pp. 1231-1238, 2013.
- [2] P. Lamberti, et al., "The Role of Pulse Repetition Rate in nsPEF-Induced Electroporation: A Biological and Numerical Investigation," IEEE Transactions on Biomedical Engineering, 62 (9), art. no. 7079377, pp. 2234 – 2243, 2015, DOI: 10.1109/TBME.2015.2419813,
- [3] P. Kuzhir, et al. "Main principles of passive devices based on graphene and carbon films in microwave - THz frequency range" JOURNAL OF NANOPHOTONICS. Vol. 11. (2017) 03250401 (19pp), doi: <http://dx.doi.org/10.1117/1.JNP.11.032504>
- [4] S. Elia, P. Lamberti, "The reproduction of the physiological behaviour of the axon of nervous cells by means of finite element models," (2013) Studies in Computational Intelligence, 442, pp. 69 – 87, DOI: 10.1007/978-3-642-32177-1_5
- [5] A. L. Hodgkin and A. F. Huxley, "A quantitative description of membrane current and its application to conduction and excitation in nerve," J. Physiol., vol. 117, no. 4, pp. 500–544, 1952.
- [6] P. Lamberti, M. Compitello, and S. Romeo, "ns Pulsed Electric Field-Induced Action Potentials in the Circuitual Model of an Axon," IEEE TRANSACTIONS ON NANOBIOSCIENCE, vol. 17, no. 2, April 2018
- [7] S. Elia, P. Lamberti, and V. Tucci, "Influence of Uncertain Electrical Properties on the Conditions for the Onset of Electroporation in an Eukaryotic Cell," IEEE Transactions on Nanobioscience, vol. 9, no. 3, pp. 204-212, Sep 2010, doi: 10.1109/Tnb.2010.2050599.
- [8] E. Sieni, et al., "Electric Field Distribution in Cell Aggregates in Presence of Nanostructures Under Electroporation Pulses," 2023 IEEE Nanotechnology Materials and Devices Conference (NMDC), Paestum, Italy, 2023, pp. 174-179.

High-precision observation and simulation of femtosecond laser ablation

Kuniaki Konishi

*Institute for Photon Science and Technology, The University of Tokyo
kkonishi@ipst.s.u-tokyo.ac.jp*

Laser processing technology using ultrashort pulsed lasers has many advantages over conventional processing technologies, such as the ability to freely fabricate ultrafine shapes on various difficult-to-process materials, including carbon fiber composite materials and glass, without contact and without the effects of thermal damage. Therefore, improving the controllability of laser processing technology is an important issue for industrial applications. Furthermore, in recent years, microstructure fabrication technology using ultrashort pulsed laser processing has also advanced remarkably, and it has become clear that it can be used to fabricate elements for terahertz light wave control [1,2,3]. However, the mechanism of laser-induced material destruction is still not fully understood due to the complex interplay of physical phenomena on various spatial and temporal scales in non-equilibrium open systems.

As a starting point to address these issues, it is important to clarify the reproducibility of femtosecond laser ablation with high accuracy. To this end, it is necessary to precisely determine the correspondence between the beam profile of the femtosecond laser pulse and the shape of the resulting laser-processed crater. We have developed an original method to measure the beam profile at the laser focus point directly and have succeeded in developing a method called fluence mapping, which provides a one-to-one correspondence between the intensity at each location in the laser spot and the depth of the laser trace by directly comparing it with the measured laser trace geometry (Figure 1)[4]. As a result, extremely high reproducibility and localization in dielectric laser processing were revealed. Furthermore, this has made it possible to match the experimental and simulation conditions of laser ablation with high accuracy.

Therefore, we have also succeeded in demonstrating that nonlinear simulations of femtosecond laser propagation in air can predict the radius of the laser-processed scar with extreme accuracy over a wide range of laser intensity [5]. This means that our simulation technique can also be used to predict processing results. Thus, it has become clear that femtosecond laser processing can process materials with high accuracy and reproducibility on the submicron order, and the groundwork is being laid for exploring the mechanism.

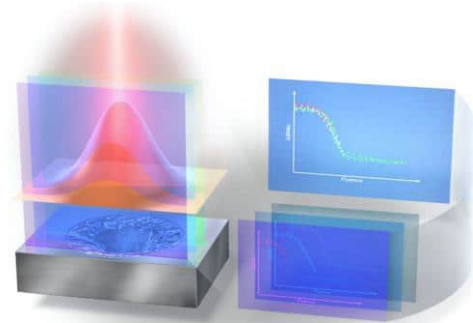


Fig.1 Conceptual diagram of fluence mapping method

References

- [1] Haruyuki Sakurai, Natsuki Nemoto, Kuniaki Konishi, Ryota Takaku, Yuki Sakurai, Nobuhiko Katayama, Tomotake Matsumura, Junji Yumoto, Makoto Kuwata-Gonokami, *OSA Continuum*, **2**, 2764 (2019).
- [2] R. Takaku, S. Hanany, H. Imada, H. Ishino, N. Katayama, K. Komatsu, K. Konishi, M. Kuwata-Gonokami, T. Matsumura, K. Mitsuda, H. Sakurai, Y. Sakurai, Q. Wen, N. Y. Yamasaki, K. Young, J. Yumoto, *Journal of Applied Physics* **128**, 225302 (2020).
- [3] Ryota Takaku, Qi Wen, Scott Cray, Mark Devlin, Simon Dicker, Shaul Hanany, Takashi Hasebe, Teruhito Iida, Nobuhiko Katayama, Kuniaki Konishi, Makoto Kuwata-Gonokami, Tomtoake Matsumura, Norikatsu Mio, Haruyuki Sakurai, Yuki Sakurai, Ryohei Yamada, Junji Yumoto, *Optics Express* **29**, 41745-41765 (2021).
- [4] Haruyuki Sakurai, Kuniaki Konishi, Hiroharu Tamaru, Junji Yumoto, Makoto Kuwata-Gonokami, *Communications Materials* **2**, 38 (2021).
- [5] Ryohei Yamada, Wataru Komatsubara, Haruyuki Sakurai, Kuniaki Konishi, Norikatsu Mio, Junji Yumoto, and Makoto Kuwata-Gonokami, *Optics Express* **31**, 7363 (2023).

Recent advances in ultrafast laser nanostructuring of transparent materials

P.G. Kazansky¹, Y. Lei¹, H. Wang¹, S. Shevtsov¹, M. Shribak² and Y. Svirko³

¹University of Southampton, Southampton, UK

²University of Chicago and Marine Biological Laboratory, Woods Hole, USA

³University of Eastern Finland, Joensuu, Finland
pgk@soton.ac.uk

In ultrafast laser writing, it has been widely accepted that higher energy density leads to stronger material changes unless thermal effects are involved. We challenge this belief by demonstrating that decreased energy density—achieved through increased scanning speed and without thermal accumulation—leads to more significant modifications in silica glass. This phenomenon is attributed to the nonlocality of light-matter interaction at tight focusing, where the intensity gradient and charge carrier diffusion play a critical role in enhancing material modification. We observed a tenfold increase in the writing speed of polarization multiplexed data storage, achieving MB/s rates using high transmission nanopore-based modification.

The temporal contrast of femtosecond pulses is also crucial in laser writing. Anisotropic nanopores in silica glass are produced by high-contrast (107) femtosecond Yb laser pulses, rather than low-contrast (103) Yb fiber laser pulses. The difference arises from the fiber laser storing a third of its energy in a post-pulse of up to 200 ps duration. This low-intensity fraction is absorbed by laser-induced transient defects with long lifetimes and low excitation energy, such as self-trapped holes, altering the energy deposition kinetics and the type of material modification. Low-contrast pulses effectively create lamellar birefringent structures, potentially driven by a quadrupole nonlinear current.

Differential interference contrast (DIC) microscopy benefits from femtosecond laser writing, which enables the creation of anisotropic nanopores with ultrahigh transmittance (>99%), producing negative form birefringence, comparable to the positive birefringence of quartz crystal.

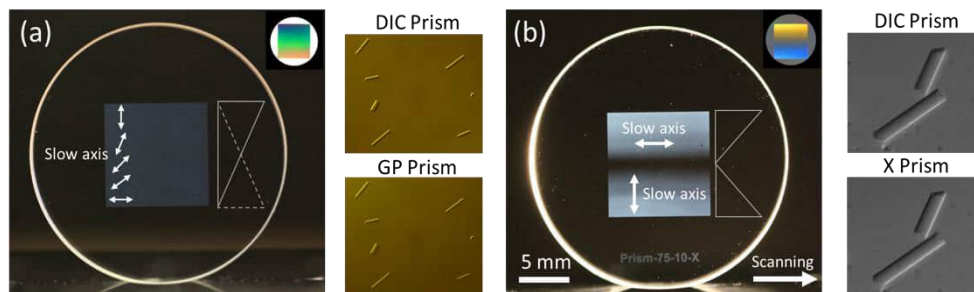


Fig. 1 (a) A 10 mm geometric phase prism (GP Prism) and (b) a 10 mm X prism written by ultrafast laser writing in silica glass. The double arrow represents the direction of the slow axis. The inset on the upper right is their image taken by polychromatic polarization microscope. The image performance of prisms was compared with a commercially available DIC prism (Olympus U-DIC20HR).

High-performance birefringent elements, such as geometric phase prism (GP prism) and retardance gradient prism (X prism), were fabricated by modulating the slow axis or retardance of the birefringent modification (Fig.1). These elements can replace standard DIC prisms without losing image quality, increase resolution, field of view and advantage of design flexibility.

This work was partially supported by H2020 RISE project #101007896 (CHARTIST) and Research Council of Finland (decision no 343393).

[1] H. Wang, Y. Lei, G. Shayeganrad, Y. Svirko, and P. G. Kazansky, Increasing Efficiency of Ultrafast Laser Writing Via Nonlocality of Light-Matter Interaction. *Laser Photonics Rev.* 2024, 2301143.

[2] Y. Lei, H. Wang, G. Shayeganrad, Y. Svirko, and P. G. Kazansky, "Controlling ultrafast laser writing in silica glass by pulse temporal contrast," *Opt. Lett.* 49, 2385-2388 (2024).

[3] Y. Lei, P. Kazansky, and M. Shribak, "Birefringent elements for optical microscopy by ultrafast laser writing," in *CLEO/Europe 2023, Technical Digest Series* (Optica Publishing Group, 2023), paper ch_7_4.

Author index

- Ahmed, F., 58
Alborghetti, L., 31, 41
Alsamsam, M. N., 8
Altman, M. S., 28
Ayyagari, S. R., 32
- Balasubramanian, P., 21
Basharin, A., 37, 53
Bertoni, B., 31, 41
Bianco, G. V., 36
Brozzesi, S., 4
Bruno, G., 36
- Cao, S., 15
Cheng, Xu, 59
Chernyakova, K., 9, 42
Chmeliov1., J., 44
Cigler, P., 21, 23
Cojocari, M., 31, 37
Copak, J., 21
Cui, X., 58
Cun, H., 28
Cígler, P., 20
- Dai, Y., 58
Dassano, G., 37
Dementjev, A., 5
Ding, Y., 15
D'Orazio, A., 36
- Fedorov, G., 17, 31
Ferrari, A. C., 60
Filonenko, E., 49
Fu, H., 27
- Gazzerro, P., 64
Gelzinis, A., 44
Genevet, P., 47
Golberg, D., 30
Golubewa, L., 9
Greber, T., 28
Grincienė, G., 9, 42
Gulka, M., 20, 21
- Hakamada, Y., 43
Halimski, I., 5, 44
Hartmann, R. R., 16
Hashiyada, S., 46
- Hemmi, A., 28
Hong, Hao, 59, 62
- Iannuzzi, M., 28
- Janonis, V., 32
Jelezko, F., 21, 22
Jorudas, J., 32
Jureviciute, M., 8
- Kanda, N., 14
Karpicz, R., 5, 9, 42
Kawano, Leo T., 48
Kawano, S., 45
Kawano, Y., 46, 52, 54
Kazansky, P. G., 66
Kašalynas, I., 5, 17, 32
Khadir, S., 47
Khun, J., 21
Kimura, W., 45
Kinoshita, Y., 48
Konishi, K., 29, 43, 45, 50, 65
Konishi, M., 46
Kopustas, A., 8
Kossowski, N., 47
Krupinski-Ptaszek, A., 6
Kubota, M., 48
Kuwata-Gonokami, M., 50
Kuzhir, P., 17, 31, 37
- Lamberti, P., 5, 31, 64
Lapkiewicz, R., 6
Lei, Y., 66
Li, Kou, 46, 48, 52, 54
Liapis, A. C., 58
Liu, K., 13, 59, 62
Liu, Wen, 15
Liu, Z., 59
- Maffucci, A., 63
Makowski, A., 6
Malykhin, S., 19, 49
Marinov, E., 47
Matekovits, L., 36, 37, 53
Matoba, M., 43, 50
Matsunaga, R., 14
Matsuzaki, Y., 46, 54
Matveev, G., 37

- Mielnicka, A., 6
Mio, N., 45, 50
Morello, S., 64
Moscotin, M., 32
Murotani, Y., 14

Nigmatulin, F., 58

Obraztsov, A. N., 18, 51
Obraztsov, P. A., 51
Odawara, R., 52
Ogrin, F. Y., 34
Okawa, H., 46
Osanova, A., 53

Padrez, Y., 9
Paksaite, J., 8
Palummo, M., 4
Paonessa, F., 36
Papadakis, V., 51
Pashnev, D., 5, 17, 32
Pawłowska, M., 6
Perebeinos, V., 3
Peter, I., 33
Pitanti, A., 31, 41
Portnoi, M., 17
Portnoi, M. E., 16
Pulci, O., 4

Quarshie, M., 49

Riaz, M. U., 36
Roddaro, S., 31, 41

Sakurai, H., 29, 43, 45
Saushin, A., 17
Scholtz, V., 21
Seitsonen, Ari P., 28
Shagieva, E., 21
Shang, N., 62
Sheraz, M., 32
Shevtsov, S., 66
Shribak, M., 66
Shundalau, M., 5, 64
Sieni, E., 64
Stehlik, S., 21
Steiner, F., 20
Streckaitė, S., 44
Strnad, G., 33
Subačius, L., 32
Sun, J., 15
Sun, Z., 58, 59, 62
Svirko, Y., 51, 66
Szczykowski, P., 6

Takai, Leo, 54
Talaikis, M., 5

Tanaka, Y., 46
Tenne, Ron, 6
Tredicucci, A., 31, 41
Tucci, V., 64
Turchanin, A., 57
Tutkus, M., 8

Uddin, Md G., 58
Urbanovič, A., 5

Valkunas, L., 44, 61
Vetrone, F., 7
Vicarelli, L., 31, 41
Virone, G., 36

Wang, H., 66
Wang, Q., 15
Wang, S., 15
Watanabe, Y., 52

Xie, Jin, 59
Xu, Bo, 49
Xu, C., 15
Xue, G., 59

Yamada, R., 45
Yamamoto, M., 52, 54
Yamamoto, Y. M., 48
Yoon, H. H., 58
Yumoto, J., 35, 50

Zaleckas, M., 9
Zanotto, S., 31, 41
Zhang, C., 30
Zhang, Qi, 46
Zobelli, A., 4

Čopák, J., 20



ISBN: 978-952-61-5287-5